Experimental Study of Ice Accumulation on Arctic Vessels and Offshore Structures

by **Jonathan R. Bennett**

A thesis submitted to the School of Graduate Studies in fulfillment of the requirements for the degree of

Master of Engineering

Faculty of Engineering and Applied Science

Memorial University of Newfoundland

June 2020

St. John's Newfoundland

Abstract

The arctic landscape has slowly been warming over the course of the 20th century resulting in a recession of ice coverage presenting ships with access and opportunity to regions previously blocked by heavy ice coverage and difficult weather conditions. A rise in global temperatures has accelerated the reduction of arctic sea ice coverage providing fishing and ships the ability to venture further north. Weather systems and frigid temperatures have historically overwhelmed ships traversing the arctic with heavy onboard ice accumulation risking the stability of the vessel and ultimately the safety of the crew. This onboard ice accretion is a combination of both ocean sea spray and freshwater precipitation and can additionally reduce the accessibility and functionality of essential mechanical and emergency equipment. The walkways, stairs and ladders can quickly become layered with ice making work and onboard navigation increasingly hazardous for the crew. While there are several methods to either prevent or remove accumulated ice, each is limited by either high costs, reductive efficiency or additional environmental concerns. Ship operators have traditionally relied on their crew to manually remove accumulated ice with shovels, baseball bats and sledgehammers putting the safety of the crew at risk as they work to remove ice on an already unsteady ocean surface. Additionally, they have generally avoided the thicker ice and colder environment of the winter choosing to work within the warmer summer months. However, with each passing year the ice coverage continues to shrink opening the arctic to more vessels and extending the shipping season further into the winter. This threat of marine icing is only going to become more extensive as the evolving arctic draws both the fishing and shipping industries further north in the pursuit of new opportunities. While there have been great advancements over the last half century in understanding the cause of marine icing there lacks insight and practical research into mitigating its onboard presence. The exposed stairways of ships are particularly dangerous as the increased slipping hazard is worsened with the risk of falling from a height or potentially overboard into the freezing arctic waters.

This thesis gives a detailed look at the history of marine icing and the environmental properties which perpetuate its onboard growth. The research examines the effect of various stair design characteristics on reducing ice accumulation through a set of experiments conducted in the climate controlled cold room located at Memorial University. An open cell tread design resulted in the least amount of ice accretion when compared to the diamond plated aluminum, steel and rubber treads. Due to its hydrophobic properties the rubber tread accrued the most ice while simultaneously demonstrating the greatest ease of removal from impact testing. Thermal conductivity appears to have no correlation with ice accumulation or adhesion as both the steel and aluminum tests attained similar results with drastically different conductivities.

Acknowledgements

I would first like to thank my supervisor Dr. Yuri Muzychka for his guidance and insight throughout this research. His knowledge and support were invaluable, without his assistance this project would have been impossible. I would also like to acknowledge Dan Oldford for his contribution in establishing the scope of this research and feedback throughout the experimental process.

Additionally, this research would not have been possible without the financial assistance provided by the American Bureau of Shipping, MITACS, Equinor and the Research and Development Corporation of Newfoundland Labrador.

To Billy Bidgood and his team within Technical Services Department at Memorial for their help in the design and fabrication of the experimental stair model. My gratitude extends to each of the laboratory technicians from the thermodynamics lab for their daily assistance in operating the equipment. Their rapid response and consistent support were greatly appreciated through the experimental process. I would like to thank Craig Mitchell for his support in operating the cold room and assistance through the troubleshooting phase of this research.

Finally, I would like to thank the staff of Coffee Matters and Jumping Bean coffee shops whose welcoming atmosphere and delicious coffee provided a space to focus, write and procrastinate.

Table of Contents

Table of Figures

Freshwater Ice Accumulation Test

Saltwater Accumulation Test

Impact Test Results

Table of Tables

Freshwater Ice Accumulation Tests

Saltwater Ice Accumulation Tests

Impact Test Results

Chapter 1 Risk and Safety Onboard Shipping Vessels

1.1 Introduction

Marine icing is the accumulation of ice on ocean superstructures and ships travelling through cold and harsh ocean waters. The arctic ocean has particularly challenged humanity as its freezing temperatures and thick ice coverage has overwhelmed ships and slowed advancement. It is impossible to know how many ships have been lost due to onboard ice accretion taking the lives of those onboard, but a changing landscape and new technology has sparked a resurgence in arctic activity. The arctic is broadly defined in most literature by the arctic circle at the 60°N longitude shown in Figure 1.1, however the winter ice growth often pushes beyond this boundary into surrounding waters (Winton, 2006). Marine icing is product of many factors but primarily hinges on freezing temperatures and is most likely to occur in any body of water bordered within the northern ice wall and the 1.5°C isotherm, both of which shift with the cycling seasons.

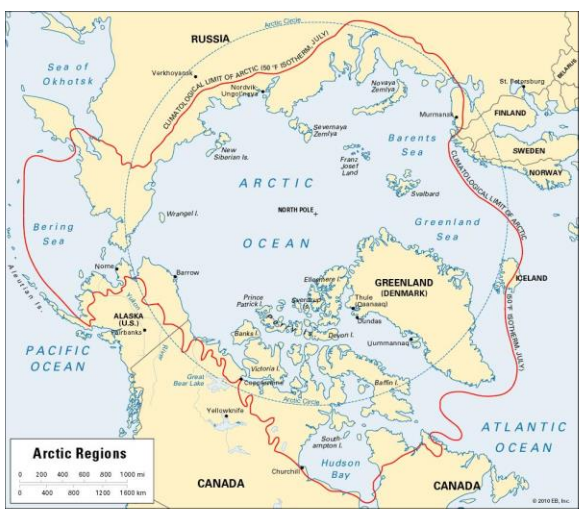

Figure 1.1 - Arctic Circle (Britanica, 2018)

When sailing through freezing ocean conditions a combination of sea spray and atmospheric precipitation results in significant onboard ice accumulation leading to structural damage, instability and the decrease in overall safety of those working at sea. Sea spray icing is generated by waves continuously crashing into the hull and showering the ship before freezing onboard as shown in Figure 1.2. Atmospheric icing is a result of precipitation covering the surfaces of a vessel by way of snow, rain or fog and freezing due to the frigid temperatures (Hay, 1956).

Figure 1.2 - Wave Generated Sea Spray from (Canadian Coast Guard, 2019)

The most notable difference between the two is the salinity of sea water resulting in different ice properties than the ice formed through precipitation. While atmospheric icing due to rain and snow does contribute to ice accretion it is widely agreed that sea spray is the main contributor of icing at sea (Minsk, 1977) (Hay, 1956) (Shellard, 1974) (Samuelsen, 2017). Wave generated spray is inevitable when at sea, whereas atmospheric precipitation is sporadic and can be minimalized with proper preparation and forecasting. Samuelsen (2015) goes on to argue that atmospheric icing is simply a side effect of strong meteorological conditions leading to stronger winds and larger waves perpetuating the problem of sea spray.

Table 1-1 - Source of Ice Accretion from (Dehghanisanij, 2017)

	Sea Spray	**Spray with fog, rain, or drizzle**	**Snow**	**Fog, rain or drizzle**
Northern Hemisphere	90%	6%	1%	3%
Arctic	50%	41%	N/A	9%

In studying reports of icing in the northern hemisphere researchers Borisenkov and Panov found that atmospheric icing was only a contributing factor in 10% of all reported incidents (Dehghanisanij, 2017). However, when focusing solely on the arctic the same study showed the influence of atmospheric icing increasing to 40%, which could be attributed to the year-round colder temperatures, stronger winds and more severe storms. The cold climate breeds opposing pressure systems creating more frequent and powerful storms, increasing the rate and severity of icing throughout the arctic (Arctic Council, 2009). As ice accumulates and the overall mass increases, the ship is forced to sit lower in the water resulting in an increase of sea spray from ocean waves as the roll of the ship dips closer to the freezing water (Shellard, 1974). The additional weight increases its center of mass, reducing its stability and increases the likelihood of capsizing risking the lives of all onboard. Smaller explorative, fishing vessels and trawlers don't have the protection of larger vessels and offshore structures as the ice reduces their already limited freeboard and increases the likelihood of sinking.

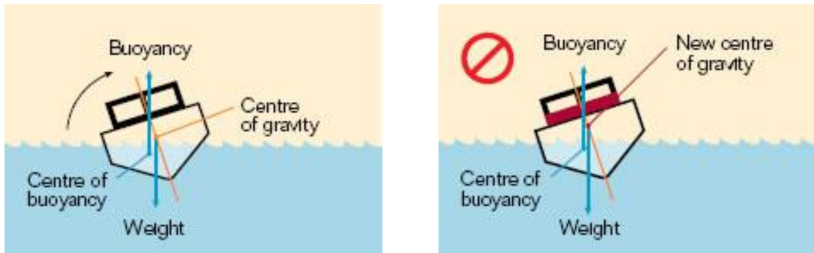

Figure 1.3 - Vessel Stability and Roll from (Government of Canada, 2015)

This was the reason for the loss of the Destination fishing vessel in 2017 as it ventured into tumultuous weather conditions and capsized due to rapid onboard ice accumulation (NTSB, 2017). Its capsizing highlights many of the problems affecting arctic vessels with limited ice removal procedures, rigorous working conditions, imposed timelines forcing difficult decisions and underdeveloped emergency protocols. There was no distress call made by the Destination leading investigators to believe that the vessel was quickly overwhelmed by ice accumulation (NTSB, 2017). The vessels emergency beacon transmitted an automatic distress signal at 0613 and just a minute later the automatic identification system linked to navigational satellites stopped transmitting (NTSB, 2017). It took hours for emergency support to arrive from the mainland with the coast guard relying on nearby vessels to risk their own safety by entering the same ocean conditions to assist the Destination (NTSB, 2017).

The size of a ship can have a big impact on onboard accretion as sea spray has a reduced effect on vessels and offshore structures with a freeboard greater than 50ft preventing the sea spray and crashing waves to reach its surface (Makkonen, 1984). Atmospheric icing becomes a larger concern for tall stationary structures as the ice adheres to antennas, masts and structural beams leading to instability and safety concerns for those working on its surface (Ryerson, 2011). The extended exposure to the atmosphere has led to multiple reports of up to 120mm of atmospheric icing and when combined with sea spray has seen up to 1000mm of ice accumulation (Wold, 2014).

Figure 1.4 - Ocean Superstructure (Ryerson, 2011)

Larger vessels offer more protection from marine icing as their size permits greater amounts of accumulation however if not properly managed the structural integrity can worsen creating issues for the crew onboard. The combination of freezing temperatures and onboard ice coverage on a rolling ship makes even the simplest tasks dangerous. The arctic can challenge ship operators as they navigate the heavy sea ice while managing onboard icing with incomplete navigational charts and an underdeveloped infrastructure (Samrat Ghosh, 2015). These ships are at a greater risk of collisions with an always shifting ice landscape resulting in hull damage or potential grounding. In the last decade reports of groundings in the arctic have increased considerably as ships continue to battle the accumulation while navigating the evolving landscape (Struzik, 2018). It is crucial that the crew and ship operators work diligently to predict and manage onboard ice accretion and avoid structural deterioration. Modern vessels can better prepare themselves to manage these risks by analyzing the source of past icing incidents and studying the various elements that influence ice accretion.

1.2 Problem Discussion

The Marine Icing Group led by Dr. Yuri Muzychka is comprised of several academics studying the hazards attributed with arctic exploration. Their research hopes to provide insight into managing the safety of those at sea by developing new technologies to better predict icing and finding the most effective methods of managing accretion.

This paper will focus on studying how ice accumulates on the exposed stairways of shipping vessels and gain better understanding of which design factors are most effective to manage ice accretion and ease its removal.

Chapter 2 Governing the Arctic

2.1 Introduction

For centuries the arctic has been considered a neutral zone with many countries using the space for exploration, colonization and trading purposes (King, n.d). It wasn't until the 17th century that the northern nations bordering the arctic coordinated to create the "Freedom of the Seas" doctrine, giving jurisdiction to their immediate shorelines leaving the rest of the arctic "free to all and belonging to none" (United Nations, n.d). This was before the world recognized the economic and strategic potential within the arctic. In the 19th century they each began withdrawing from the agreement in order to claim the rights to the resources along their continental shelves. In 1982, the United Nations signed "The Law of the Sea" giving each country the rights to any resources up to 200 nautical miles from their shoreline (King, n.d).

In the last few decades the arctic ice coverage has slowly been fading offering the fishing and shipping industries access to regions previously too dangerous to navigate. Additionally, the energy sector sees massive arctic potential as an estimated 17% of the worlds oil supply and 33% of its natural gas resources are trapped within the arctic (Gautier, 2009). In 2012, the Norwegian Prime Minister awarded 26 production licenses to multiple oil companies for offshore oil areas in the Norwegian and Barents Sea (Schiermeier, 2012). With a growing global population expected to reach 9.8 Billion by the year 2050 (United Nations, 2017) there comes the need for new and expansive energy sources. Even though there has been great progress in the way of renewable energies, the oil and gas industries continue to play a large role in supplying the worlds demand. Arctic activity is on the rise and will continue to grow as the ice coverage disappears requiring new research to build safe regulations and shipping practices. The Arctic Council is the leading international body for overseeing modern day activity in the arctic. Comprised of Canada, Denmark, Finland, Iceland, Norway, Russia, Sweden and the United States, the council focuses on issues of environmental protection and sustainable development for the arctic states, the indigenous people and all other life in the arctic (Young, 2000).

While most research recognizes the impact marine icing has had throughout history they all cite an absence of data and documentation (Minsk, 1977) (Hay, 1956). It was with the loss of the RMS Titanic off the coast of Newfoundland in 1912 which sparked the creation of the International Convention for the Safety of Life at Sea (SOLAS) who to this day commit to adapt and improve the standard for shipping safety (Caddell, 2010). Marine icing became a central issue during the second world war as transport ships with supplies for the allied forces tried to navigate the northern oceans (Navy, 1988). These vessels experienced extremely cold temperatures and icing resulting in the loss of many lives and ships, in one particular mission only 11 of the 33 vessels made it to its destination (Navy, 1988). It wasn't until 1955 with the loss of two British trawlers, Lorella and Roderigo, that significant research into icing began (Minsk, 1977). Both ships were lost within 5 miles of each other on the same day prompting what is recognized as the beginning of modern marine icing research. With Hay (1956) confirming that both sea spray and atmospheric icing were the main contributors to their loss, the British Shipbuilding Association opened the first climate controlled test chamber to perform experimental tests on scaled down trawlers (Shellard, 1974). The United Nations reacted by instructing the International Maritime Organization (IMO) to expand on SOLAS to include international safety regulations for the growing shipping industry (IMO, 2014). In response to the growing interest in the Arctic the IMO adopted the Polar Code which covers " the full range of design, construction, equipment, operational, training, search and rescue and environmental protection matters relevant to ships operating in the inhospitable waters surrounding the two poles" (IMO, 2019). The Arctic Council recognizes the standards set by the International Maritime Organization having implemented the Polar Code within their respective countries.

2.2 American Bureau of Shipping

While there are a number of organizations operating today with the intention of better understanding the arctic, the American Bureau of Shipping (ABS) has a long history developing safety and operational standards for the shipping industry. Founded in 1862, ABS recognized the need for those working on ships to meet some standard prior to heading out to navigate the oceans. They required shipmasters to obtain certification to demonstrate awareness and competency in order to build a more safe and responsible landscape (Joe Evangelista, 2013). They have evolved into a vessel classification society working hard to improve on the technical and operational regulations that govern the industry as the worlds rapidly changing climate produces both new opportunities and new challenges. They have published the “Guide for Vessels Operating in Low Temperature Environments” which denotes industry accepted standards for “vessels designed, intended and operated in low temperature environments” (Shipping, 2015). This document assigns a three-level classification to any vessel travelling through sub-zero environment with each class permitting access to different polar regions. They continuously update their regulations to better the industry while working to protect the vessel, the ocean environment and most importantly the crew onboard. The American Bureau of Shipping is just one example of the many research organizations studying the arctic for academic, environmental, and industrial purposes. Each attempting to better understand the changing climate and make reasoned decisions for the development of the arctic without compromising the safety of those working within.

2.3 Changing Climate

Trading in the 15th century was limited to the southern oceans, although northern countries were exploring the arctic as an alternative to avoid piracy and difficult inland routes (Samrat Ghosh, 2015). John Cabot initially conceived of the Northern Sea Route in 1497 on a failed arctic expedition hoping to find a more direct trading route with the west as shown in Figure 2.1. Due to a lack of global awareness, limited technology and heavy sea ice their ship instead inadvertently landed in North America (Arctic Council, 2009).

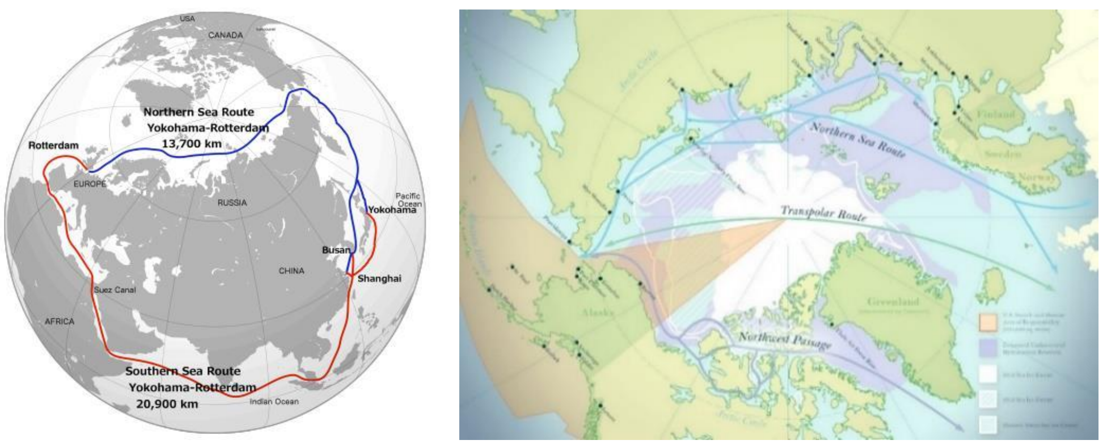

Figure 2.1 - Arctic Shipping Routes taken from (Samrat Ghosh, 2015)

European explorers continued to navigate the oceans looking for new land and opportunity with each settlement relying solely on shipping services in order to trade resources with the “Old World” (Heaver, 2006). Today the two most common shipping routes through the arctic are the Northern Sea Route (NSR) which follows the Russian shoreline and the North West Passage (NWP) remaining close to the northern territories of Canada. A third route known as the Transpolar Sea Route does provide a direct route through the arctic but the presence of year-round ice currently prevents any vessel from passing through (Samrat Ghosh, 2015). For centuries human curiosity and global expansion pushed north in the pursuit of knowledge but it wasn't until 1906 that the first vessel managed to fully traverse the NWP requiring three years and an escorting icebreaker to guide them through the thick ice (Arctic Council, 2009). Young (2000) estimates that only 50 vessels managed to duplicate that voyage by the year 2000 citing the heavy sea ice and high cost of necessary icebreakers as the main deterrents. The arctic ice coverage naturally cycles with the changing seasons as shown in Figure 2.2, where the warmer summer months melts the ice before reforming through the winter. This can effect activity as the arctic sees a 36% reduction in traffic during winter months as the thick ice and freezing temperatures discourages ships from entering.

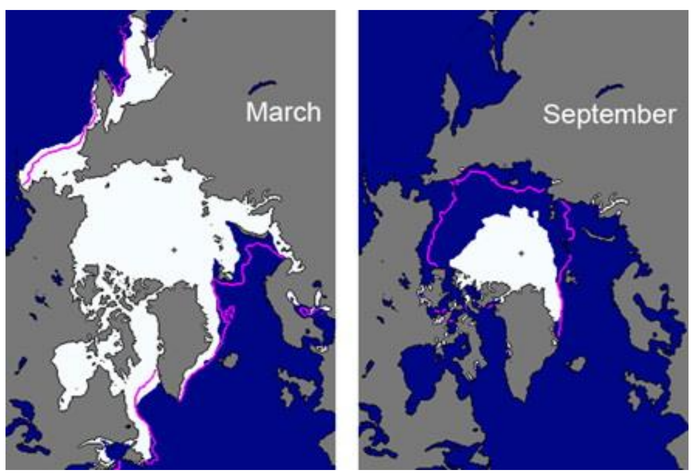

Figure 2.2 - Polar Ice Coverage from (Donald K. Perovich, 2008)

Over the last few decades the arctic ice coverage has been receding as demonstrated in Figure 2.2 in which the purple contour compares the median average ice coverage from 1979 - 2000 with that of 2012. This trend is only going to continue as global warming has caused the average arctic temperature to double since 1980 (Samrat Ghosh, 2015). While this does raise environmental concerns, an underlying upside is that it does create appealing new routes for commercial shipping as research predicts a 50% reduction in transit time (Samrat Ghosh, 2015). Not only does this reduce expense and risk of misfortune but it effectively cuts their emissions rates in half as well. With growing global interest in the arctic and ongoing technological advancements modern vessels are evolving to better manage the landscape. The cost to traverse the arctic is decreasing as new ships are designed with ice hardened hulls capable of breaking through 2.5m thick ice, eliminating the need for an escorting icebreaker. In 2017, the Eduard Atoll became the first ship to complete an unescorted trip through the arctic winter (gCaptain, 2018). A similar vessel arrived at its destination a full week faster than the route previously taken through the Southern Sea Route (gCaptain, 2018).

Figure 2.3 - The Eduard Atoll Navigating the Arctic from (Schuler, 2018)

Arctic shipping is on the rise as these technological advancements and warming global temperatures permit longer and deeper access to the known resources and reduced shipping times. This will inevitably increase the rate of marine icing incidents as the arctic conditions continue to breed ice accumulation. The photographs taken from the Eduard Atoll's arctic expedition shown in Figure 2.3 show proof of the continuing threat of icing in 2017. These photos highlight the need for continued research to improve the standards and safety practices with the growing arctic interest.

2.4 Safety Concerns on Arctic Waters

The majority of marine icing incidents occur in the oceans and seas surrounding the arctic with shipping activity has remained near the shorelines to avoid isolation and the heavy polar ice (Struzik, 2018).

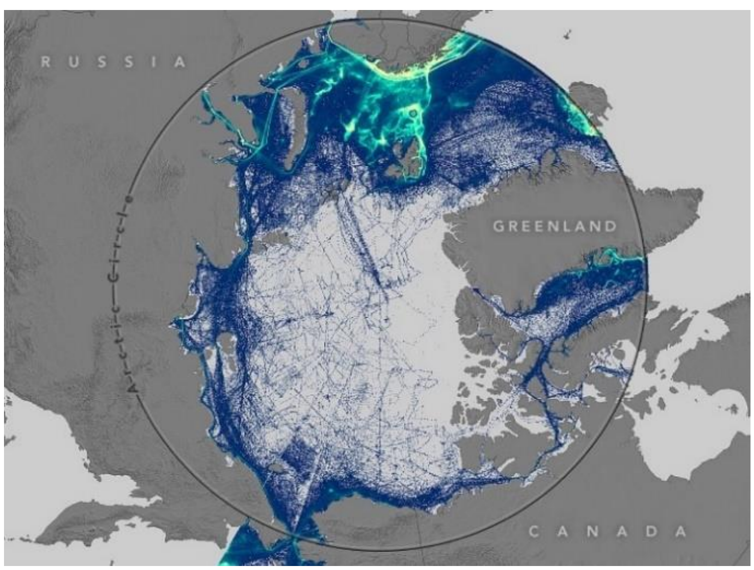

Figure 2.4 - Arctic Activity from (gCaptain, 2018)

The distribution of arctic ships between 2009 and 2016 can be seen in Figure 2.4 with blue dot representing a single ship. High traffic areas are shown with a brighter blue whereas the individual blue dots represent the lesser travelled routes. Although the concentration of ships noticeably decreases as you move in towards the north, research has shown the mean of arctic activity has shifted 300 miles further offshore (gCaptain, 2018). While this does create opportunity with shorter shipping routes and access to previously unreachable resources it also alienates vessels from emergency services and mainland support. In studying the geography of icing incidents from the 1970s, two independent researchers found that over a third of all recorded incidents occurred in the Barents and Norwegian Sea as shown in Table 2-1 (Efimov, 2012). It is important to note that the high traffic areas shown in Figure 2.4 are also those who have the most recorded incidents.

Table 2-1 - Icing Incidents by Region from Panov (1976) Vasileva (1971)

Region	**Panov (1976)**	**Vasileva (1971)**
Barents and Norwegian	34.5%	38.6%
Bering Sea	25.5%	25.2%
Sea of Okhotsk	18.0%	19.3%
Western Pacific Ocean	10.5%	8.0%
Sea of Japan	8.1%	6.2%
Baltic Sea	2.4%	1.9%
Black and Azov Seas	1.0%	0.8%

Even though the arctic is experiencing the effects of global warming more than any other region on earth (Arctic & Global Warming, 2020), the region is still prone to dangerous icing conditions. The receding ice coverage and warming temperatures have been linked to more frequent and erratic weather systems making it difficult to forecast sea conditions and predict icing potential (IMO, 2019). Within the first five years of a study done by the International Maritime Organization they found that of 407 reports, 25% of vessels in the United Kingdom experienced ice accumulation equal to or exceeding the amount deemed allowable by the IMO, with 8 cases exceeding the allowable limit by 100% or more. Reports submitted in 1970 by the USSR and Republic of Germany, the probability of severe icing was found to be as high as 76% and 80% respectively (Shellard, 1974). Marine icing threatens each type of arctic vessel differently as smaller fishing vessels are more easily overtaken than large shipping carriers. A study showed that in the early 1970s workers in the commercial fishing industry were 20 times more likely to experience a fatal injury than any mainland industry, increasing to 30 for those working as north as Alaska (Jensen, 2000). In the last 80 years, 80% of the vessels lost due to icing were less than 100m in length (Efimov, 2012). It has been reported that the likelihood of capsizing increases with a weight displacement of just 15% (Shellard, 1974) which can accumulate rapidly for smaller ships. Once icing initiates these ships have very little time to react and can be overwhelmed before assistance can arrive. In one case emergency services arrived just 20 minutes after receiving the distress call to find the ship had already sank and its crew lost at sea (Dotter, 2002).

Winter shipping has especially challenged vessels as the freezing temperatures and harsh winds increase the severity and reach of marine icing. The summer months provide some relief from icing as the warmer air and sea temperatures won't result in onboard accretion. In an analysis of icing incidents in the Far East Russian Sea, Efimov (2012) observed a drastic increase in severe icing incidents during the winter months as demonstrated in Figure 2.5.

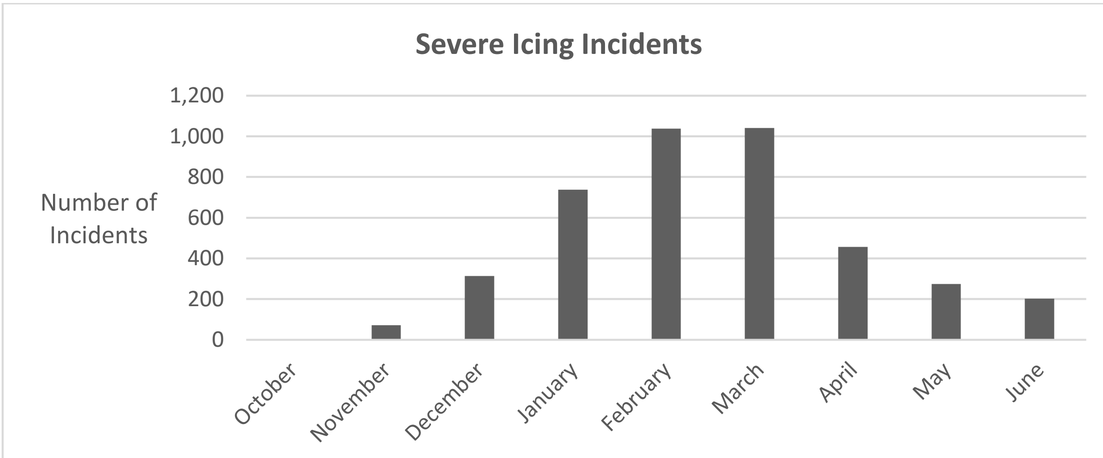

Figure 2.5 - Severe arctic icing incidents by month

As global warming creates a more accessible arctic with longer shipping seasons smaller trawlers are going to expand in search of new opportunities. Larger shipping carriers are used for extended expeditions that push further into the arctic as their size offers protection from the polar ice and onboard ice accumulation. These ships tend to have longer shipping seasons that carry into the winter, they can spend weeks at sea leaving them exposed to prolonged onboard icing which can quickly deteriorate the vessels integrity if not properly managed. The ice can impede communication and navigation equipment making it difficult to determine the proper course or communicate with emergency services and nearby vessels if assistance is needed. The crew must work diligently to manage the ice as it can quickly blanket the decking and important onboard equipment. This is especially dangerous due to the increased potential for loss of life as these vessels are commissioned with a larger capacity for personnel. In 2011, an oil rig capsized in arctic Russian waters as its structural components and onboard decking became layered in a thick ice taking the lives of the 37 onboard (Schiermeier, 2012). The forecastle and decking are most compromised to icing due to their exposure to the elements and sea spray (Shellard, 1974). This subjects the crew to dangerous working conditions as they attempt to manage the accumulated ice in freezing temperatures which can lead to frostbite, exhaustion and personal injury. Slips and falls account for 25% of all injuries at sea making onboard ice prevention crucial to onboard safety (Jensen, 2000). While the likelihood of capsizing due to onboard ice accretion is lowered, their lack of maneuverability in remote arctic water puts them at risk of ice collision and groundings. In 2018, an arctic carrier ran aground in the arctic with 120 passengers but fortunately a nearby vessel managed to rescue those onboard (Struzik, 2018). With less than 10% of the arctic properly charted, the lack of infrastructure leaves arctic vessels and those on board more vulnerable and inaccessible to emergency response (Struzik, 2018).

2.5 Loss of the Destination Fishing Vessel

In February of 2017 the Destination fishing vessel was crossing the Bering Sea carrying over 200 crab pots when it was overcome by rapid onboard ice accumulation and capsized claiming all of those onboard (Marex, 2018). The weather forecast predicted strong winds with high waves and warnings of heavy freezing spray along the Destination’s trajectory as documented in Table 2-2 convincing similar vessels to avoid the region that day (NTSB, 2017). The captain had 32 years of arctic shipping experience and with full knowledge of the forecast yet decided the vessel and its crew were well equipped to safely make the journey. However, within minutes of leaving the shelter of St. Georges Island, the Destination drastically changed its heading in what is believed to be an attempt to manage the rapid onboard ice accretion.

Table 2-2 - Weather predictions for surrounding zones at time of Destination incident taken from (NTSB, 2017)

	Zone 1	**Zone 2**	**Zone 3**
Winds	North-to-northeast at 25-35 knots; gale warnings	Northeast at 15-25 knots, increasing to 30 knots by morning	Northeast at 15 knots, increasing to 30 knots; small craft advisory through overnight hours
Seas	7-13 feet	7-12 feet	7 feet, increasing to 9 feet
Icing	Heavy freezing spray warning for evening and overnight hours	Heavy freezing spray warning through overnight hours	Heavy freezing spray warning

Reports from other vessels in the area at the same time provide additional details giving some indication to the hazards the Destination may have faced that morning. The “Clipper Surprise” had accrued 4in of ice before deciding to remain in the shelter of the island whereas the “Polar Sea” stopped four separate times to remove the excessive ice buildup with the crew ranking the severity of the icing they experienced as an 8 out of 10 (NTSB, 2017). Even though the two were at one point only 37 miles apart, the Sandra Five managed to make it to port safely. Figure 2.6 shows the seriousness of the ice accumulation experienced that day. Investigators believe that the exposed surface area of 200 crab pots onboard the "Destination" had been a significant factor in rapid ice adhesion and weight increase leading to vessel instability (NTSB, 2017). A research group at Memorial University performed an in-depth analysis in which they estimate that the ship had experienced an additional 92.4 and 154.0 metric tonnes of ice accretion leading to instability and capsize (NTSB, 2017). Based on their models and the weather forecast for that day they estimate that in just 15 minutes the vessel would have accrued 2.7 metric tonnes of ice which could explain the rapid deterioration and absence of distress call as the crew scrambled to mitigate the inevitable disaster (NTSB, 2017).

Figure 2.6 - Ice Accumulation on the Sandra Five fishing trawler taken from (Marex, 2018)

The growing push into the arctic is only going to amplify these concerns as even more shipping and fishing vessels venture further north and oil corporations expand their reach. In 2011, the number of commercial vessels traversing the arctic grew from 4 to 34, to 46 in 2012 and 72 in 2013 (Samrat Ghosh, 2015). This increase in arctic activity will bring a large influx of new workers with inexperience to the hazards of marine icing as workers under the age of 20 and seasoned workers over 50 account for 40% of all reported accidents. Working at sea is arduous with long hours, lack of sleep resulting in physical and mental exhaustion which is a dangerous when coupled with corporate pressure to meet quotas and deadlines (NTSB, 2017). Human errors, technical and mechanical failure, and environmental factors all play an underlying role in shipping accidents. It is essential that further research be done to better understand how to better manage the ice accretion onboard the ships sailing in the arctic waters.

Chapter 3 Properties of Icing

3.1 Introduction

Marine icing is not limited to the artic and can affect shipping operations in any body of water so long as certain meteorological conditions are met (Samuelsen, 2015). As the ship pushes forward the rolling waves impact the hull breaking it apart resulting in a cloud of tiny sea spray droplets which falls to the ships surface. The wind propels that spray to cover more of the ships surface with stronger winds further perpetuating icing with larger waves, more rolling and greater sea spray coverage (Shellard, 1974).

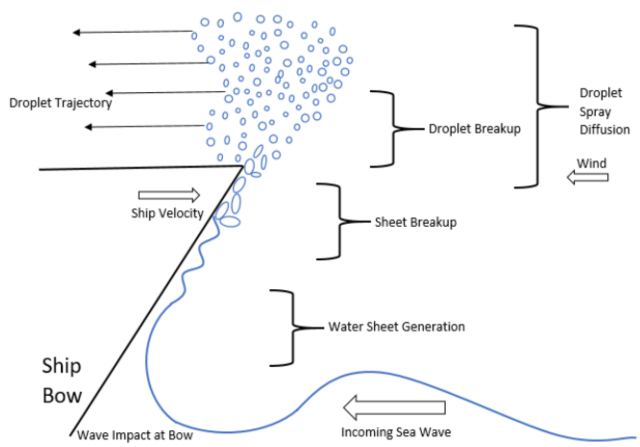

Figure 3.1- Wave Break Up Diagram

The wave break-up generates water droplets of varying size with the smaller drops reaching further while larger droplets fall more immediately (Dehghanisanij, 2017). With enough force the wind can pull droplets off the crest of neighbouring waves to increase onboard wetting although this only affects the smaller vessels with shorter freeboards (Dehghanisanij, 2017). For these smaller vessels the pitching and rolling motions experienced on board further exposes the deck to the wave spray. As the ice accumulates the additional weight raises its center of gravity resulting in a more drastic roll enabling the effects of marine icing (Shellard, 1974). The formation and properties of the accumulated ice depends on the environment in which the vessel is found and the source of water. While sea spray comes from the surrounding ocean, fog, rain, snow, and ice pellets are all examples of freshwater precipitation relying on different meteorological properties in their creation. Marine icing is the amalgamation of each type which together decreases vessel stability, interferes with mechanical equipment and creates dangerous working conditions leaving the ship and its crew vulnerable (Ryerson, 2011). Ryerson generated an onboard safety matrix shown in Figure 3.2, ranking the areas of most concern with the various forms of icing. A vessels stability and integrity were both assigned the highest safety rating of 10 since their failure can be the most catastrophic leading to the loss of the vessel and its crew. This is followed by essential mechanical and emergency equipment which are crucial to accident prevention and safe onboard operations. Sea spray is ranked as the most concerning form of marine icing as it is the leading cause of ice accumulation and consequentially loss of vessel at sea. The constant flooding from wave generated spray and propulsion from the wind leads to heavy ice accumulation affecting every aspect of a vessel's operation. The salt within the sea spray creates pockets of trapped oxygen resulting in a thick spongy white ice. This not only reduces its hardness but forces the brine downward increasing the salinity near the interface reducing its adhesion with the surface (Shellard, 1974).

Hazard rating	Safety rating	Spray ice 10	Snow 8	Glaze 7	Rime 6	Frost 4	Sleet 1
Stability	10	100	80	70	60	40	10
Integrity	10	100	80	70	60	40	10
Fire and rescue	9	90	72	63	54	36	9
Communications	8	80	64	56	48	32	8
Helicopter pad	8	80	64	56	48	32	8
Air vents	8	80	64	56	48	32	8
Flare boom	7	70	56	49	42	28	7
Handles, valves	6	60	48	42	36	24	6
Windows	5	50	40	35	30	20	5
Cranes	4	40	32	28	24	16	4
Winches	4	40	32	28	24	16	4
Stairs	4	40	32	28	24	16	4
Decks	3	30	24	21	18	12	3
Railings	3	30	24	21	18	12	3
Hatches	2	20	16	14	12	8	1
Cellar deck	1	10	8	7	6	4	1
Moon pool	1	10	8	7	6	4	1

Figure 3.2 - Ranking of Icing Threats Onboard Vessels from (Ryerson, 2011)

Even though snowfall doesn't directly lead to icing its added weight can affect the vessels stability by reducing the ships freeboard, again increasing the exposure to sea spray which can then wet and harden the fallen snow. Additionally, the snow can drastically reduce visibility making it difficult to navigate the already ice infested arctic ocean. Some of the worst icing events have been recorded with storm-force winds and simultaneous snowfall, the resulting ice being very tenacious and difficult to remove (Hay, 1956). It focuses on horizontal surfaces but develops strong adhesion properties if wetted and can adhere to vertical surfaces before freezing. Snow can also damage onboard equipment, prevent valves from opening and impede access to equipment in the case of an emergency (Ryerson, 2011). Snowfall can last for days and even though the wind can help clear snow from the vessel it can also push into corners and stairways requiring immediate attention.

Figure 3.3 - Onboard Ice Accumulation from (United States Navy, 2017)

In below zero temperatures rainfall will quickly freeze to a ships horizontal surfaces, hardening into what is known as glaze ice. This ice coats pathways and stairs with a slick translucent ice creating a dangerous slipping hazard for the crew as it is hard to detect and difficult to remove due to its higher density (Makkonen, 1984). Glaze ice can make its way into the mechanics of onboard equipment, disabling cranes, valves and winches with its dense ice (Wold, 2014). Rime ice is also composed of freshwater yet is less dense and is formed when super cooled fog or cloud droplets get caught by the wind and swept across the ship adhering to vertical surfaces. This icing can freeze release mechanisms for lifeboats, coat communication equipment and create slippery decking increasing the risk and managing crew safety in emergency situations (Ryerson, 2011). Both glaze and rime are hazardous to tall stationary ocean structures where the proportion of ice increases with height, as does the ability to manage it. The Ernest Holt was a vessel operating in the 1950s which one researcher estimates had experienced atmospheric icing at a rate of 2.5 tons of ice per hour (Shellard, 1974). Those onboard must be prepared for all forms of icing as their vessels as fluctuating meteorological conditions can quickly change bringing each form of ice (Overland, 1990).

3.2 Variables in Marine Icing

The key variables in determining icing severity are wind speed, air and sea temperature as well as the characteristics of the vessel and its velocity in relation to the wind (Overland, 1990). Sailing into the wind increases the frequency and force at which the waves crash into the hull resulting in more onboard flooding and icing. (Samuelsen, 2017) states that wind speed and wave height are the two leading causes of icing severity and that with enough force the wind can pull droplets from the crest of nearby waves to further perpetuate icing. A side wind can be especially dangerous as ocean spray accumulates to one side producing a dangerous imbalance that only gets worse as the ice accumulates. Panov and Moltanov discovered the relationship between intensity of sea spray and the impact of angle and size of incoming waves (Dehghanisanij, 2017). The intensity of the sea spray appears to be greatest with smaller waves hitting the hull of the ship at 40° from its trajectory as shown in Figure 3.4. As the wave height increases, the angle that produces the largest spray intensity shifts closer to the ships forward hull (Overland, 1990).

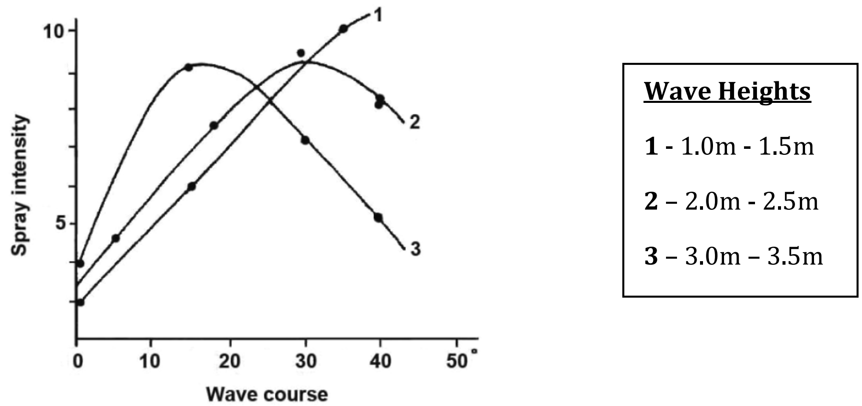

Figure 3.4 - Severity of sea spray in relation to angle of impact and Wave height from (Overland, 1990)

While the wind is certainly the driving force of sea spray, the severity and rate of icing can be amplified by several factors. The ambient temperature surrounding a ship is one of the main forecasters of marine icing as both sea spray and atmospheric icing require below zero temperatures in order to freeze. The severity of icing has been shown to increase with both higher wind speeds and decreasing surrounding air temperatures (Shellard, 1974). Once the ambient temperature drops below -16°C the droplets from sea spray will rapidly cool and freeze prior to landing on the vessel and won't adhere to ships surface (Hay, 1956). This ice can still be concerning as it acts similar to snow yet creates a much more slippery surface. The upper and lower limits of icing can be seen in Figure 3.5 in which Lundqvist and Swada show the increase in icing severity with both air temperature and wind speed (Overland, 1990). The freezing points of both fresh (0°C) and salt water (-1.8°C) differ slightly due to the intrinsic salinity of seawater (Canadian Coast Guard, 2019). The temperature of the artic seawater can have an impact on the rate at which icing accumulates as shown in Figure 3.6. While the temperature of water ultimately determines whether it will transition into ice, it is the atmospheric temperature and wind acting together to create a heat sink further reducing its temperature and perpetuating the freezing process.

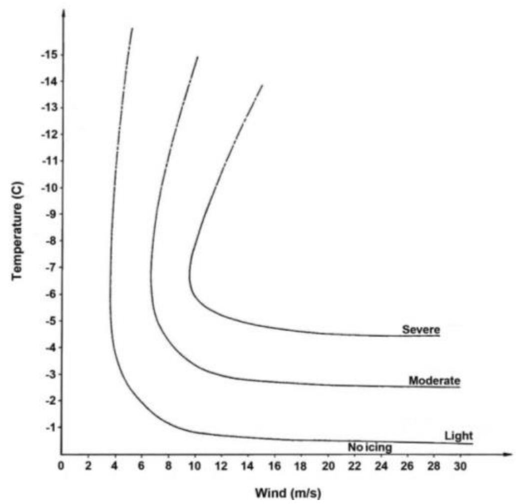

Figure 3.5 - Effect of Wind Speed and Air Temperature on Ice Accretion from (Overland, 1990)

There have been reports of icing with sea temperatures well above the freezing point of saltwater at +5° C with warmer water simply taking longer to cool before eventually freezing to the surface(Hay, 1956). These cases are mostly outliers acting during the winter transition as it is rare to have warm sea temperatures in a cold environment. With that said it is in these windows that vessels can be caught off-guard by unexpected icing, especially those which are smaller and less equipped to manage it.

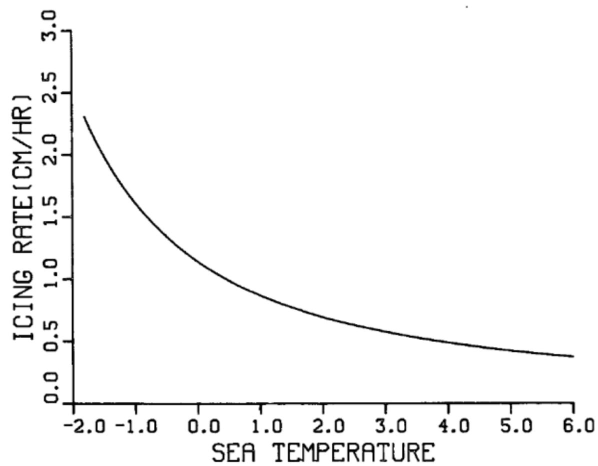

Figure 3.6 - Effect of Sea Temperature on Rate of Icing from (Overland, 1990)

The rate and severity of onboard ice accumulation depends on all these factors working together, creating unique environments that perpetuate icing. Using data from multiple icing events, Overland (1990) created an algorithm to predict the severity of icing using wind speed, air temperature and sea temperature.

As previously stated, the severity of icing worsens as the air temperature drops and the speed of wind relative to the ship's velocity increases. The visual representation of that algorithm is demonstrated at four different water temperatures in Figure 3.7 with the severity being defined as:

Light Icing – Less than 0.7cm of ice accumulated per hour

Medium Icing – Between 0.7cm to 2.0cm of ice accumulated per hour

Heavy Icing – Greater than 2.0cm/hr of ice accumulated per hour

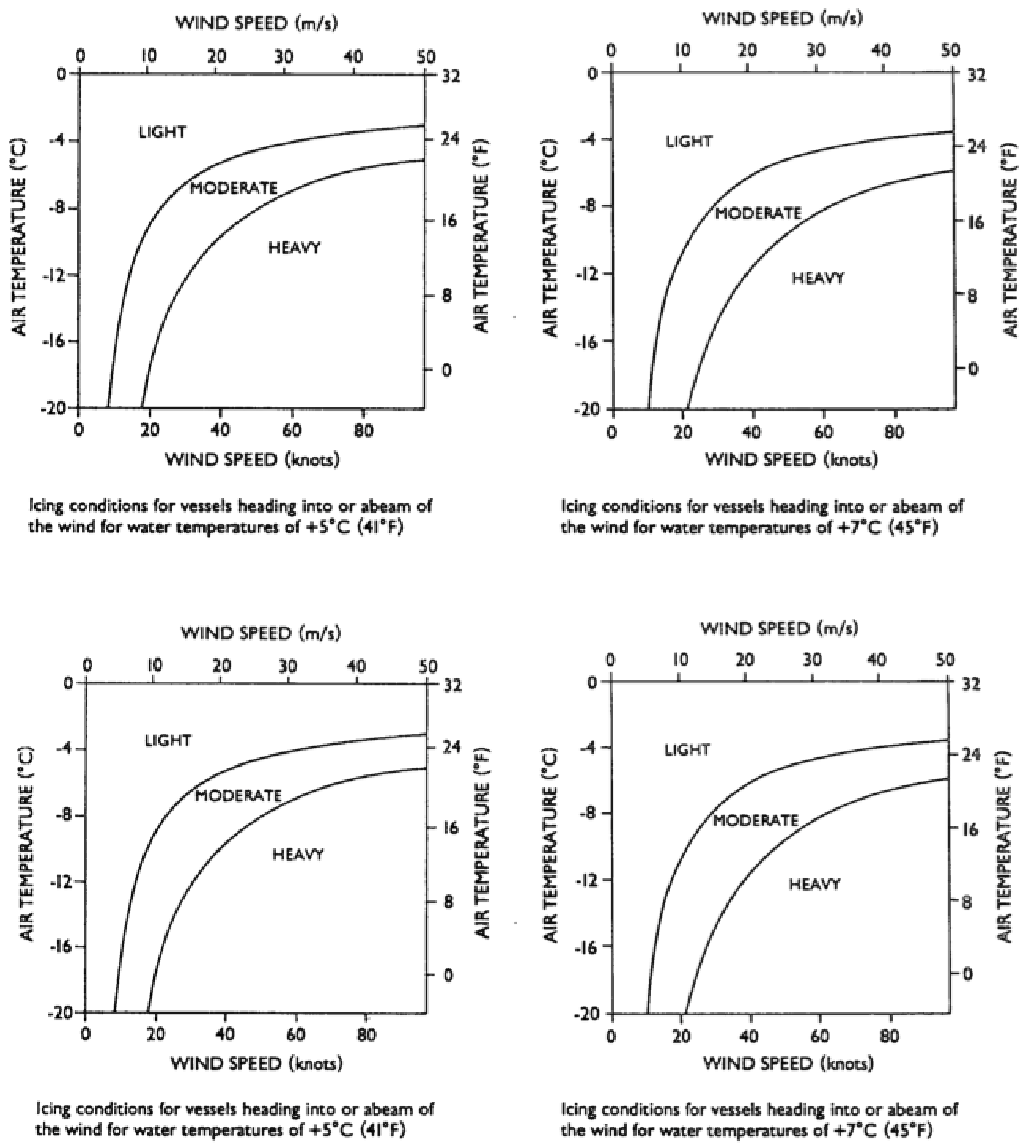

Figure 3.7 - Meteorological Effect on Icing Severity from (Overland, 1990)

3.3 Current Solutions

The American Bureau of Shipping's "Guide for Vessels Operating in Low Temperature Environments" assigns ships different classifications depending on how frequently they traverse low temperature environments (Brazil, 2013). De-icing is optional for ships which only occasional find themselves in arctic waters however all fire safety systems must be designed to remain fully active down to a certain temperature (Ryerson, 2011). If a ship frequently finds itself in low temperature environments solutions must be in place for stairways, open decking, gangways and all railings (Brazil, 2013). Ice accumulation is an inevitability and while there are methods to help minimize its growth many of them are limiting or far too expensive for practical use.

There are two methods of ice management, anti-icing technology delays the growth of ice whereas de-icing reduces the adhesion strength making it easier to remove any accumulated ice. The following solutions are the leading technologies adopted by shipping vessels operating today.

3.3.1. Chemicals and Coatings

There are up to 14 varying types of de-icing and anti-icing chemicals with varying properties for a wide range of purposes (Ryerson, 2011). They are commonly used in the aviation and highway shipping industries for ice prevention and removal. The chemicals can be in solid or liquid form and applied either before, during or after accretion to reduce adhesions strength or melt the accumulated ice (Wold, 2014). The goal is to find a suitable non-corrosive chemical which is effective in low temperature environments. The most promising chemical options are potassium acetate and propylene glycol which offer both minimal corrosion and low temperature effectiveness and could be useful in offshore operations (Wold, 2014). The biggest concern when it comes to chemical use onboard is the constant flooding from ocean waves pulling the chemicals into the sea polluting the oceans and affecting the surrounding wildlife. Additionally, the sea spray and waves can dilute the chemicals making them less effective and leaving a slick residue creating and even worse slipping hazard (Ryerson, 2011). While chemicals are regarded as effective, the high cost, reductive efficiency and environmental concerns are enough to discourage as potential solution (Ryerson, 2011).

3.3.2. Heat Tracing

Heat can be used to reduce or prevent ice buildup through directional venting of hot air or electrothermal heat tracing. The main issue with using heat to reduce or prevent ice accretion is the high cost in supplying the energy required to generate enough heat to counter the freezing arctic temperatures (Ryerson, 2011). Heat tracing is an attractive solution as it can be installed and left to remove ice on its own. The electrical coils can be built into the handrails, decking and mechanical equipment so that the heat can conduct through and melt the ice. Much of the heat is absorbed by the substrate between the elements and ice reducing its effectiveness especially in events of extreme icing. Placing the heating elements directly on the surface to make direct contact with the ice has been shown to reduce the adhesion of ice stuck to the ship, making it easier to remove. Intermittent pulse heating has been found to be anywhere from 20% to 50% more efficient but the same studied claimed that the amount of energy required to melt the entirety of ice accumulated is much too high (Brazil, 2013).

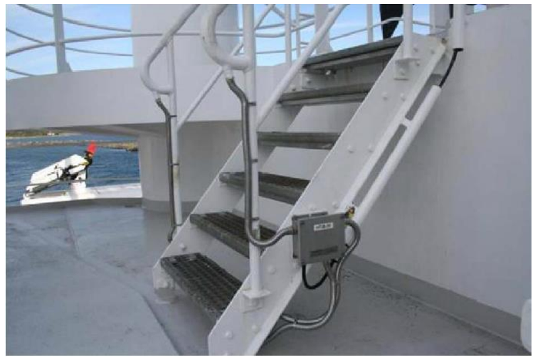

Figure 3.8 - Heat Trace installed on vessel stairs from (Brazil, 2013)

The vast ice infested shipping lanes create a lot of unpredictability in traversing the arctic making heat tracing unreliable. Its reliance on a power supply limits heat tracing as emergency situations in which the ship loses power or gets stuck as it will lose the ability to generate the heat required to remove the ice. Heat tracing while initially enticing has been shown to be too expensive and unreliable of a solution for many companies to opt into. Not only would it be costly to operate the electrothermal heat tracing, but to retrofit it into a ships structure would be a massive undertaking.

3.3.3. Adhesive Coatings

Adhesive coatings offer a cheaper alternative to chemicals without the environmental concerns and risks of corrosion which can degrade a ships structure (Brazil, 2013). They are easy to apply and can be used to reduce ice adhesion to the ships surface by coating equipment, decking and stairs. Most coatings are hydrophobic with a low surface energy holding liquid drops to the surface but while coatings can reduce adhesion, they haven't been shown to effectively reduce ice accumulation on board (Jing Chen, 2012). Additionally, a layer of the coating is removed with the ice as the cohesive forces of the coating are significantly less than the adhesive force with the ice (Ryerson, 2011). Coatings also have a finite lifespan requiring recursive application and the coating can become less effective if it becomes contaminated by another substance. Most coatings do not result in less ice accretion and Ryerson warns of using coatings on decking and stairs as they they can increase the slipping hazard for the crew when wetted (Ryerson, 2011).

While covering the surface of decking and stairs with an alternative substrate with lower adhesion properties may not result in less ice accretion it can present more promising adhesive properties. Hydrophobic surfaces have low wettability resulting in a greater contact angle resulting in less adhesion strength between the ice and its surface. Rubber is an example of a hydrophobic surface with optimistic adhesion for accumulated ice leading to easier removal and a greater coefficient of friction offering better traction for the crew than commonly used metallic alloys used on ships.

3.3.4. Mechanical De-Icing and Design

While there have been many advancements in ice prevention and removal, ship operators continue to depend on manual methods of removal as the most reliable and cost-effective solution to the problem (Ryerson, 2011). This solution requires the onboard personnel to be in good health in order to repeatedly swing heavy shovels, hammers or bats to break off accumulated ice. All of which creates dangerous working conditions as extreme weather conditions and slippery decking can lead to personal injury or falling overboard. The repeated impact on some mechanical equipment can lead to damage and although it is the most cost effective it can come at the expense of those onboard.

Figure 3.9 - Manual de-icing of accumulated ice from (Brazil, 2013)

Many vessels have been saved by mechanical de-icing, but a significant number have also been lost as it was their only remaining option. (Ryerson, 2011) believes that structural design is the most effective method for reducing ice hazards onboard. Certain design elements can be made to not only make it easier to remove ice but also limit the ice accumulation. Accumulation can be slowed by reducing surface area and small diameter objects which benefit ice growth as well as providing shelter for walkways and stairs preventing sea spray from reaching them (Ryerson, 2011). Unfortunately, many vessels are already designed to maximize their limited space and cannot afford to re-engineer their ships. When it comes to ice accumulation the modern-day solutions are either too expensive or ineffective for practical use forcing the ship operators and their crew to manually remove the ice putting them at risk of injury.

These experiments will focus on the exposed stairways of ships, examining the effects of tread design and slope on ice accumulation and ease of removal. While there have been advancements in new technologies to control ice accretion, the preferred method to remove ice from stairways and other onboard equipment is for a crewmember to physically hit the iced stairs with a large hammer. This continues to be the most reliable and cost-effective solution of removing ice once it has accrued. The hope is that this research can prevent further accidents and provide a safer work environment for the crew while providing insight for companies and operators to lead a more responsible workplace.

Chapter 4 Experimental Design

4.1 Introduction

A set of stairs were designed and built using the standards set by the American Bureau of Shipping in their “Guide for Vessels Operating in Low Temperature Environment”. The guide assigns an allowable range to specific design parameters from which the stairs must meet in order to operate at sea. Working within the allowable specifications creates experimental parameters to ultimately find the most appropriate design for reducing ice accumulation without making use of any additional technology or energy. Any set of stairs can be broken up into three sections each of which are exposed and shielded differently from the elements: the top stair, bottom stair and all those in between. A simple three step design allows for a scaled down experimental model while still permitting a full-scale analysis of each differently shielded step. As part of these experiments involve repeatedly striking the stairs with a large force, the frame was made of steel for its strength and durability.

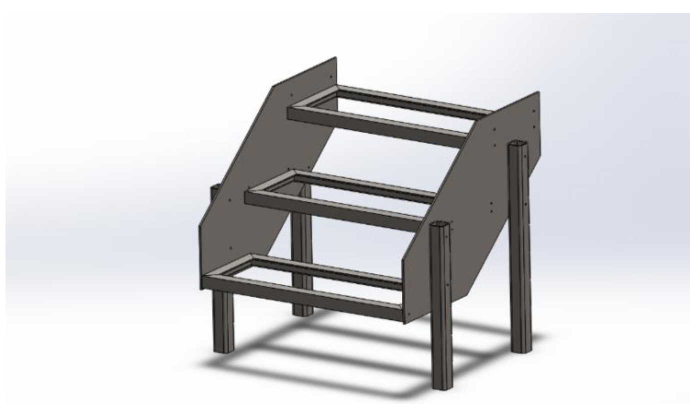

Figure 4.1 - CAD image of the frame for the experimental stair model

The frame of the stairs is made of two side panels with three angled frames which can accommodate each of the various tread designs. According to the standards set by the American Bureau of Shipping the vertical rise between each step could be no greater than 9in with a rate of inclination between 38° and 45°. The depth of each step was limited to 11in and there was to be an overhang of exactly 1in.

Table 4-1 - Design Requirements of Exposed Stairways from (Shipping, 2015)

Dimension	**Requirements**
Tread Depth	11 in
Rise	≤ 9 in
Step Overhang	1 in
Angle of Inclination	38-45 deg.

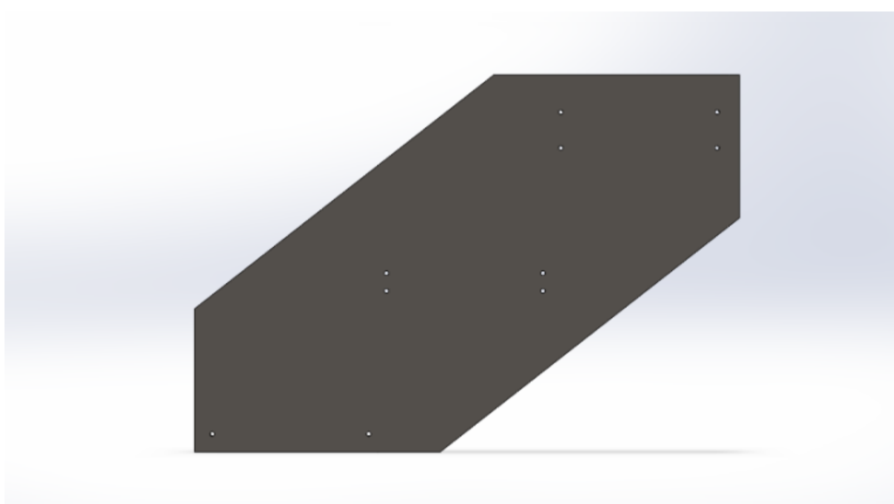

Figure 4.2 - CAD image of the side panel of experimental stair model

The side panels have two-hole configurations to hold the three steps allowing for two different rates of inclinations, both of which fit within the ABS regulations in Table 4-1. The goal was to differentiate the two as much as possible while still working within the design requirements set by ABS. This resulted in two rates of inclination as demonstrated in Figure 4.3 and Figure 4.4

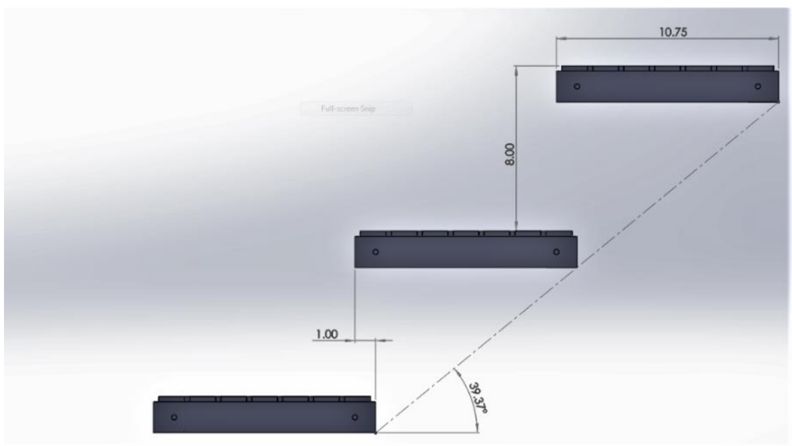

Figure 4.3 - First Rate of Inclination

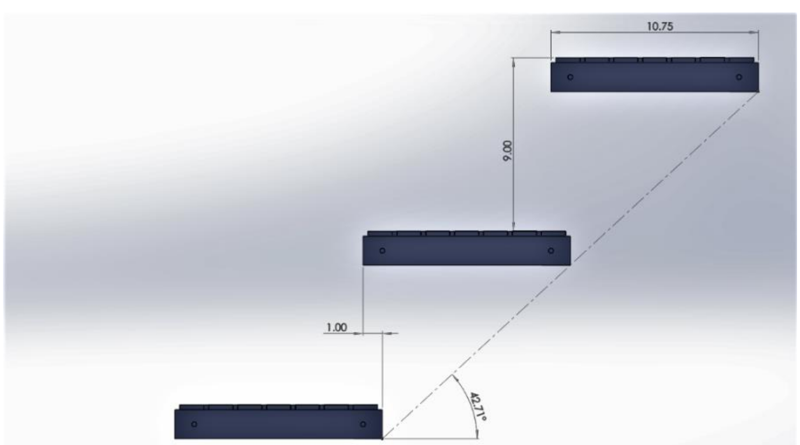

Figure 4.4 - Second Rate of Inclination

Four different tread designs were chosen based on common industrial practice, thermal properties and surface wettability. Open cell steps are frequently commissioned for shipping vessels as the limited surface area allows the sea spray to fall through its gaps while still providing enough support for the weight of the crewmembers. However, in the event of severe icing the open cells have been shown to rapidly bridge the gap between cells and ice over in the arctic (Ryerson, 2011). These open cell steps were made of aluminum and designed to sit inside the angled frames as seen in Figure 4.5.

Figure 4.5 - Open cell and aluminum diamond plated tread designs

The next design was an aluminum flat diamond plated tread design which allows for a direct comparison with the open cell to determine its effectiveness at reducing ice accumulation. Aluminum is hydrophilic with a high thermal conductivity which defines its ability to both repel water droplets and conduct heat. Steel plated steps were chosen as an alternate hydrophilic material with a substantially lower thermal conductivity as seen in Table 4-2 which compares the conductivities of the various tread designs.

Table 4-2 - Thermal Properties of Material from (Thermtest Inc, 2019)

	Thermal Conductivity	**Contact Angle**	**Wettability**
Rubber	0.14 W/mK	greater than 90°	Hydro**phobic**
Steel	50.8 W/mK	less than 90°	Hydro**philic**
Aluminum	236 W/mK	less than 90°	Hydro**philic**

Both the steel and aluminum are diamond plated with a thickness of 0.125in and fastened to the angled frame for testing. Their varying thermal conductivities will provide insight into its effect on ice accumulation and adhesion properties. The surfaces of both steel and aluminum are hydrophilic and attracts the water molecules to spread across its surface. Rubber has the opposite effect and repels water resulting in a higher contact angle between the droplet and its surface. The rubber matting was slightly thinner than the metal plates at 0.100in thick and was mounted to the frame of the stairs with the aluminum plate for additional support.

Figure 4.6 - Steel and Rubber Diamond Plated Step

4.2 Simulation of Arctic Conditions

Marine icing research has become a large focus at Memorial University as the province of Newfoundland has relied on the resources found at sea. This research will have a direct impact on numerous industries both at home and around the world. With three large climate-controlled research bays, Memorial University can study large scale arctic simulations and perform extensive ice related research. The largest of the rooms is 375 sqft which allows for additional test equipment to suit experimental needs as demonstrated in the test setup in Figure 4.7. Each of the rooms are connected by sliding insulated doors and windows for observation and can maintain temperatures as low as -30°C simulating the extreme conditions of the arctic.

Figure 4.7 - Cold Room Set up with Stairs

The cold room has a water spray system to simulated both saltwater sea spray and freshwater precipitation. The spray system is equipped with two nozzles to spray a cloud of water upwards into an air stream produced by an industrial sized fan to simulating ocean winds and propel the water spray forward. The model number of these nozzles is 1/8GG-316SS3 which indicates a 1/8 inlet connection, type GG nozzle head and 316SS representing stainless steel corrosion resistant material allowing for both fresh and saltwater testing. The water was pumped from an external reservoir at a discharge pressure of 90psi resulting in a conical spray cloud with an average droplet size of 792μm.

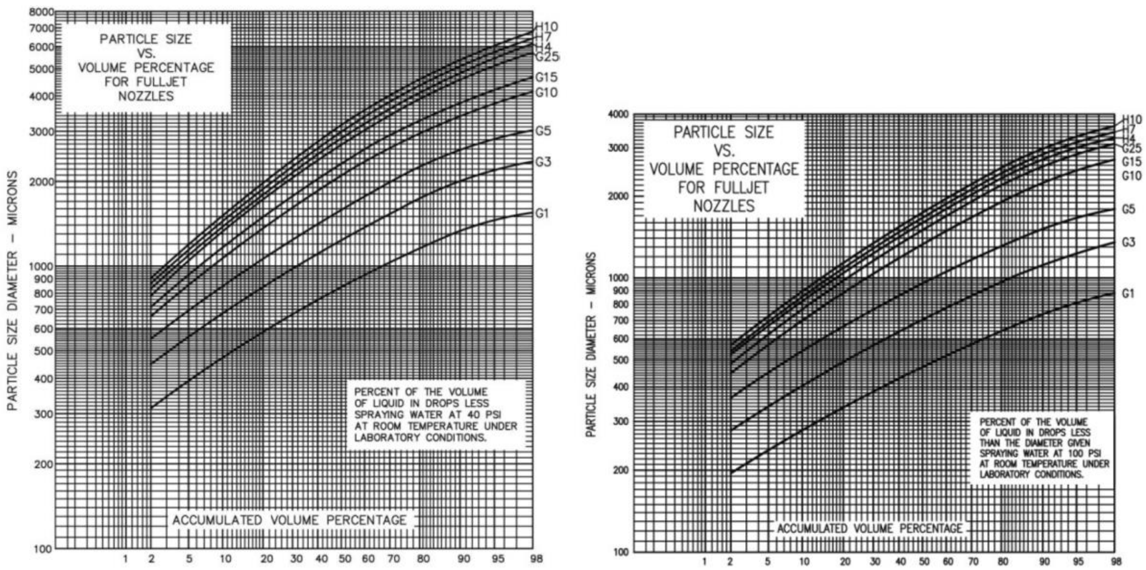

Figure 4.8 - Droplet Size Specification for 1/8GG-316SS3 at 40psi and 100psi

The two charts in Figure 4.8 Figure 4.8show the droplet size characteristics ($Dv_{0.5}$) for the two nozzles at 40psi and 100psi through which the following linear relationship was determined.

$$Dv_{0.5} = -9.1667P + 1616.7 \tag{1}$$

With a diameter of 93.98cm the fan was large enough to create airflow simulating ocean winds and propel the water spray forward. With a built-in variable frequency drive the fan can generate a wide range of wind speeds for experimental flexibility. In order to permit saltwater testing the fan and its housing were all coated in a corrosion resistant paint. All other fan specifications are shown in Figure 4.9 detailing expected performance and power requirements.

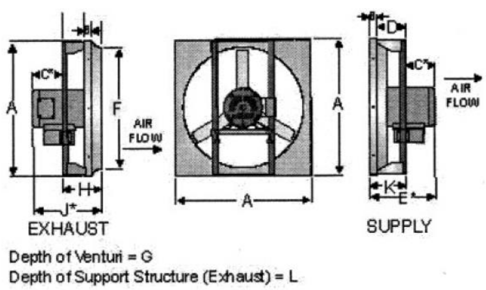

Dimensions (Inches)									
A	42	B	2	C	11	D	9	E	21
F	37	G	3	H	9	I		J	20
K	11	L	4	M		N		O	
P		Q		R		S		T	
U		V		W		X		Y	

Note: Accessories may effect dimensions shown.

Performance

Fan RPM	Flow (CFM)	SP (in W.G.)	Power (HP)	SE	ME	FPM (TS)	FPM (OV)
1160	16080	.475	3.317	36%	1.18	10933	2155

Altitude (Feet): 600 **Temperature (Centigrade):** 21 **Density (Lb/Ft3):** .073

DBA	SONE
81.2	40

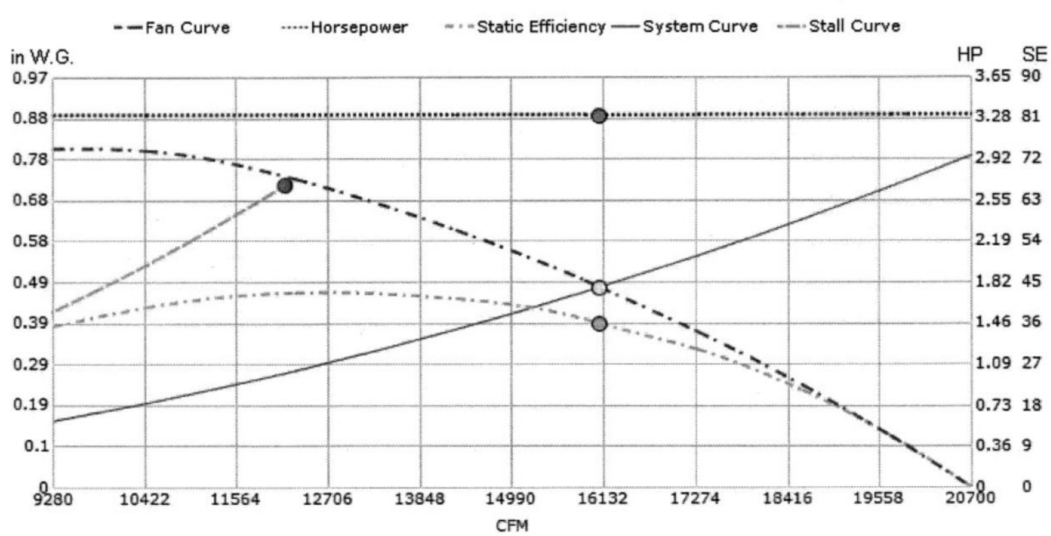

Figure 4.9 - Specifications of Wind Inducing Fan

A two-way digital solenoid was implemented with a digital timer to create a periodic spray within the cold room, simulating the crashing of sea waves. The cycle was set to spray water for 5 seconds with a 30 second delay. The specifications for both the pressure system can be seen in Table 4-3 showing the these tests work within their limits.

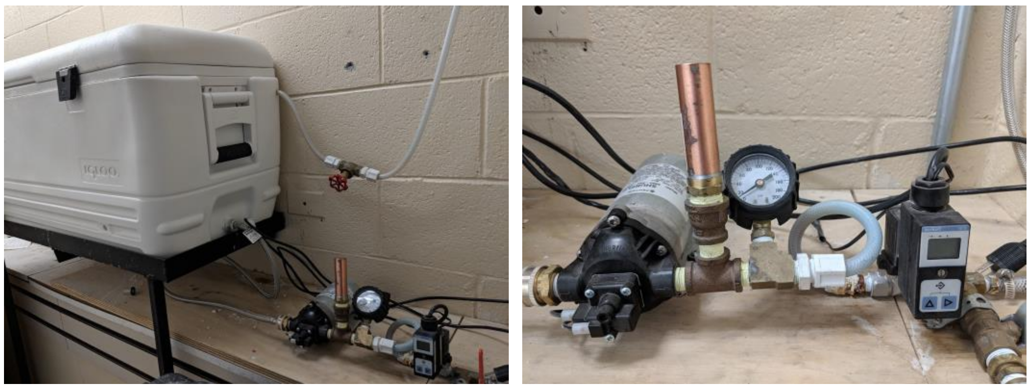

Figure 4.10 - Water Supply and Pump Setup

Table 4-3 - Specifications for Digital Solenoid and Timer

Instrument	Description
Burkert Zero Differential Pressure 2-Way Solenoid Valve	2/2-way valve, 6213 EV Series Solenoid valve, ¼” NPT Working Pressure: 0-145 PSI Cv: 4.2 Body: Stainless Steel, Seal Material: FKM Volt: 120-60
Burkert 1078-2 Series Digital Timer	Timing Range: 0.2 s to 9999 h, Continuous Switch Status: LED Supply: 110-230V/50 Four Switching Functions Mounting: DIN 43650 form A (standard coil plug)

In order to keep it from freezing, the water reservoir for these tests was kept outside of the cold room before being pumped through the spray system and into the test setup. The temperature of the water would begin to cool once it had entered the cold room and forced through the spray nozzles and diffused into droplets of various diameters. The droplets go through three phases of cooling as they are propelled through the air: liquid droplet cooling, droplet nucleation, and solid droplet cooling. The first phase happens almost immediately as the fan induced air flow forces the heat transfer process in the -18°C cold room. The time it takes for the droplet to reach its freezing point can be determined using a lumped sum analysis defined by Eq.2. It is important that the droplets be cooled prior to hitting the stairs as to best simulate the conditions at sea. The time it takes for droplets with an average diameter of 792μm to reach its freezing point can be seen in Figure 4.11, showing that even larger droplets of 1mm will have dropped to 0°C in under a second.

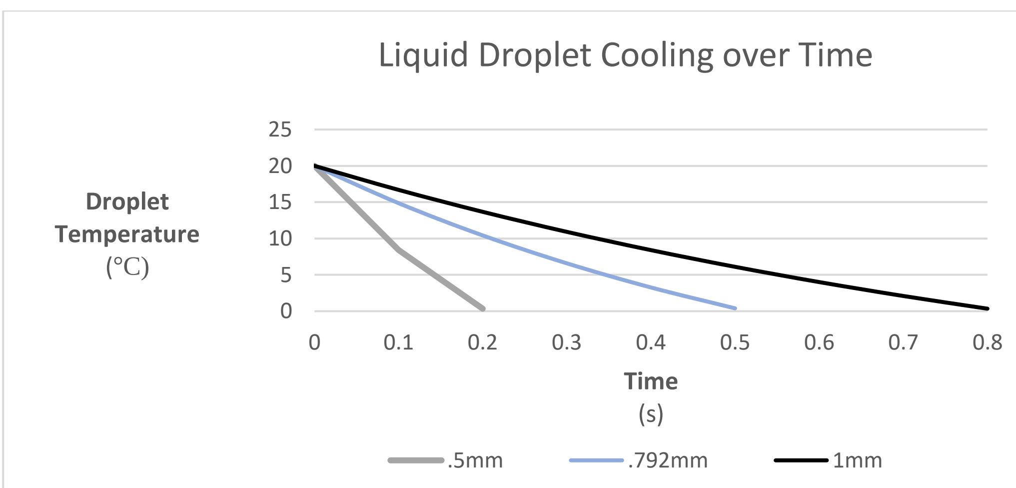

Figure 4.11 - Liquid Cooling Stage for various diameters

These results are based on a forced convection analysis using the induced air flow of 7.487 m/s in the -18°C cold room temperature. Complete calculations and fully defined workings can be found in Appendix F.

$$\frac{\phi(t)}{\phi_0} = \exp(-3Bi_r Fo_r) = \frac{T - T_\infty}{T_0 - T_\infty} \tag{2}$$

The droplets need to be cooled from room temperature prior to reaching the stairs in order to simulate the icing conditions experienced in the arctic. The distance between the fan, spray nozzles and stair model can be seen in Figure 4.12 , and with an air speed of 7.487m/s the droplets will have reached the model in under a second. This demonstrates that the droplets will indeed have cooled to the temperature of the water experience in marine icing reports by the time they reach the stair model.

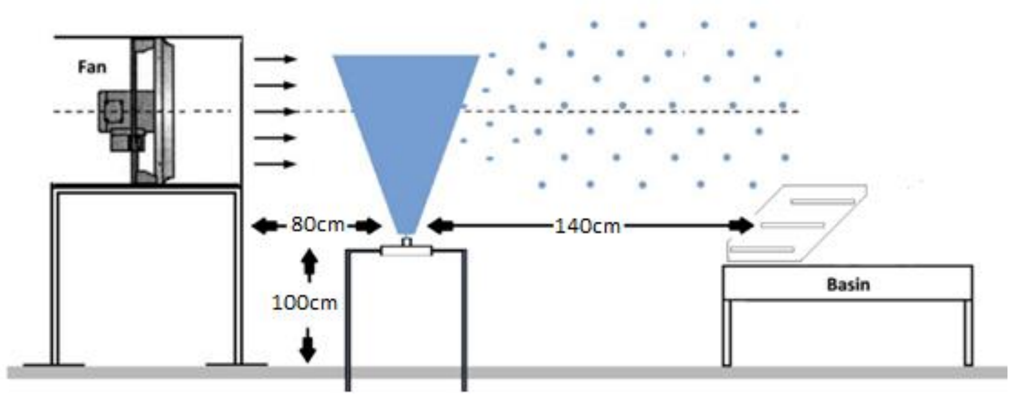

Figure 4.12 - Layout of Equipment in Cold Room

It is once the droplets have settled on the step that the droplets adhere to its surface and foster growth. The process of droplet nucleation is non-linear as the outer shell of each droplet will be the first to freeze before moving in towards the center. This phenomenon is demonstrated in Figure 4.13 in which the moving boundary creates a non-linear problem which can only be solved through computational analysis.

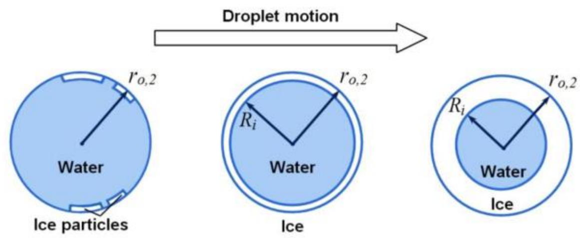

Figure 4.13 - Nucleation of a spherical water droplet from (A.R. Deghani-Sanij, 2019)

In a 2019 report, Deghani-Sanij studied the effects of droplet freezing and calculated the time it would take for droplets of varying salinities to go through all three phases to becoming fully crystallized (A.R. Deghani-Sanij S. M., 2019). The phase lengths for this research could be found by applying the cold room experimental conditions to his findings.

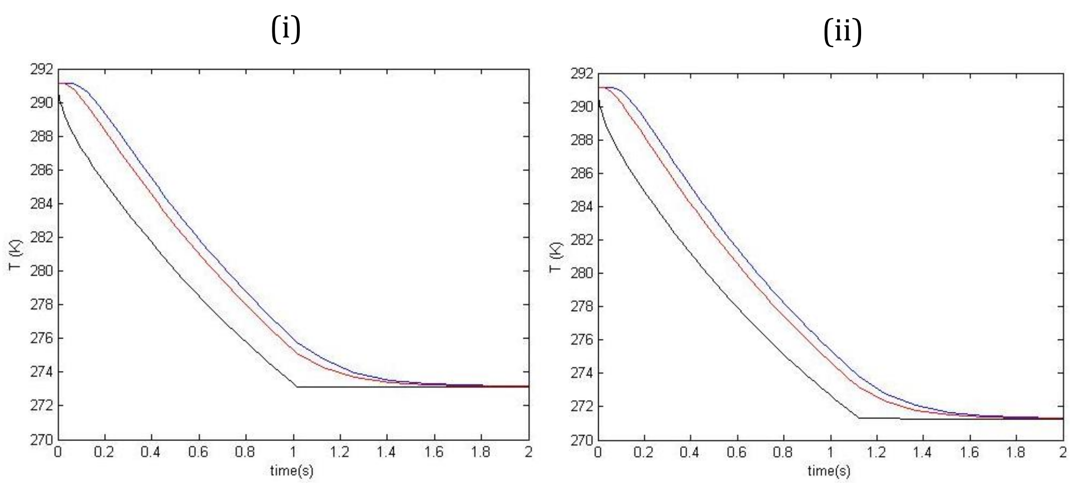

Figure 4.14 – Salt (i) and freshwater (ii) theoretical liquid cooling time

The time it takes to reach freezing temperatures can be seen in Figure 4.14 where both the salt and freshwater droplets reach 0° within a second of being exposed to the -18° ambient temperature of the cold room. This confirms the earlier estimate made through a lumped sum analysis. The total time for both fully salinized and fresh water freezing can be seen in Figure 4.15, showing that it takes almost a full two minutes to reach cold room equilibrium. The nucleation and ice cooling phases take the most time, the cooling process slows once the droplet has solidified before eventually reaching equilibrium with the ambient temperature.

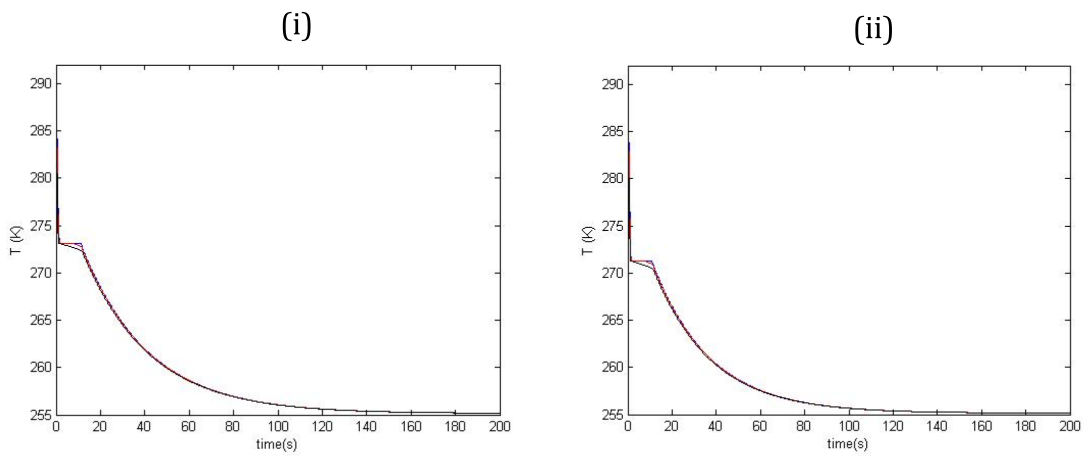

Figure 4.15 – Time for salt (i) and freshwater (ii) liquid droplets to fully transform into ice in equilibrium with ambient temperature(A.R. Deghani-Sanij, 2019)

By applying these test parameters to the algorithm created by Deghani-Sanij (2019) it was found that it would take 2 minutes for the droplets to fully transform from liquid water at room temperature to ice in equilibrium with its surrounding. More importantly it showed that the room temperature water will reach arctic sea temperatures by the time the droplets landed on the model.

4.3 Measuring Tools

4.3.1. Temperature

The temperature of the cold room was monitored and recorded using a type J thermistor linked to a Keithley 2700 DAQ and computer software for instant feedback. The cold room also has its own built in thermometer which was used to compare and confirm the accuracy of the thermistor.

4.3.2. Airflow

The airflow created by the fan was measured using a Reed Anemometer which provides accurate readings from 0-30 m/s with a resolution of 0.1m/s. Measurements were averaged across the fans profile for multiple frequencies 40 cm from the blades at the edge of the housing unit.

Table 4-4 - Wind Speed for Varying Frequencies

	Wind Speed	
50 HZ	6.785	m/s
55 HZ	7.847	m/s
60 HZ	8.855	m/s

All the tests were performed at 55hz inducing an average wind speed of 7.847 m/s. This allowed for optimal conditions producing a uniform spray pattern.

4.3.3. Relative Humidity

The humidity of the cold room was measured using BiOS weather station rated to -40°C outdoor temperatures. Data was recorded every 30 minutes through remote sensors placed in opposite corners of the cold room. These sensors have a range of -40°C to 70°C with a resolution of 0.1°C.

4.3.4. Salinity

The saltwater was prepared by mixing standard table salt with the freshwater in the lab and using a Thermo Fischer Scientific Salinity Meter Pen to ensure its concentration. The range of the salinity pen was 70ppt with a resolution of 0.01ppt.

Figure 4.16 – Measuring salinity of saltwater mix

4.3.5. Ice Accumulation

The amount of ice accumulation on each of the stair designs is a primary focus of this project. This can be obtained by weight and thickness measurements prior to and post spray testing. Thickness measurements were taken at 3 points on both the front and back edge of each step using a set of digital Vernier calipers. The weight of each step was taken using KWS 301 with a 15.000kg weight capacity and graduation of 0.0005kg.

Figure 4.17 - Weight Measurements with KWS 301 Scale

4.4 Experimental Design

The Marine Icing Group have performed several experiments using the cold room and spray unit to simulate the arctic ocean environment. Through their experience and some trial and error the following control variables were set.

- Fan speed of 7.85 m/s
- Cold room temperature of -18°C
- 2.2m between fan and stairs
- 0.8m between spray nozzle and fan
- Spray cycle of 5s on and 30s off
- 2hr long tests

The following independent variables were chosen in order to determine their impact on ice accretion and which of the various designs is easiest to manage and remove.

1. By the standards set by American Bureau of Shipping, the rate of inclination of exterior stairs must remain within 38° to 45° while maintaining a vertical rise no greater more than 9in. This resulted in a low and high rate of inclination, 39.3° and 42.7° respectively.
2. Two different salinities were observed fresh water at 0% and saltwater at 33%.

3. Four different tread designs were tested: steel plated, aluminum plated, open cell aluminum and rubber matting.

Each test was assigned a unique code to easily differentiate between the data sets and easily reference results throughout this paper. The various test parameters can be immediately recognized within each test: T-15_ROI38_0PPT_Rub refers to the test performed at -15°C, with a rate of inclination of 38° using freshwater spray on rubber tread. Alternatively, T-15_ROI42_33PPT_Cell is assigned to saltwater testing of the open cell design at a rate of inclination of 42° at -15°C.

4.5 Impact Test Design

The most effective and preferred method of ice removal is using the impact force of a baseball bat, shovel or sledgehammer to break the accumulated ice. A simple pendulum swing was designed to impact the stair so that the sledgehammer would transfer consistent impact energy to the steps through a 90° free fall rotation.

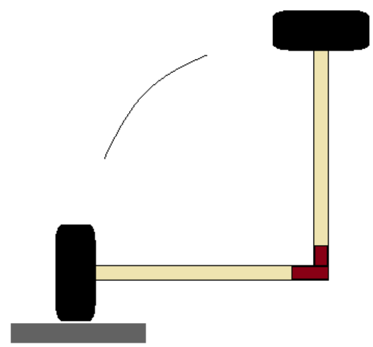

Figure 4.18 - Sledgehammer for Impact Testing

The amount of energy transferred to the step on impact is equal to the kinetic energy it absorbed through its free fall rotation. The moment of inertia for the sledgehammer was simplified to a point mass with its handle length as the radial arm.

$$I_{sledgehammer} = mr^2 = \mathbf{4.69\ kg \cdot m^2} \tag{3}$$

Using the conservation of energy, the angular velocity at impact was found to be 4.39 rad/s. With a head mass of 4.54kg and a 1.016m radius the sledgehammer impacts the step of approximately 50J of energy.

$$E_{gravitaional} = E_{kinetic} \tag{4}$$

$$mgh = \frac{1}{2}I\omega^2 = \mathbf{49.83\ J} \tag{5}$$

$$\omega = \sqrt{\frac{2 * 49.93}{4.69}} = 4.39\ rad/s \tag{6}$$

Figure 4.19 - Cold Room Impact Test Setup

Chapter 5 Data Collection

The run time for each test was 2 hours long with approximately an hour for pre-test set up and another hour for data collection for a total of 4hrs per test. Once the test was complete the temperature of the cold room would remain at -18°C allowing ice thickness and weight measurements to be recorded. The relative humidity remained relatively consistent across all tests with an average starting humidity of 72%. The humidity would slowly climb during each test due to the water spray to a final humidity of 82% on average, with the highest recorded humidity being 85%. There were no outliers when it came to relative humidity, each test appeared to follow the same pattern. The room and stairs were brought to its test temperature before initiating the spray system ensuring that both were mimicking arctic conditions prior to wetting.

5.1 Ice Accumulation Test

The thickness of the accumulated ice was one of the metrics used to compare ice accretion across each test and various step orientations. Measurements were taken at three points along the front and back edge of each of the three steps and documented in **Error! Reference source not found.** which shows recorded thickness measurements prior to and post spray testing. Another metric used to compare ice accumulation was in comparing the weight of the ice accrued as demonstrated in Table 5-2 where the weight of each step prior to icing was subtracted from the final result to give the weight of ice accumulated from each spray test.

Table 5-1 - Thickness Measurements for T-15_ROI38_0PPT_Rubb

	Thickness (mm)							
	Initial			Final			**Avg**	**Slope**
Front Edge	48.84	48.82	49.37	54.95	54.79	52.56	**5.09**	**-0.940**
Back Edge	47.89	47.73	48.82	54.71	54.08	53.74	**6.03**	
Front Edge	47.48	47.85	48.1	55.2	53.69	55.39	**6.95**	**2.663**
Back Edge	47.59	47.91	48.04	52.49	52.22	51.69	**4.29**	
Front Edge	48.62	48.38	48.32	54.87	53.41	52.13	**5.03**	**1.453**
Back Edge	47.98	47.66	47.85	51.97	51.59	50.66	**3.58**	

Figure 5.1 - Accumulated Ice Weight Measurements

Table 5-2 - Weight Measurements for T-15_ROI38_0PPT_Rubb

	Weight (kg)		
	Initial	Final	**Total Ice**
Top	10.02	11.116	**1.096**

Middle	9.92	10.852	**0.932**
Bottom	9.983	10.818	**0.835**

Table 5-3 - Fresh Water Accumulation for T-15_ROI38_0PPT_Rubb

		38 deg			
			Front	Back	
		Weight kg	**Thickness** mm		**Slope** mm
Rubber	Top	0.994	4.063	4.993	-0.930
	Mid	0.872	5.190	3.477	1.713
	Bot	0.824	5.323	3.827	1.496

The weight, thickness and observed slope of the accumulated ice observed from the T-15_ROI38_0PPT_Rubb test were then combined into Table 5-3 allowing for a detailed analysis in Chapter 6. The full set of data for each test can be found in Appendix A for freshwater testing and Appendix B for saltwater tests.

5.2 Impact Test

The objective of the impact test is to determine which of the materials has the lowest adhesion strength and highest ease of removal. The top and bottom steps were removed from the model leaving just the middle step fully exposed to the water spray. In order to determine the amount of ice removed from the sledgehammer pendulum the weight of the step was recorded at three essential stages as seen in

Table 5-4 below. The amount of ice removed from the pendulum swing is easily found by comparing the weight of the ice measured prior to impact.

Table 5-4 - Fresh Water Impact Test Results

	Fresh Water									
	Dry Weight		Pre-Impact		Ice		Post-Impact		Ice	
Rubber	9.920	kg	10.587	kg	0.667	kg	10.264	kg	0.344	kg
Steel	11.948	kg	12.418	kg	0.470	kg	12.324	kg	0.376	kg
Aluminum	8.361	kg	8.821	kg	0.460	kg	8.464	kg	0.103	kg
Open Cell	8.776	kg	9.133	kg	0.357	kg	8.983	kg	0.207	kg

5.3 Experimental Replication

These types of practical experimentation benefit from experimental replication which produces comparable results to further validate the accuracy of the collected data. Due to the limited resources, lengthy of the tests and scheduling these tests were constrained to just one run through. While these tests could certainly benefit from replication there is a basic level of replication built into the test. Each of the four tread designs were tested under four separate yet unique test conditions which allows for substantial comparison and analysis.

Chapter 6 Data Analysis

6.1 Accumulated Ice

This section will focus on the ice accumulation of all four types of tread design before expanding into the influence of water salinity and rise of the steps has on ice accretion. This analysis will observe the effect of thermal conductivity and wettability on ice accretion while ultimately determining the ideal step design to minimize accumulation.

6.1.1. Tread Design

The total ice accumulation from all 16 tests is accumulated into Table 6-1 and divided by tread type and step position. The rubber steps accumulated the most ice out of the various tread designs with the open cell steps producing the least amount of accretion.

Table 6-1 - Tread Type Weight Analysis

	Weight Analysis Tread Type			
	Rubber	**Steel**	**Open Cell**	**Aluminum**
All	10.13 kg	8.58 kg	7.25 kg	8.53 kg
Top	3.82 kg	2.90 kg	2.46 kg	3.14 kg
Middle	3.26 kg	2.72 kg	2.27 kg	2.53 kg
Bottom	3.05 kg	2.97 kg	2.52 kg	2.87 kg

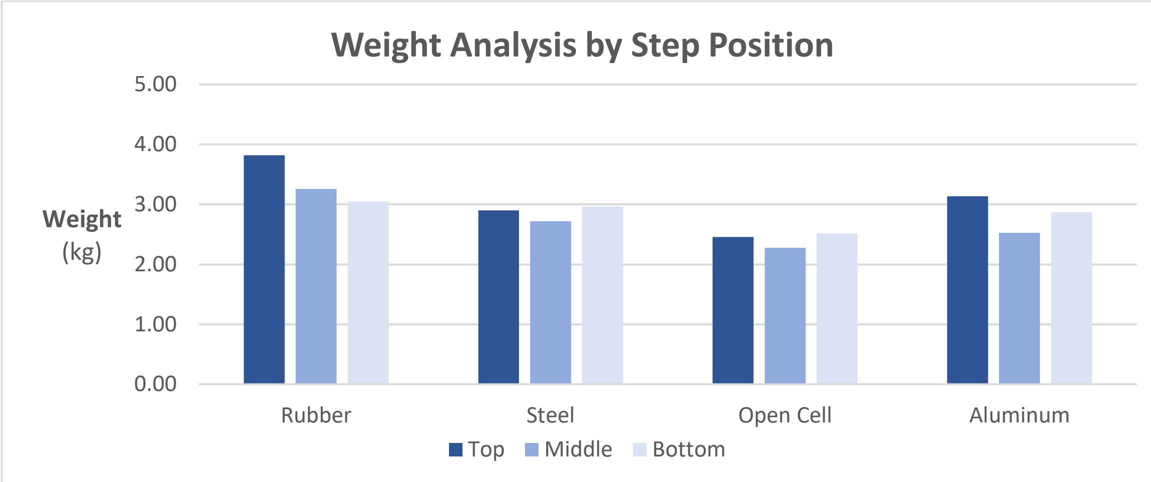

Figure 6.1 - Accumulated Ice vs Tread Design by Step Position

Both the steel and aluminum tread designs accumulated very similar amounts of ice with two considerably different thermal conductivities. Rubber has a very small thermal conductivity and produced the most amount of ice, but the conductivity of aluminum is 4 times that of steel with no large difference in accumulation. This demonstrates that the thermal conductivity does not have any effect on ice accumulation.

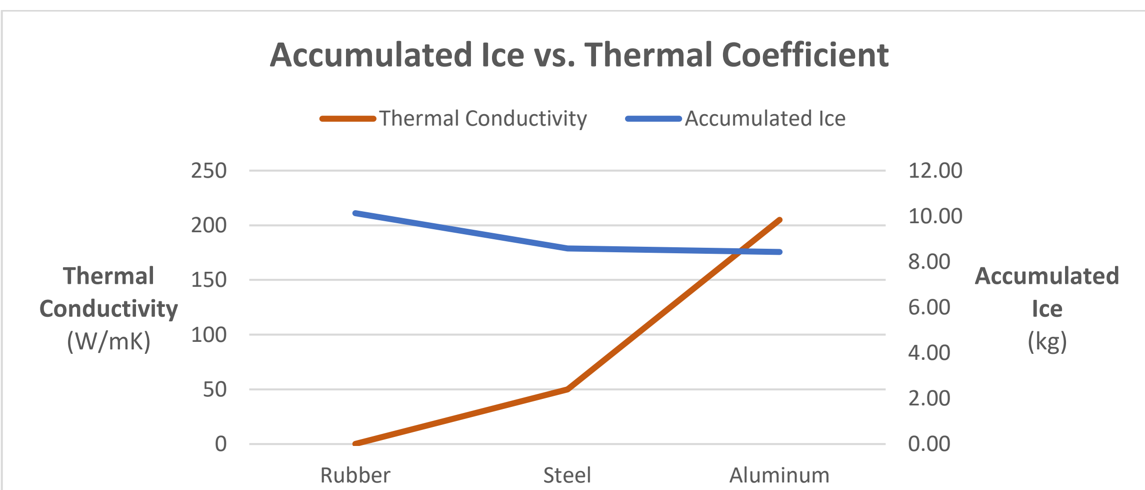

Figure 6.2 - Accumulated ice vs. Thermal Conductivity

The front edge of each step accumulated a significant amount of icing as its horizontal surface was directly in line with both the spray and constant flow of air. This phenomenon was observed on the bottom, middle and top step of each test as well as the side panels as seen in Figure 6.3 demonstrating that ice will adhere to any exposed surface.

Figure 6.3 - Full Ice Coverage of Stairs

The bottom step appeared to experience this phenomenon more than the other two. This is likely a product of the spray trajectory which is a product of both its proximity to the fan and its placement within the cold room and surrounding equipment.

The open cell step design did result in the least amount of ice given its significantly minimal surface area exposed to the spray. It has been reported that over time that the ice growth will eventually accumulate between the gaps of the open cells. The rate at which this happens is dependent on the severity of the icing. These tests have highlighted the initial icing properties of the different treads and their ability to affect the rate at which icing initiates. The open cell design appears to slow the initial development of icing while the rubber surface promotes its growth. The wettability of the tread design may have some effect on the development of icing and can account for the higher levels of ice accumulation on the rubber tread. After 30 minutes of testing the rubber steps appear to have accumulated more ice than that of the steel and aluminum.

Figure 6.4 - Early accumulation comparison on rubber and steel tread

The hydrophobic rubber repels the water and prevents it from spreading creating a thick layer of droplets which quickly freeze. Both aluminum and steel are hydrophilic allowing the droplets to spread across their surface. This also makes it easier for the droplets to slide off the back of the step before fully adhering to it. However, once the initial coating of ice has been established the material of the tread appears to become irrelevant as the spray no longer adheres to the tread but to the already accumulated ice.

6.1.2. Rate of Inclination

The rate of inclination proved to have a significant effect on the amount of ice accretion with the greater slope resulting in 20% more ice across all tests. A larger rate of inclination increases the vertical rise between each step creating a larger window for the water spray to cover each step.

Table 6-2 - Weight Analysis for varying rates of inclination

	Weight Analysis Rate of Inclination		
	All	**38**	**42**
All	33.75 kg	15.28 kg	18.47 kg
Top	12.01 kg	5.26 kg	6.75 kg
Middle	10.58 kg	4.55 kg	6.02 kg
Bottom	11.16 kg	5.47 kg	5.70 kg

At a 42° slope there is a 9in rise between steps compared to only 8in for the 38° rate of inclination. That extra inch allows more coverage from the spray and additionally results in less shelter from the next step. The top step of the design doesn't have that protection which is why it accrued more ice than the others. This is again reflected when comparing the slope of the accrued ice across each step as demonstrated in Table 6-3. This was done by taking ice thickness measurements on both the front and back edge of each step, creating an ice growth profile. Without the shelter of another step the droplet spray could evenly count its surface resulting in no slope.

Table 6-3 - Slope of ice for varying rates of inclination

	Slope of Ice Rate of Inclination					
	38			**42**		
	Front	Back	**Slope**	Front	Back	**Slope**
All	4.29	2.80	**1.48**	4.65	3.54	**1.11**
Top	3.76	3.66	**0.11**	4.52	4.34	**0.17**
Middle	4.25	2.31	**1.94**	5.00	3.14	**1.86**
Bottom	4.85	2.45	**2.40**	4.43	3.14	**1.29**

The back surface of the bottom and middle steps are shielded from the spray preventing the ice from reaching its full surface as shown in Figure 6.5. This effect was amplified with the lower rate of inclination creating an even greater slope from front to back edge.

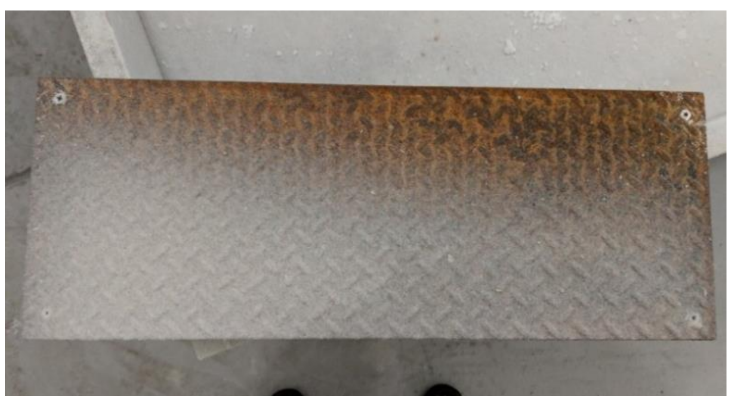

Figure 6.5 - Slope of ice at lower rates of inclination

The open cell tread further reinforces this as it showed very little slope on all three steps across each test. The grated surface doesn't provide the same shelter afforded by the other materials with fully covered surfaces. While the reduced surface area of the open cells was shown to reduce accumulation, the gaps do not provide the same shelter afforded by the other designs.

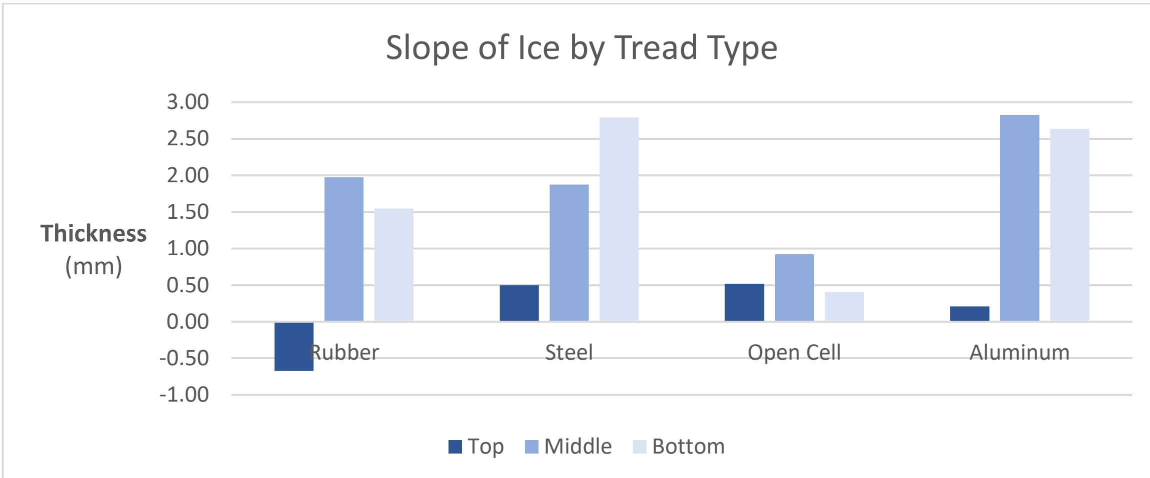

Figure 6.6 - Slope of ice by step position

The disparity between the slope developed on the top step compared to the others can be seen in Figure 6.6. These values are based on the average thickness measurements taken for each test. The open cell treads performed the best across all tests, accruing the least amount of ice with uniform surface coverage.

6.1.3. Salinity

In a direct comparison the freshwater spray tests resulted in 18% more ice accumulation than saltwater spray. This is interesting considering the slightly higher density of saltwater at 1029 kg/m^3 compared to just 1000 kg/m^3 for freshwater. With a lower freezing point of -1.8°C the saltwater has the potential to run off the step prior to freezing which is enabled by the constant airflow and growing slope induced by the rate of inclination.

Table 6-4 - Salinity Weight Analysis

	Weight Analysis Salinity		
	All	**Fresh**	**Salt**
All	33.75 kg	18.26 kg	15.49 kg
Top	12.01 kg	6.50 kg	5.51 kg
Middle	10.58 kg	5.86 kg	4.71 kg
Bottom	11.16 kg	5.90 kg	5.26 kg

Freshwater accumulation was larger on each of the various tread designs as shown in Table 6-4, with steel and aluminum producing very similar results despite their drastically differing thermal conductivities. This is a consistent observation across all tests again demonstrating the similarities between steel and aluminum ice accretion despite aluminum being 4.6 times more conductive.

The rubber tread continues to be the design with the highest amount of ice accumulation while the open cell tread is the lowest.

Figure 6.7 - Icicle formation post saltwater testing

The ice formed from saltwater testing produced a much softer ice and sometimes wet to the touch. Throughout these tests small icicles appeared to form on the edges of the steps as show in Figure 6.7 which emphasizes the slower nucleation of salt water and its potential to runoff prior to adhering to the steps.

6.2 Impact Testing

The freshwater impact tests were much more effective when compared to the saltwater ice. The fresh water produces a very brittle ice with each impact propagating though the ice and breaking it apart. The aluminum impact test was especially effective for freshwater ice as Figure 6.8 showing the smaller shards of ice created after impact. Aluminum is not as stiff as its steel counterpart allowing more of the impact energy to the ice rather than being absorbed by the structure.

Figure 6.8 - Freshwater versus Saltwater Impact

The saltwater produces a much softer ice as the pockets of trapped brine and air can produces the ability to locally absorb more energy from the impact resulting in less cracking. This can make removing the accumulated ice difficult as it requires more energy in order to break it apart. In contrast the brittleness of the freshwater allows cracks to propagate, promoting its destruction with each impact.

Table 6-5 - Amount of ice removed from impact test

	Impact Test Ice Removed			
	Freshwater		Saltwater	
	Weight	Perct.	Weight	Perct.
Rubber	0.323 kg	48%	0.111 kg	21%
Steel	0.094 kg	20%	0.052 kg	7%
Aluminum	0.517 kg	72%	0.062 kg	11%
Grated	0.15 kg	27%	0.063 kg	15%

While the open cell treads do reduce the amount of accumulated ice, they don't present any benefit to the ease of ice removal. Their design lacks the rigidity of a fully covered tread allowing the tread to absorb some of the energy from the impact minimizing its effect. The open cell does have a larger and more intricate surface area which enhances ice bondage. The sledgehammer only appears to have removed ice from where it made direct impact as seen in Figure 6.9 showing the post impact condition of the open cell tread.

Figure 6.9 - Post impact of open cell tread

Taking both the salt and freshwater tests into consideration the rubber tread showed the greatest results in removing the ice. This is most likely due to its hydrophobic properties and flexibility as a material. With each impact the ice become dislodged from its surface as seen in Figure 6.10, even the ice which remained after impact easily came loose.

Figure 6.10 - Post impact of rubber tread

Rubber is a hydrophobic material with a contact angle greater than 90° forcing the droplets to sit on the surface. Both steel and aluminum are hydrophilic which allows the water droplets to flatten and spread across its surface more easily. For rubber, its hydrophobic properties appear to promote stronger adhesion as even the remaining ice post impact was very easily removed.

Figure 6.11 - Rubber ice adhesion properties

Even during spray testing while disassembling the stairs for the next experimental trial the lower adhesion properties associated with the rubber were observed. The ice would easily peel away from the rubber in large chunks as shown in Figure 6.11, but for the steel and aluminum surfaces the ice would stick to their surfaces and break off in smaller fragments. Even though the hydrophobic properties of the rubber does reduce the adhesion forces it is likely further aided by the heavily localize brine at the interface of the saltwater accretion.

Chapter 7 Summary

The capability to study the effects of marine icing on such a large scale is an invaluable research technique which can provide representations of real-life problems. Through a series of ice accumulation tests it was found that the rubber tread design resulted in the most amount of ice accumulation in both fresh and saltwater tests. The hydrophobic properties of the rubber promoted early ice growth while the steel and aluminum flat plate designs resulted in less accumulated ice with nearly identical results for both. The open cells did successfully reduce the amount of ice accretion, showing the least amount of growth but there were signs of adhesion and ice growth within the cells that would eventually lead to its redundancy. The variance in ice accumulation appears to be linked to the initial phase of ice accumulation with the surface properties becoming irrelevant once a primary layer of ice has formed. The surface properties appear to play a large role in the adhesion of ice and its ease of removal. Even though rubber resulted in the most ice accretion of the four potential designs it also was the best design for removing ice. The fresh water was unpredictable as its brittle structure led to a 78% ice removal on the aluminum tread whereas the saltwater proved more difficult to remove with force. While varying surface type does result in different rates of accretion, it was also observed that a larger rate of inclination between steps promotes ice growth. While further research is needed to observe the early growth of ice on these variant surfaces it is clear that the rubber surface both accumulate more ice and its surface properties make it easiest to manage when trying to remove the ice.

7.1 Lessons Learned

There were some issues with the cooling system of the cold room as the air intake would accumulate ice due to the rising humidity resulting in erratic temperature drops. The summer weather during this program was especially humid which likely played a role in this difficulty. In order to help manage this the tests were limited to one per day and the door connecting the adjacent cold room was opened to assist in maintaining the temperature.

In order to ensure a consistent droplet diameter of 792μm these experiments were designed with a discharge pressure of 90psi. Occasionally the pressure would become irregular as any sort of air bubble or ice buildup in the line would result in pressure fluctuations affecting the force of the spray and the size of the droplets. Whenever the pressure would begin to waver the compressor was used to clear the lines and remove the disturbance. While not ideal this process allowed the pressure to quickly return to its designed limit of 90psi. This occurred during multiple tests and required constant monitoring.

Even though the fan, spray unit and steps were all aligned in the center of the room the water spray favored the left side. This resulted in uneven ice accumulation on the left side of the stair model as shown in Figure 7.1. This was likely due to a smaller current created by the cooling unit and other uncontrollable factors in room conditions. To minimize those effects, the equipment remained in the same position throughout all test as to keep the experiments consistent.

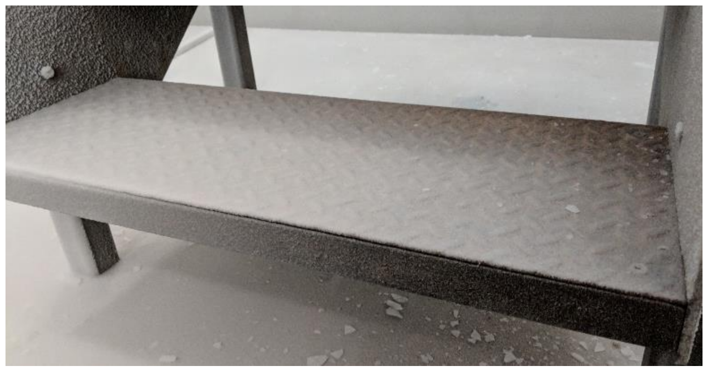

Figure 7.1- Ice accumulation favoring left side

7.2 Recommendations

While this research has provided great insight in the accumulation of marine icing on stairs and its ease of removal for different designs, it has revealed several questions that can be examined with future research. The rubber surface experienced the most ice accretion across all tests, but thickness measurements were only taken at the end of each test. Rubber is a hydrophobic element which repels water droplets, but as ice accumulates the rubber surface becomes layered in a sheet of ice making its tread type redundant. The rate of icing likely changes as the tread material recedes; this could be confirmed with incremental thickness measurements during the initially icing phase.

To remain consistent each step was exposed to 2hr of spray prior to the impact tests which inadvertently varied the thickness of ice for each tread. As already shown in the accumulation tests, in that two hours the rubber accrued more ice than the other three tread designs. Even though the same amount of energy was applied to each step it is impossible to say whether the thickness of ice had any effect on the ease of removal. The impact tests compared the weight of ice removed prior to and post impact showing the percentage of ice removed for each design. The results clearly showed that the fresh water was easier to remove than saltwater and that the rubber tread exhibited lower adhesion properties, but it ignored the thickness of the ice. This question could be further examined by coating each tread with the same thickness of ice prior to impact. Additionally, the tests could gradually increase the thickness to determine the ideal thickness for ice removal.

Some of the issues experienced during these tests could be solved for future marine icing researchers. A more precise tool for measuring the relative humidity of the cold room during testing would result in more accurate readings. The water lines supplying the spray system in the current set-up would slowly freeze impeding the flow of water and affect the supply pressure. Better line insulation or thermal heat trace to prevent ice from forming would help keep the pressure constant and reduce wait time between tests. The appearance of air bubbles in the line would also induce pressure fluctuations but the monitoring station was on the other side of the room. A pressure sensor linked to the data acquisition unit would allow the researcher to monitor the pressure, temperature and spray unit from the one station. This could prevent irregular spray phenomenon and a more consistent testing environment.

Finally, it would be advantageous to design a step that combines the minimal accretion rates of the open cell design with the low adhesion properties of the rubber surface. This would result in a reduced surface area for ice to adhere with the proven ease of removal that is afforded through the rubber tread.

References

A.R. Deghani-Sanij, S. M. (2019). Multistage cooling and freezing of a saline spherical water droplet. *International Journal of Thermal Sciences*, 16.

A.R. Deghani-Sanij, S. M. (2019). *Multistage Cooling and Freezing of a Saline Spherical Water Droplet.* Waterloo.

Council, Arctic & Authors, Coordinating & Brigham, Contributing & Zolotaryov, V.. (2009). Arctic Marine Shipping Assessment 2009 Report.

Brazil, H. (2013). Electric Heat Tracing for Surfaces Heating on Arctic Vessels and Structures to Prevent Snow and Ice Accumulation. *49*, 5.

Britanica. (2018). *Isotherm.* Retrieved from Encyclopeadia Britannica: https://www.britannica.com/technology/isotherm

Caddell, R. (2010). Convention for the Safety of Life at Sea. *Berkshire Encyclopedia of Sustainability: The Law and Politics of Sustainability*.

Canadian Coast Guard. (2019, 02 08). *Navigation in Ice Covered Waters*. Retrieved from Governmnent of Canada: http://www.ccg-gcc.gc.ca/Icebreaking/Ice-Navigation-Canadian-Waters/Navigation-in-ice-covered-waters

Dehghanisanij, A. (2017). *Theroretical and Experimental Study of Heat Loss and Ice Accretion for Large Structures on Marine Vessels and Offshore Structures.* St. John's: Memorial University of Newfoundland.

Perovich, D. K., Richter-Menge, J. A., Jones, K. F., & Light, B. (2008). Sunlight, water, and ice: Extreme Arctic sea ice melt during the summer of 2007. Geophysical Research Letters, 35(11).

Dotter, E. (2002). Winter harvest of danger: fishing on board a Maine trawler in the storm-tossed North Atlantic. *Public Health Reports*, *117*(4), 324.

Efimov, Yaroslav & Kornishin, Konstantin. (2012). Vessel Icing on the Shtokman FPSO. 10.4043/23718-MS. Gautier, D. B. (2009). Assessment of Undiscovered Oil and Gas in the Arctic. *Science, New Series*, 6.

gCaptain. (2018, April 12). *Researchers Map Seven Years of Arctic Shipping*. Retrieved from https://gcaptain.com/researchers-map-seven-years-of-arctic-shipping/

Government of Canada. (2015, 05 25). *Keep Your Vessel Stable*. Retrieved from Marine Transportation: https://www.tc.gc.ca/eng/marinesafety/tp-tp14070-3586.htm

Hay, R. F. M. (1956). Ice accumulation upon trawlers in northern waters. *Meteorological Magazine*, *85*(1010), 225.

Heaver, T. D. (2006, February 7). *Shipping Industry*. Retrieved from The Canadian Encyclopedia: https://www.thecanadianencyclopedia.ca/en/article/shipping-industry

Husain, A. (2014, 04 14). *Here's Why Russia and Canada Are Clamouring for the Arctic*. Retrieved from Vice News:

https://news.vice.com/en_us/article/zm5w73/heres-why-russia-and-canada-are-clamoring-for-the-arctic

IMO. (2014, October 24). *IMO in the United Nations*. Retrieved from International Maritime Organization: http://www.imo.org/en/KnowledgeCentre/IMOAndTheUnitedNations/Pages/default.aspx

IMO. (2019). *Shipping In Polar Waters*. Retrieved from International Maritime Organization: http://www.imo.org/en/MediaCentre/HotTopics/polar/Pages/default.aspx

Jensen, Olaf. (2000). Non-fatal occupational fall and slip injuries among commercial fishermen analyzed by use of the NOMESCO injury registration system. American journal of industrial medicine. 37. 637-44. 10.1002/(SICI)1097-0274(200006)37:63.0.CO;2-3..

Jing Chen, J. L. (2012). Superhydrophobic surfaces cannot reduce ice adhesion. 4.

Joe Evangelista, S. H. (2013). *The History of the American Bureau of Shipping.* Houston: ABS.

King, H. M. (n.d). Who Owns the Arctic? *Geoscience News and Information*. Retrieved from Geology.

Makkonen, L. (1984). *Atmospheric Icing on Sea Structures.* Philadelphia : Cold Regions Research and Engineering Labratory.

Marex. (2018, July 13). *Icing Led to Deadly Fishing Boat Sinking*. Retrieved from The Maritime Executive: https://www.maritime-executive.com/article/ntsb-icing-led-to-deadly-fishing-boat-sinking

Minsk, L. D. (1977). *Ice Accumulation on Ocean Structures.* Hanover: US Army Cold Regions Research and Engineering Labratories.

Navy, U. (1988). *Cold Weather Handbook for Surface Ships.* Washington D.C.: Chief of Naval Operations .

NTSB. (2017). *Capsizing and Sinking of Fishing Vessel Destination.* National Transportation Safety Board.

Overland, J. E. (1990). Prediction of Vessel Icing for Near-Freezing Sea Temperatures. *Weather and Forecasting*.

Ryerson, Charles. (2011). Ice protection of offshore platforms. Cold Regions Science and Technology. 65. 97-110. 10.1016/j.coldregions.2010.02.006.

Samrat Ghosh, C. R. (2015). The emergence of Arctic Shipping: issues, threats, costs, and risk-mitigating strategies. . *7*(3), 13.

Samuelsen, E. M. (2015). *Ship Icing Prediction Methods Applied in Operational Weather Forecasting.* Stavanger: University of Stavanger.

Samuelsen, E. M. (2017). *Modelled and Observed Sea-Spray Icing in Arctic-Norwegian Waters.* Norway: Cold Regions Scuebnce and Technology.

Schiermeier, Q. (2012). The great arctic oil race begins: conservationists fear spills in icy waters as Norway awards oil-production licences. *Nature*, *482*(7383), 13-15.

Schuler, M. (2018, February 1). *Teekay's New Icebreaking LNG Carrier 'Eduard Toll' Makes Historic Northern Sea Route Passage*. Retrieved from gCaptain: https://gcaptain.com/photos-teekays-new-icebreaking-lng-carrier-eduard-toll-completes-northern-sea-route-passage/

Shellard, H. (1974). *The Meterorological Aspect of Ice Accretion on Ships.* Geneva, Switzerland: World Meterological Organization.

Shipping, A. B. (2015). *Vessels Operating in Low Temperature Environments.* Houston: ABS.

Struzik, E. (2018, September 4). *As ice recedes, the Arctic isn't prepared for more shipping traffic.* Retrieved from The Conversation: https://theconversation.com/as-ice-recedes-the-arctic-isnt-prepared-for-more-shipping-traffic-102312

The Arctic & Global Warming. (2020). Retrieved 21 February 2020, from https://www.greenpeace.org/usa/arctic/issues/global-warming/

United Nations. (2017). *World Population Prospects.* New York: United Nations.

United Nations. (n.d). *Oceans and Law of the Sea*. Retrieved from United Nations: http://www.un.org/en/sections/issues-depth/oceans-and-law-sea/

United States Navy. (2017, 2 17). *McCampbell Conducts Bilateral Sonar Training*. Retrieved from America's Navy: https://www.public.navy.mil/surfor/ddg85/Pages/McCampbell-Conducts-Bilateral-Sonar-Training.aspx

Winton, M. (2006, February 1). Amplified Arctic Climate Change. *Geophysical Research Letters*. Retrieved from Geophysical Research Letters.

Wold, L. E. (2014). *A study of the changes in freeboard, stability and motion response of ships and semi-submersible platforms due to vessel icing.* Stavanger: University of Stavanger.

Young, O. R. (2000). Arctic Politics: Conflict and Cooperation in the Circumpolar North. In O. R. Young, *Arctic Politics: Conflict and Cooperation in the Circumpolar North* (pp. 118-125). Darthmouth: Darthmouth College Press.

Appendix A - Freshwater Ice Accumulation Results

Table A-1 - Test Properties for T-15_ROI38_0PPT_All

Test Properties	
Tread	Aluminum
Rate of Inclination	38
Salinity	0
RHumidity	76%
.5hr	68%
1hr	74%
1.5hr	79%
2hr	82%

Table A-2 - Weight Measurements for T-15_ROI38_0PPT_All

	Weight (kg)		
	Initial	Final	**Total Ice**
Top	8.354	9.107	**0.753**
Middle	8.361	9.001	**0.64**
Bottom	8.348	9.102	**0.754**

Table A-3 - Thickness Measurements for T-15_ROI38_0PPT_All

	Thickness (mm)							
	Initial			Final			**Avg**	**Slope**
Front Edge	42.62	42.33	42.25	46.34	46.2	45.34	**3.56**	**0.280**
Back Edge	42.19	41.76	42.11	45.47	45.8	44.63	**3.28**	
Front Edge	41.55	41.42	41.65	46.79	46.25	45.81	**4.74**	**3.960**
Back Edge	42.92	42.45	42.33	43.48	43.69	42.88	**0.78**	
Front Edge	41.43	41.54	41.35	48.93	47.03	44.74	**5.46**	**3.000**
Back Edge	42.3	42.28	42.04	45.15	45.41	43.43	**2.46**	

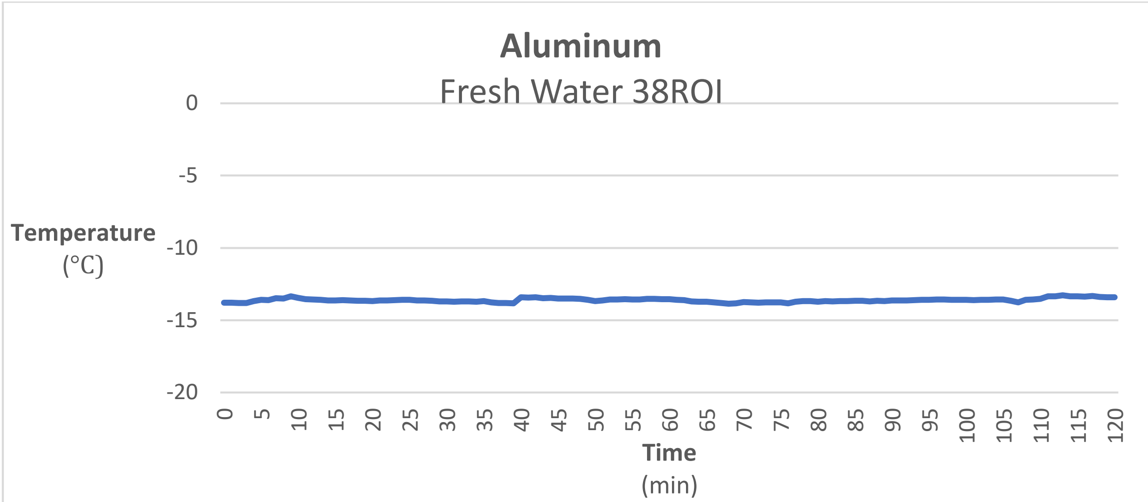

Figure A.1 - Transient Temperature Readings for T-15_ROI38_0PPT_All

Figure A.2 - Intermittent Pictures for T-15_ROI38_0PPT_All (30,60,90,120 minutes)

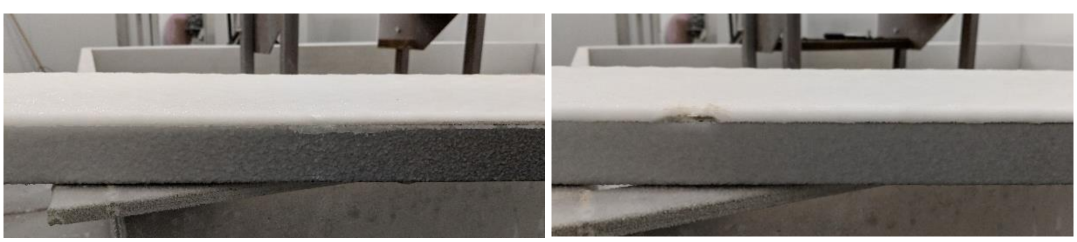

Figure A.3 - Step Thickness Pictures for T-15_ROI38_0PPT_All (Top, Middle, Bottom)

Table A-4 - Test Properties for T-15_ROI38_0PPT_OCell

Test Properties	
Tread	Open Cell
Rate of Inclination	38
Salinity	0
RHumidity	77%
.5hr	71%
1hr	76%
1.5hr	78%
2hr	81%

Table A-5 - Weight Measurements for T-15_ROI38_0PPT_OCell

	Weight (kg)		
	Initial	Final	**Total Ice**
Top	8.739	9.352	**0.613**
Middle	8.776	9.383	**0.607**
Bottom	8.773	9.415	**0.642**

Table A-6 - Thickness Measurements for T-15_ROI38_0PPT_OCell

	Thickness (mm)							
	Initial			Final			**Avg**	**Slope**
Front Edge	38.42	38.35	38.74	43.61	42.6	41.47	**4.06**	**0.250**
Back Edge	38.88	38.27	39.16	44.29	42.04	41.4	**3.81**	
Front Edge	39.06	38.02	38.32	45.05	42.33	42.24	**4.74**	**1.120**
Back Edge	38.31	37.96	38.44	42.42	41.89	41.26	**3.62**	
Front Edge	39.83	39.3	39.64	45.11	42.17	41.36	**3.29**	**0.330**
Back Edge	38.36	38.74	39.26	41.69	41.84	41.71	**2.96**	

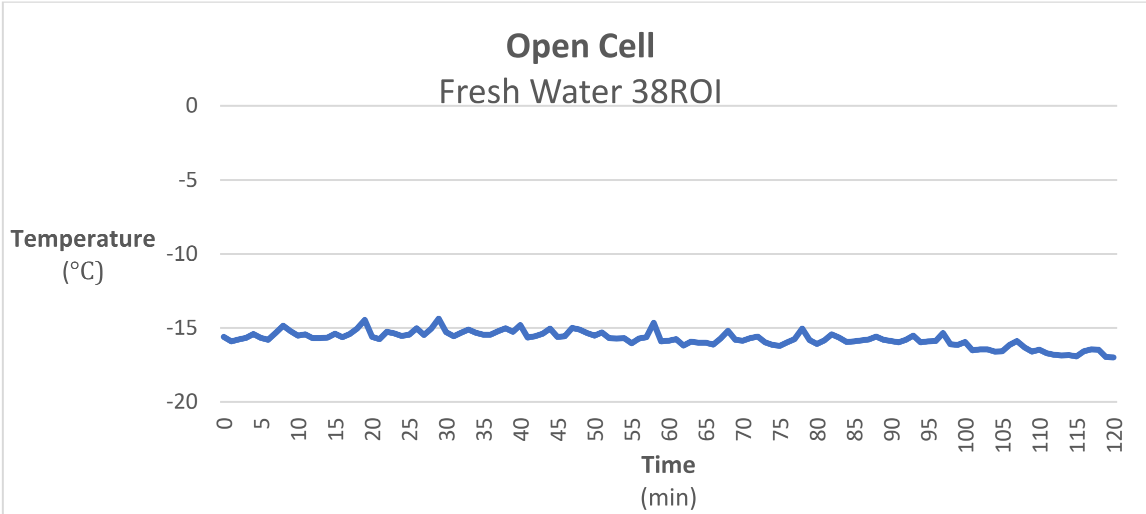

Figure A.4 - Transient Temperature Readings for T-15_ROI38_0PPT_OCell

Figure A.5 - Intermittent Pictures for T-15_ROI38_0PPT_OCell (30,60,90,120 minutes)

Figure A.6 - Step Thickness Pictures for T-15_ROI38_0PPT_OCell (Top, Middle, Bottom)

Table A-7 - Test Properties for T-15_ROI38_0PPT_Stl

Test Properties	
Tread	Steel
Rate of Inclination	38
Salinity	0
RHumidity	78%
.5hr	73%
1hr	76%
1.5hr	79%
2hr	82%

Table A-8 - Weight Measurements for T-15_ROI38_0PPT_Stl

	Weight (kg)		
	Initial	Final	**Total Ice**
Top	11.984	12.695	**0.711**
Middle	11.948	12.654	**0.706**
Bottom	11.915	12.69	**0.775**

Table A-9 - Thickness Measurements for T-15_ROI38_0PPT_Stl

	Thickness (mm)							
	Initial			Final			**Avg**	**Slope**
Front Edge	42.33	42.98	42.75	46.94	46.9	45.17	**3.65**	**0.087**
Back Edge	42.83	43.96	43.5	47.18	47.71	46.09	**3.56**	
Front Edge	43.34	43.33	42.73	46.7	46.75	45.37	**3.14**	**0.013**
Back Edge	42.21	42.34	42.71	45.34	46.16	45.14	**3.13**	
Front Edge	42.18	42.34	42.12	49.46	48.31	45.92	**5.68**	**4.037**
Back Edge	42.53	43.81	43.69	46.25	45.68	43.04	**1.65**	

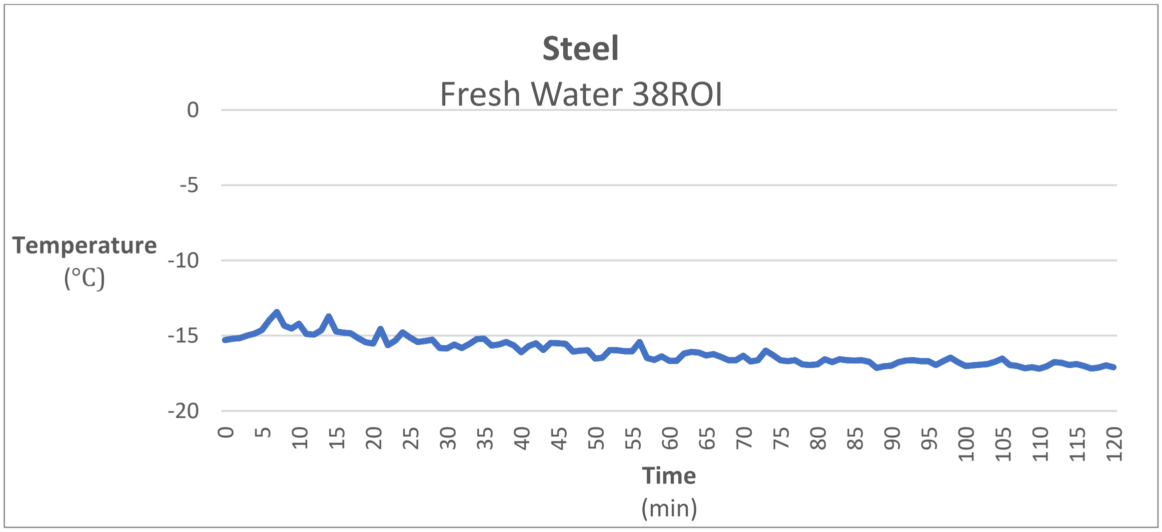

Figure A.7 - Transient Temperature Readings for T-15_ROI38_0PPT_Stl

Table A-10 - Test Properties for T-15_ROI38_0PPT_Rub

Test Properties	
Tread	Rubber
Rate of Inclination	38
Salinity	0
RHumidity	76%
.5hr	70%
1hr	74%
1.5hr	79%
2hr	80%

Table A-11 - Weight Measurements for T-15_ROI38_0PPT_Rub

	Weight (kg)		
	Initial	Final	**Total Ice**
Top	10	11.116	**1.116**
Middle	9.92	10.852	**0.932**
Bottom	9.983	10.818	**0.835**

Table A-12 - Thickness Measurements for T-15_ROI38_0PPT_Rub

	Thickness (mm)							
	Initial			Final			**Avg**	**Slope**
Front Edge	48.84	48.82	49.37	54.95	54.79	52.56	**5.09**	**-0.940**
Back Edge	47.89	47.73	48.82	54.71	54.08	53.74	**6.03**	
Front Edge	47.48	47.85	48.1	55.2	53.69	55.39	**6.95**	**2.663**
Back Edge	47.59	47.91	48.04	52.49	52.22	51.69	**4.29**	
Front Edge	48.62	48.38	48.32	54.87	53.41	52.13	**5.03**	**1.453**
Back Edge	47.98	47.66	47.85	51.97	51.59	50.66	**3.58**	

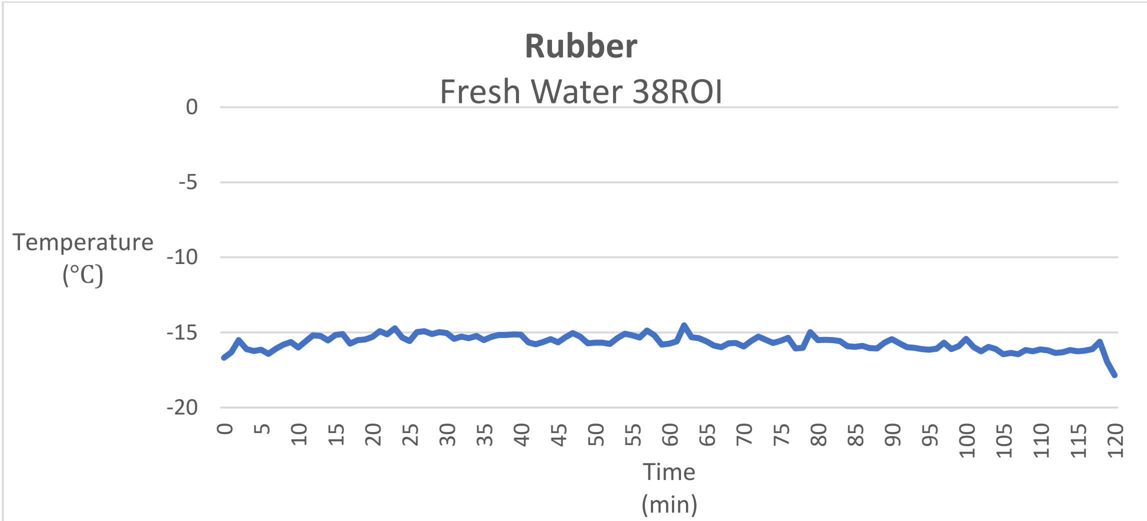

Figure A.8 - Transient Temperature Readings for T-15_ROI38_0PPT_Rub

Figure A.9 - Intermittent Pictures for T-15_ROI38_0PPT_Rub (30,60,90,120 minutes)

Figure A.10 - Step Thickness Pictures for T-15_ROI38_0PPT_Rub (Top, Middle, Bottom)

Table A-13 - Test Properties for T-15_ROI42_0PPT_All

Test Properties	
Tread	Aluminum
Rate of Inclination	42
Salinity	0
RHumidity	#DIV/0!
.5hr	
1hr	
1.5hr	
2hr	

Table A-14 - Weight Measurements for T-15_ROI42_0PPT_All

	Weight (kg)		
	Initial	Final	**Total Ice**
Top	8.354	9.231	**0.877**
Middle	8.361	9.101	**0.74**
Bottom	8.348	9.071	**0.723**

Table A-15 - Thickness Measurements for T-15_ROI42_0PPT_All

	Thickness (mm)							
	Initial			Final			**Avg**	**Slope**
Front Edge	42.62	42.33	42.25	47.94	46.43	46.18	**4.45**	**0.213**
Back Edge	42.19	41.76	42.11	46.87	46.41	45.49	**4.24**	
Front Edge	41.55	41.42	41.65	47.71	47.09	46.1	**5.43**	**3.510**
Back Edge	42.92	42.45	42.33	44.67	44.77	44.01	**1.92**	
Front Edge	41.43	41.54	41.35	47.26	45.44	45.05	**4.48**	**1.897**
Back Edge	42.3	42.28	42.04	45.34	44.89	44.13	**2.58**	

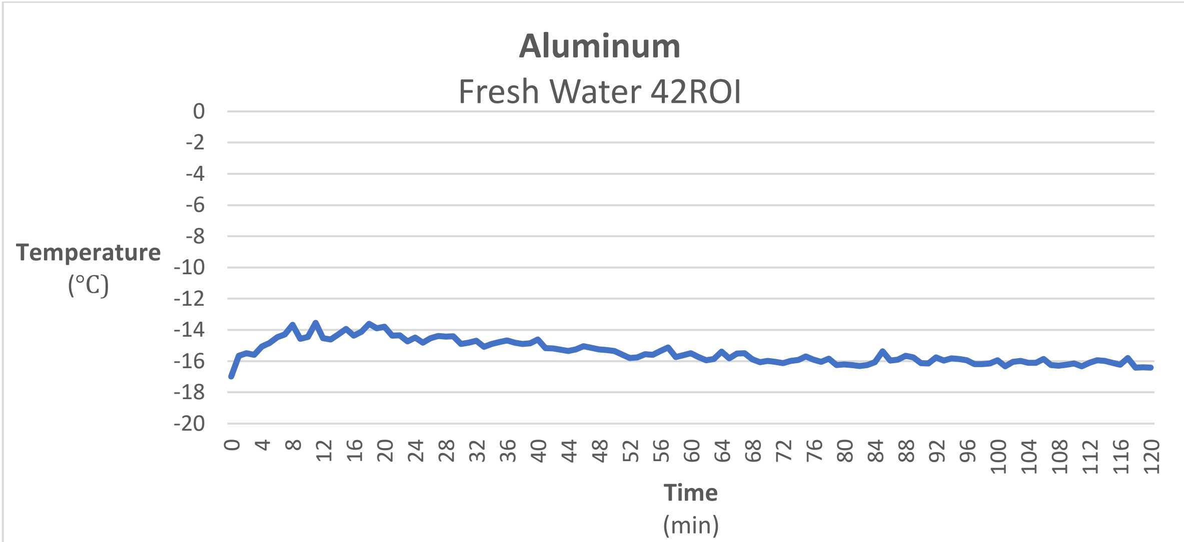

Figure A.11 - Transient Temperature Readings for T-15_ROI42_0PPT_All

Figure A.12 - Intermittent Pictures for T-15_ROI42_0PPT_All (30,60,90,120 minutes)

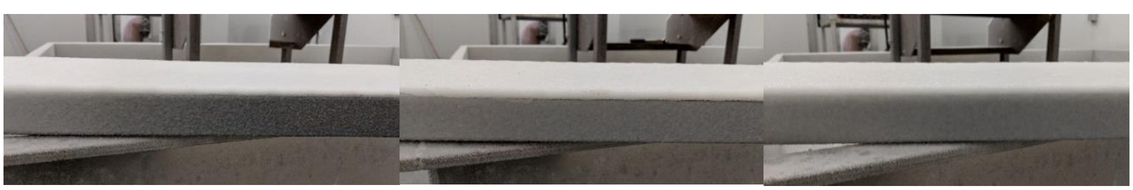

Figure A.13 - Step Thickness Pictures for T-15_ROI42_0PPT_All (Top, Middle, Bottom)

Table A-16 - Test Properties for T-15_ROI42_0PPT_OCell

Test Properties	
Tread	Open Cell
Rate of Inclination	42
Salinity	0
RHumidity	#DIV/0!
.5hr	
1hr	
1.5hr	
2hr	

Table A-17 - Weight Measurements for T-15_ROI42_0PPT_OCell

	Weight (kg)		
	Initial	Final	**Total Ice**
Top	8.739	9.393	**0.654**
Middle	8.776	9.376	**0.600**
Bottom	8.773	9.344	**0.571**

Table A-18 - Thickness Measurements for T-15_ROI42_0PPT_OCell

	Thickness (mm)							
	Initial			Final			**Avg**	**Slope**
Front Edge	38.42	38.35	38.74	44.22	43.99	43.35	**5.35**	**0.800**
Back Edge	38.88	38.27	39.16	43.78	43.47	42.71	**4.55**	
Front Edge	39.06	38.02	38.32	44.02	43.09	43.74	**5.15**	**0.840**
Back Edge	38.31	37.96	38.44	43.23	41.9	42.51	**4.31**	
Front Edge	39.83	39.3	39.64	44.4	42.55	42.87	**3.68**	**-0.407**
Back Edge	38.36	38.74	39.26	43.29	42.17	43.17	**4.09**	

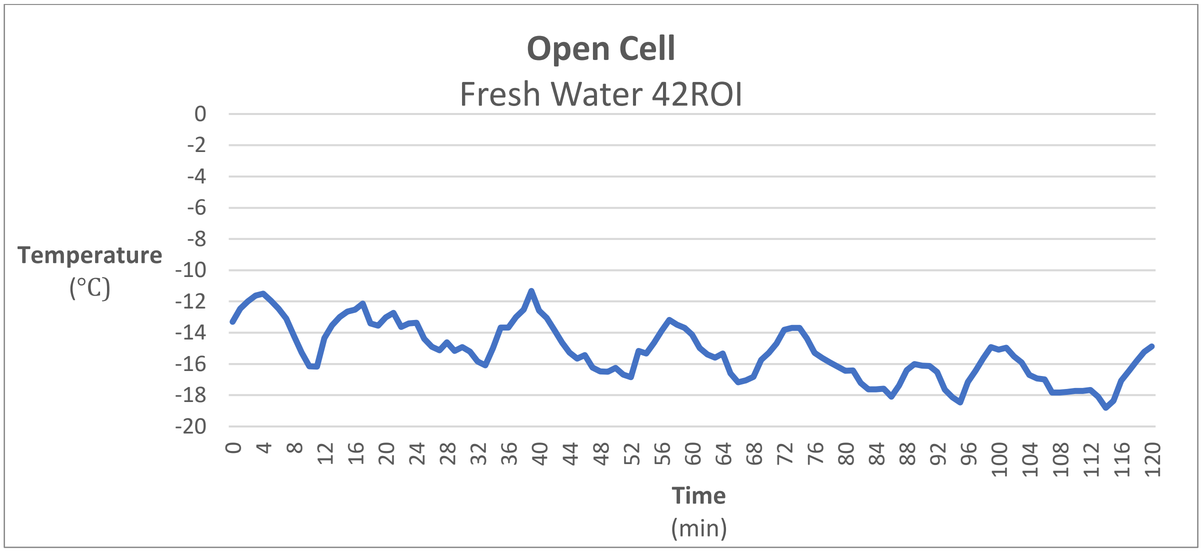

Figure A.14 - Transient Temperature Readings for T-15_ROI42_0PPT_OCell

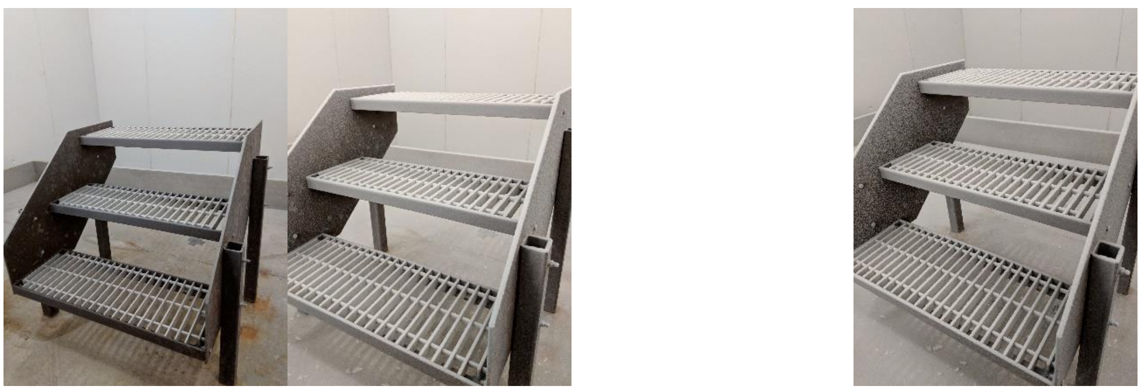

Figure A.15 - Intermittent Pictures for T-15_ROI42_0PPT_OCell (30,60,90,120 minutes)

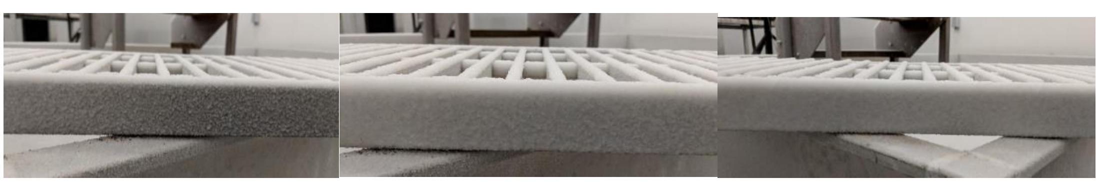

Figure A.16 -Step Thickness Pictures for T-15_ROI42_0PPT_OCell (Top, Middle, Bottom)

Table A-19 - Test Properties for T-15_ROI42_0PPT_Stl

Test Properties	
Tread	Steel
Rate of Inclination	42
Salinity	0
RHumidity	#DIV/0!
.5hr	
1hr	
1.5hr	
2hr	

Table A-20 - Weight Measurements for T-15_ROI42_0PPT_Stl

	Weight (kg)		
	Initial	Final	**Total Ice**
Top	11.984	12.767	**0.783**
Middle	11.948	12.712	**0.764**
Bottom	11.915	12.691	**0.776**

Table A-21 - Thickness Measurements for T-15_ROI42_0PPT_Stl

	Thickness (mm)							
	Initial			Final			**Avg**	**Slope**
Front Edge	42.33	42.98	42.75	47.63	46.95	46.65	**4.39**	**0.280**
Back Edge	42.83	43.96	43.5	47.93	48.04	46.65	**4.11**	
Front Edge	43.34	43.33	42.73	47.63	47.93	46.61	**4.26**	**2.263**
Back Edge	42.21	42.34	42.71	44.38	44.71	44.15	**1.99**	
Front Edge	42.18	42.34	42.12	48.66	47.64	45.59	**5.08**	**2.240**
Back Edge	42.53	43.81	43.69	46.31	46.83	45.42	**2.84**	

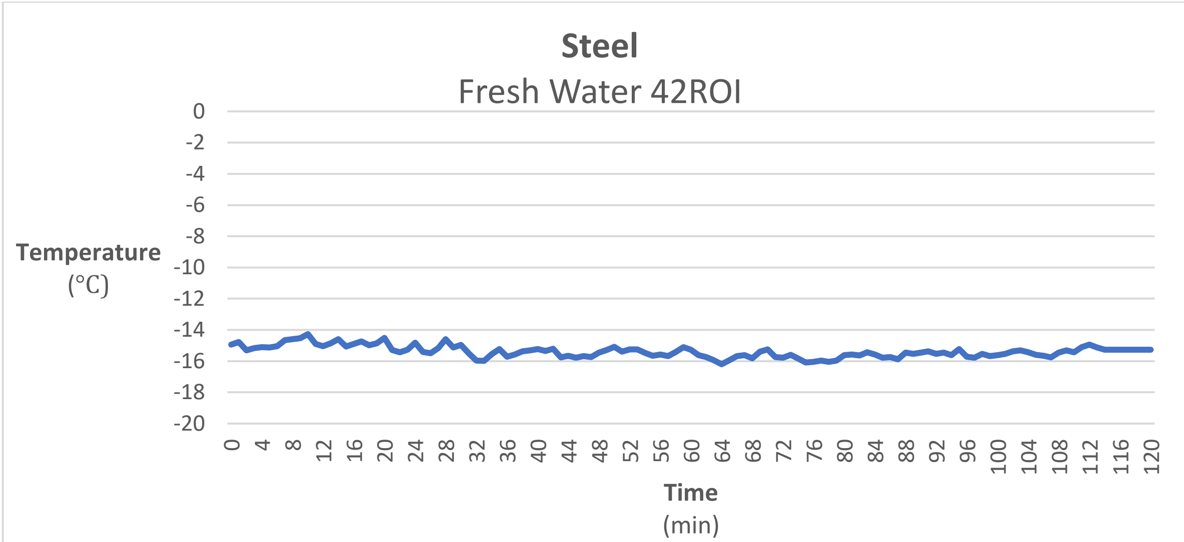

Figure A.17 - Transient Temperature Readings for T-15_ROI42_0PPT_Stl

Figure A.18 - Intermittent Pictures for T-15_ROI42_0PPT_Stl (30,60,90,120 minutes)

Figure A.19 - Step Thickness Pictures for T-15_ROI42_0PPT_Stl (Top, Middle, Bottom)

Table A-22 - Test Properties for T-15_ROI42_0PPT_Rub

Test Properties	
Tread	Rubber
Rate of Inclination	42
Salinity	0
RHumidity	#DIV/0!
.5hr	
1hr	
1.5hr	
2hr	

Table A-23 - Weight Measurements for T-15_ROI42_0PPT_Rub

	Weight (kg)		
	Initial	Final	**Total Ice**
Top	10	10.562	**0.562**
Middle	9.92	10.305	**0.385**
Bottom	9.983	10.719	**0.736**

Table A-24 - Thickness Measurements for T-15_ROI42_0PPT_Rub

	Thickness (mm)							
	Initial			Final			Avg	Slope
Front Edge	48.84	48.82	49.37	53.36	52.79	52.12	**3.75**	**0.743**
Back Edge	47.89	47.73	48.82	50.94	50.56	51.95	**3.00**	
Front Edge	47.48	47.85	48.1	53.6	51.93	51.29	**4.46**	**3.443**
Back Edge	47.59	47.91	48.04	49.42	48.85	48.33	**1.02**	
Front Edge	48.62	48.38	48.32	55.97	54.05	51.97	**5.56**	**3.850**
Back Edge	47.98	47.66	47.85	51.01	49.35	48.25	**1.71**	

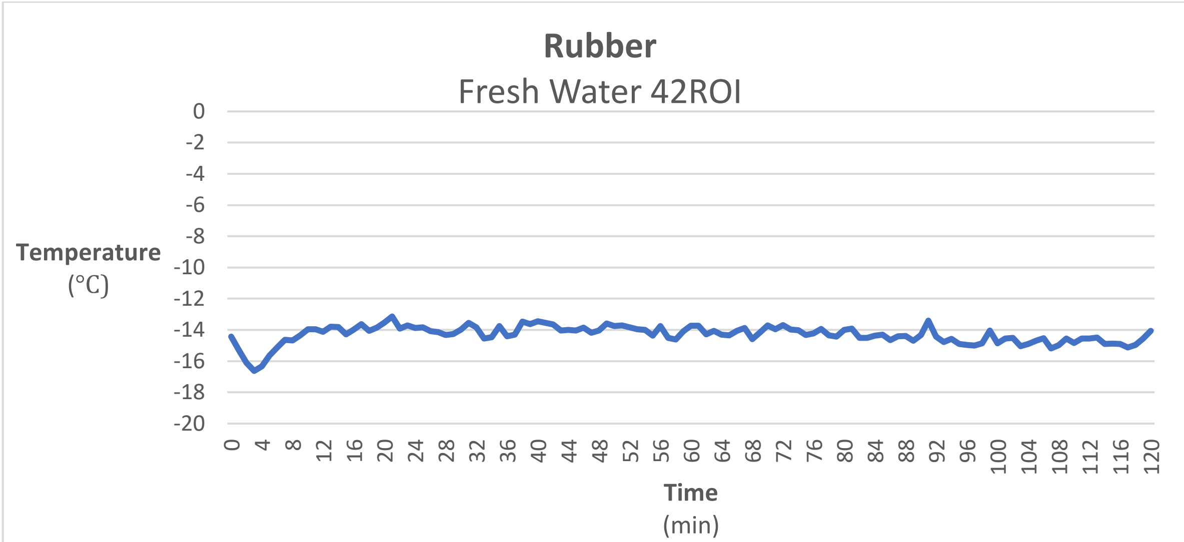

Figure A.20 - Transient Temperature Readings for T-15_ROI42_0PPT_Rub

Figure A.21 - Intermittent Pictures for T-15_ROI42_0PPT_Rub (30,60,90,120 minutes)

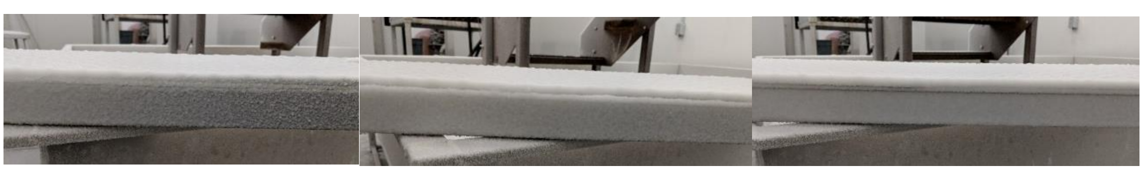

Figure A.22 - Step Thickness Pictures for T-15_ROI42_0PPT_Rub (Top, Middle, Bottom)

Appendix B - Saltwater Ice Accumulation Test Results

Table B-1 - Test Properties for T-15_ROI38_33PPT_All

Test Properties	
Tread	Aluminum
Rate of Inclination	38
Salinity	33.9
RHumidity	81%
.5hr	78%
1hr	82%
1.5hr	83%
2hr	81%

Table B-2 - Weight Measurements for T-15_ROI38_33PPT_All

	Weight (kg)		
	Initial	Final	**Total Ice**
Top	8.354	9.001	**0.647**
Middle	8.361	8.772	**0.411**
Bottom	8.348	9.026	**0.678**

Table B-3 - Thickness Measurements for T-15_ROI38_33PPT_All

	Thickness (mm)							
	Initial			Final			**Avg**	**Slope**
Front Edge	42.62	42.33	42.25	46.03	46.28	45.25	**3.45**	**0.023**
Back Edge	42.19	41.76	42.11	45.56	45.83	44.96	**3.43**	
Front Edge	41.55	41.42	41.65	46.24	44.98	44.82	**3.81**	**3.080**
Back Edge	42.92	42.45	42.33	43.41	43.34	43.13	**0.73**	
Front Edge	41.43	41.54	41.35	48.56	46.23	45.59	**5.35**	**3.883**
Back Edge	42.3	42.28	42.04	43.73	43.77	43.53	**1.47**	

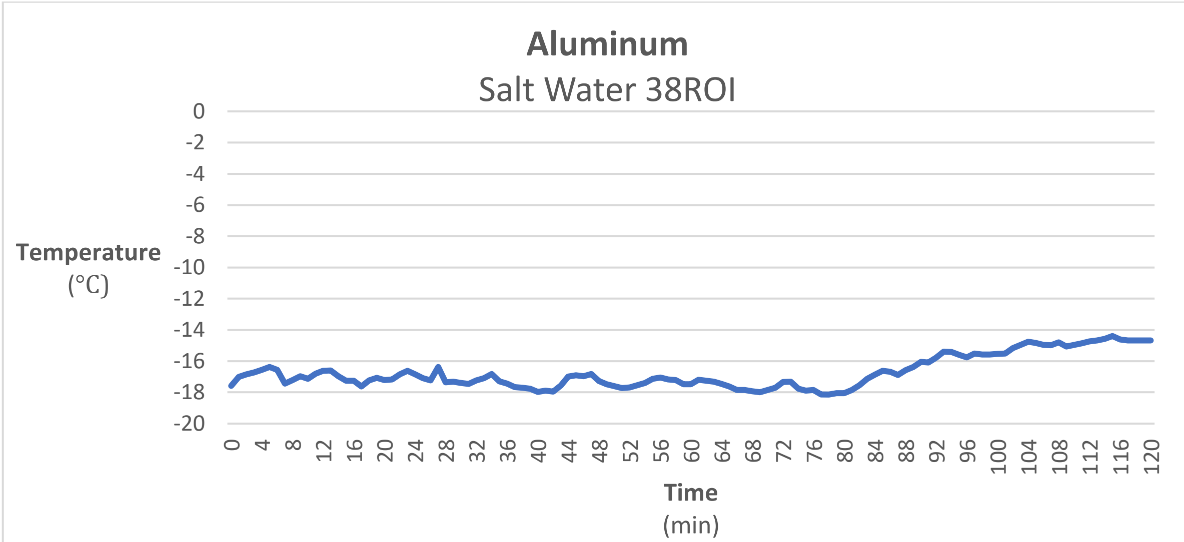

Figure B.1 - Transient Temperature Readings for T-15_ROI38_33PPT_All

Figure B.2 - Intermittent Pictures for T-15_ROI38_33PPT_All (30,60,90,120 minutes)

Figure B.3 - Step Thickness Pictures for T-15_ROI38_33PPT_All (Top, Middle, Bottom)

Table B-4 - Test Properties for T-15_ROI38_33PPT_OCell

Test Properties	
Tread	Open Cell
Rate of Inclination	38
Salinity	36.1
RHumidity	78%
.5hr	74%
1hr	77%
1.5hr	79%
2hr	81%

Table B-5 - Weight Measurements for T-15_ROI38_33PPT_OCell

	Weight (kg)		
	Initial	Final	**Total Ice**
Top	8.739	9.187	**0.448**
Middle	8.776	9.136	**0.360**
Bottom	8.773	9.256	**0.483**

Table B-6 - Thickness Measurements for T-15_ROI38_33PPT_OCell

	Thickness (mm)							
	Initial			Final			**Avg**	**Slope**
Front Edge	38.42	38.35	38.74	41.62	41.42	41.28	**2.94**	**0.327**
Back Edge	38.88	38.27	39.16	41.82	41.74	40.58	**2.61**	
Front Edge	39.06	38.02	38.32	41.12	40.76	40.4	**2.29**	**0.053**
Back Edge	38.31	37.96	38.44	40.86	40.14	40.43	**2.24**	
Front Edge	39.83	39.3	39.64	43.86	41.45	41.14	**2.56**	**-0.167**
Back Edge	38.36	38.74	39.26	42.76	41.52	40.26	**2.73**	

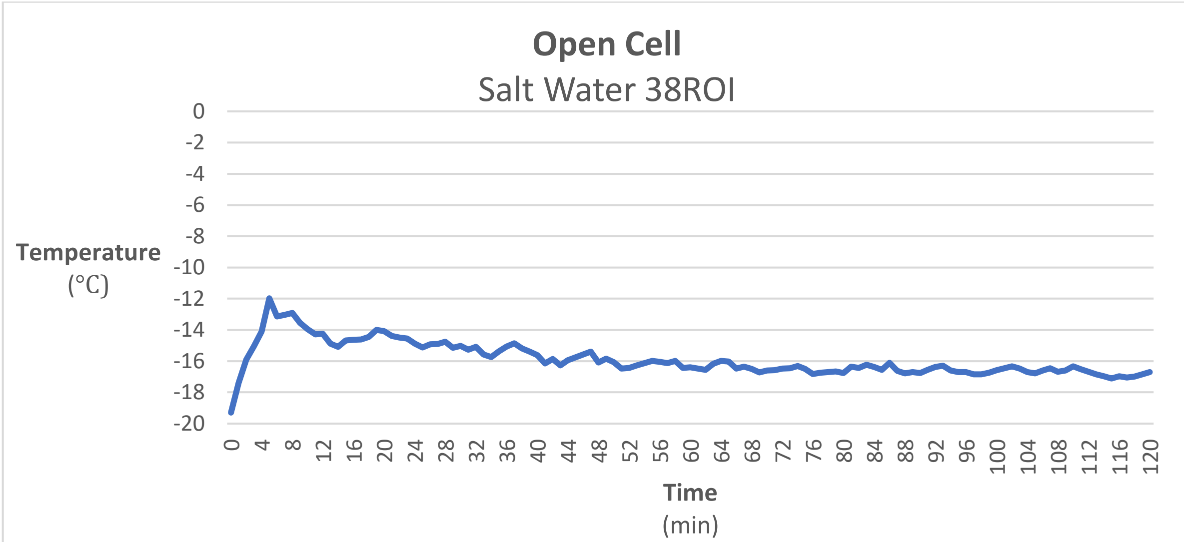

Figure B.4 - Transient Temperature Readings for T-15_ROI38_33PPT_OCell

Figure B.5 - Intermittent Pictures for T-15_ROI38_33PPT_OCell (30,60,90,120 minutes)

Figure B.6 - Step Thickness Pictures for T-15_ROI38_33PPT_OCell (Top, Middle, Bottom)

Table B-7 - Test Properties for T-15_ROI38_33PPT_Stl

Test Properties	
Tread	Steel
Rate of Inclination	38
Salinity	0
RHumidity	77%
.5hr	71%
1hr	75%
1.5hr	78%
2hr	82%

Table B-8 - Weight Measurements for T-15_ROI38_33PPT_Stl

	Weight (kg)		
	Initial	Final	**Total Ice**
Top	11.984	12.637	**0.653**
Middle	11.948	12.511	**0.563**
Bottom	11.915	9.256	**-2.659**

Table B-9 - Thickness Measurements for T-15_ROI38_33PPT_Stl

	Thickness (mm)							
	Initial			Final			**Avg**	**Slope**
Front Edge	42.33	42.98	42.75	46.97	46.82	45.99	**3.91**	**0.870**
Back Edge	42.83	43.96	43.5	46.45	47.03	45.92	**3.04**	
Front Edge	43.34	43.33	42.73	47.7	47.18	46.3	**3.93**	**2.083**
Back Edge	42.21	42.34	42.71	44.28	44.56	43.95	**1.84**	
Front Edge	42.18	42.34	42.12	49.87	48.17	46.39	**5.93**	**4.880**
Back Edge	42.53	43.81	43.69	44.64	44.34	44.2	**1.05**	

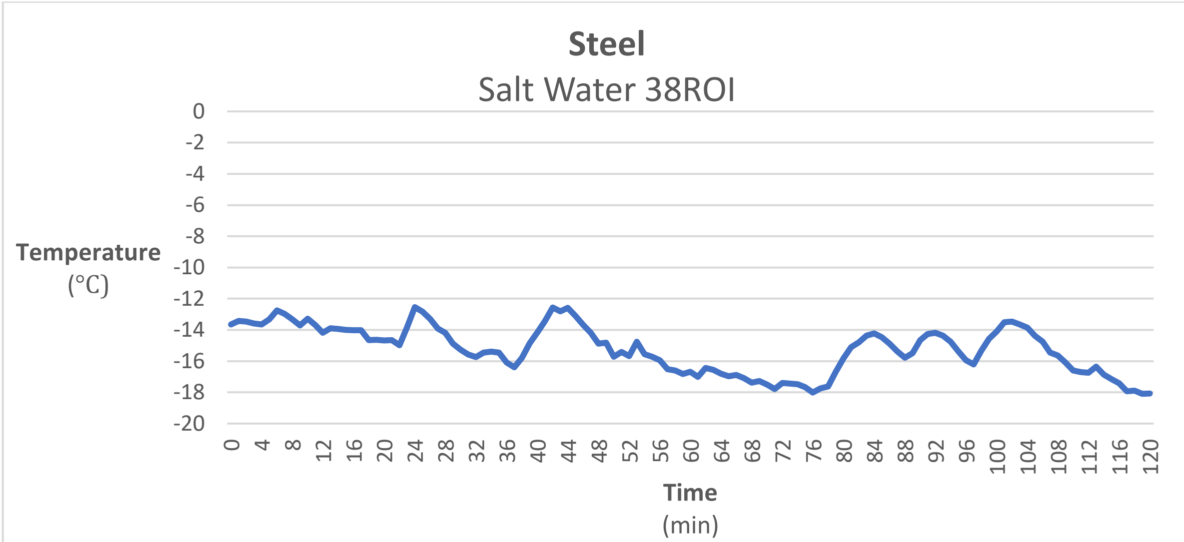

Figure B.7 - Transient Temperature Readings for T-15_ROI38_33PPT_Stl

Figure B.8 - Intermittent Pictures for T-15_ROI38_33PPT_Stl (30,60,90,120 minutes)

Figure B.9 - Step Thickness Pictures for T-15_ROI38_33PPT_Stl (Top, Middle, Bottom)

Table B-10 - Test Properties for T-15_ROI38_33PPT_Rub

Test Properties	
Tread	Rubber
Rate of Inclination	38
Salinity	35.7
RHumidity	79%
.5hr	75%
1hr	79%
1.5hr	80%
2hr	83%

Table B-11 - Weight Measurements for T-15_ROI38_33PPT_Rub

	Weight (kg)		
	Initial	Final	**Total Ice**
Top	10	10.54	**0.54**
Middle	9.92	10.313	**0.393**
Bottom	9.983	10.574	**0.591**

Table B-12 - Thickness Measurements for T-15_ROI38_33PPT_Rub

	Thickness (mm)							
	Initial			Final			**Avg**	**Slope**
Front Edge	48.84	48.82	49.37	52.91	51.77	52.28	**3.31**	**-0.667**
Back Edge	47.89	47.73	48.82	52.2	52	52.17	**3.98**	
Front Edge	47.48	47.85	48.1	53.07	51.15	51.29	**4.03**	**2.627**
Back Edge	47.59	47.91	48.04	49.48	48.92	49.34	**1.40**	
Front Edge	48.62	48.38	48.32	54.86	51.82	50.81	**4.06**	**2.647**
Back Edge	47.98	47.66	47.85	50.25	48.97	48.5	**1.41**	

Figure B.10 - Intermittent Pictures for T-15_ROI38_33PPT_Rub (30,60,90,120 minutes)

Figure B.11 - Step Thickness Pictures for T-15_ROI38_33PPT_Rub (Top, Middle, Bottom)

Table B-13 - Test Properties for T-15_ROI42_33PPT_All

Test Properties	
Tread	Aluminum
Rate of Inclination	42
Salinity	35.8
RHumidity	82%
.5hr	79%
1hr	81%
1.5hr	84%
2hr	84%

Table B-14 - Weight Measurements for T-15_ROI42_33PPT_All

	Weight (kg)		
	Initial	Final	**Total Ice**
Top	8.354	9.212	**0.858**
Middle	8.361	9.095	**0.734**
Bottom	8.348	9.062	**0.714**

Table B-15 - Thickness Measurements for T-15_ROI42_33PPT_All

	Thickness (mm)							
	Initial			Final			**Avg**	**Slope**
Front Edge	42.62	42.33	42.25	47.69	46.71	45.97	**4.39**	**0.240**
Back Edge	42.19	41.76	42.11	46.61	46.13	45.77	**4.15**	
Front Edge	41.55	41.42	41.65	47.39	47.48	45.72	**5.32**	**3.057**
Back Edge	42.92	42.45	42.33	45.46	44.69	44.35	**2.27**	
Front Edge	41.43	41.54	41.35	46.23	46.38	45.37	**4.55**	**1.757**
Back Edge	42.3	42.28	42.04	45.34	45.44	44.23	**2.80**	

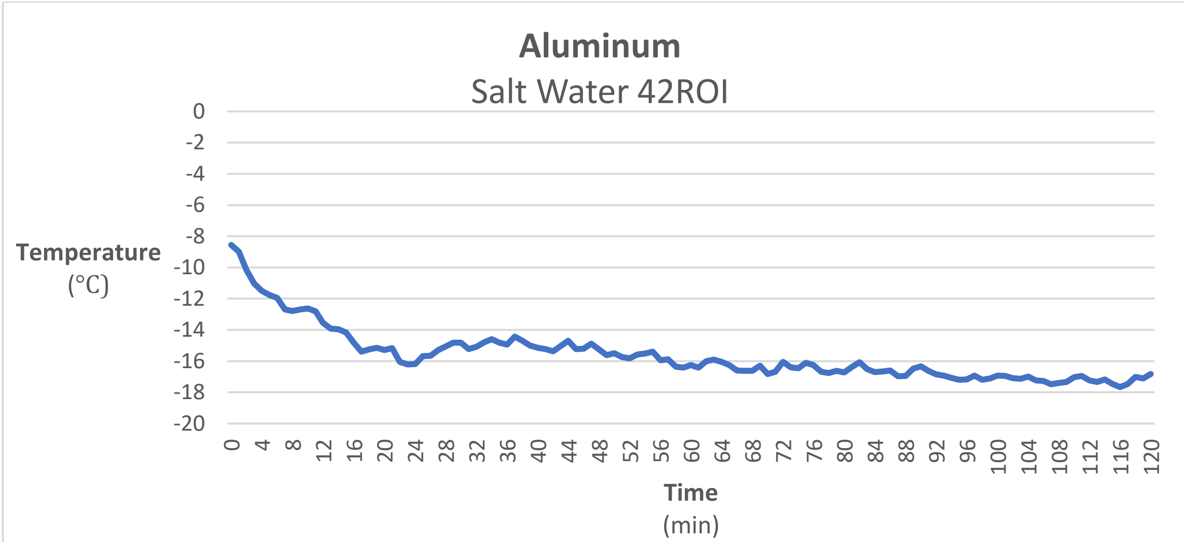

Figure B.12 - Transient Temperature Readings for T-15_ROI42_33PPT_All

Figure B.13 - Intermittent Pictures for T-15_ROI42_33PPT_All (30,60,90,120 minutes)

Figure B.14 - Step Thickness Pictures for T-15_ROI42_33PPT_All (Top, Middle, Bottom)

Table B-16 - Test Properties for T-15_ROI42_33PPT_OCell

Test Properties	
Tread	Open Cell
Rate of Inclination	42
Salinity	33.7
RHumidity	76%
.5hr	79%
1hr	74%
1.5hr	74%
2hr	78%

Table B-17 - Weight Measurements for T-15_ROI42_33PPT_OCell

	Weight (kg)		
	Initial	Final	**Total Ice**
Top	8.739	9.275	**0.536**
Middle	8.776	9.28	**0.504**
Bottom	8.773	9.357	**0.584**

Table B-18 - Thickness Measurements for T-15_ROI42_33PPT_OCell

	Thickness (mm)							
	Initial			Final			**Avg**	**Slope**
Front Edge	38.42	38.35	38.74	42.04	41.81	41.68	**3.34**	**0.160**
Back Edge	38.88	38.27	39.16	42.16	41.73	41.96	**3.18**	
Front Edge	39.06	38.02	38.32	44.87	41.78	41.67	**4.31**	**1.343**
Back Edge	38.31	37.96	38.44	41.35	41.47	40.78	**2.96**	
Front Edge	39.83	39.3	39.64	44.79	42.2	42.35	**3.52**	**0.803**
Back Edge	38.36	38.74	39.26	41.97	41.35	41.2	**2.72**	

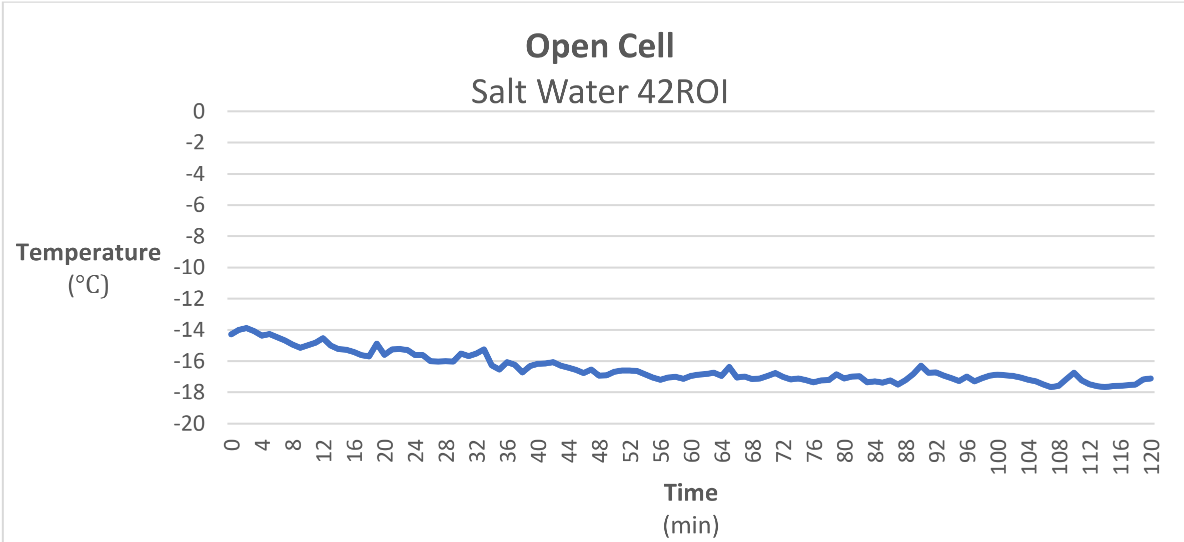

Figure B.15 - Transient Temperature Readings for T-15_ROI42_33PPT_OCell

Figure B.16 - Intermittent Pictures for T-15_ROI42_33PPT_OCell (30,60,90,120 minutes)

Figure B.17 - Step Thickness Pictures for T-15_ROI42_33PPT_OCell (Top, Middle, Bottom)

Table B-19 - Test Properties for T-15_ROI42_33PPT_Stl

Test Properties	
Tread	Steel
Rate of Inclination	42
Salinity	0
RHumidity	79%
.5hr	75%
1hr	78%
1.5hr	80%
2hr	83%

Table B-20 - Weight Measurements for T-15_ROI42_33PPT_Stl

	Weight (kg)		
	Initial	Final	**Total Ice**
Top	11.984	12.738	**0.754**
Middle	11.949	12.633	**0.684**
Bottom	11.915	12.611	**0.696**

Table B-21 - Thickness Measurements for T-15_ROI42_33PPT_Stl

	Thickness (mm)							
	Initial			Final			**Avg**	**Slope**
Front Edge	42.33	42.98	42.75	47.8	47.63	46.69	**4.69**	**1.767**
Back Edge	42.83	43.96	43.5	46.47	46.59	45.99	**2.92**	
Front Edge	43.34	43.33	42.73	47.98	47.26	46.38	**4.07**	**2.440**
Back Edge	42.21	42.34	42.71	44.16	44.34	43.66	**1.63**	
Front Edge	42.18	42.34	42.12	47.64	46.58	45.55	**4.38**	**2.003**
Back Edge	42.53	43.81	43.69	46.67	45.86	44.62	**2.37**	

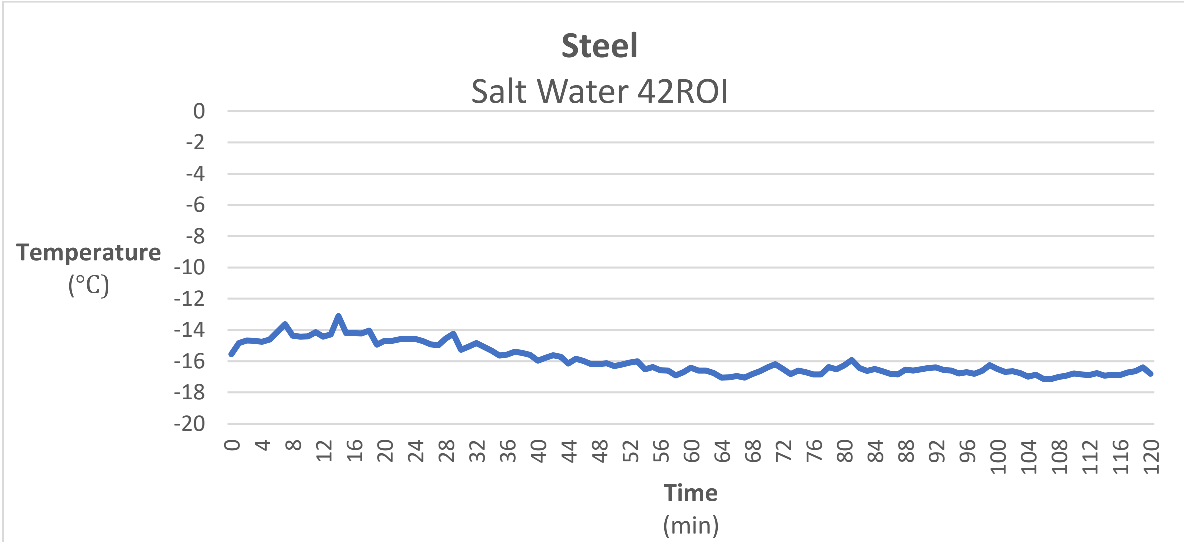

Figure B.18 - Transient Temperature Readings for T-15_ROI42_33PPT_Stl

Figure B.19 - Intermittent Pictures for T-15_ROI42_33PPT_Stl (30,60,90,120 minutes)

Figure B.20 - Step Thickness Pictures for T-15_ROI42_33PPT_Stl (Top, Middle, Bottom)

Table B-22 - Test Properties for T-15_ROI42_33PPT_Rub

Test Properties	
Tread	Rubber
Rate of Inclination	42
Salinity	35.7
RHumidity	81%
.5hr	77%
1hr	80%
1.5hr	83%
2hr	85%

Table B-23 - Weight Measurements for T-15_ROI42_33PPT_Rub

	Weight (kg)		
	Initial	Final	**Total Ice**
Top	10	11.171	**1.171**
Middle	9.92	10.984	**1.064**
Bottom	9.983	10.783	**0.8**

Table B-24 - Thickness Measurements for T-15_ROI42_33PPT_Rub

	Thickness (mm)							
	Initial			Final			**Avg**	**Slope**
Front Edge	48.84	48.82	49.37	54.56	53.11	52.65	**4.43**	**-1.147**
Back Edge	47.89	47.73	48.82	54.82	53.54	52.81	**5.58**	
Front Edge	47.48	47.85	48.1	54.29	54.92	53.98	**6.59**	**1.123**
Back Edge	47.59	47.91	48.04	53.19	53.41	53.33	**5.46**	
Front Edge	48.62	48.38	48.32	53.34	53.11	52.17	**4.43**	**-0.103**
Back Edge	47.98	47.66	47.85	53.21	51.92	51.97	**4.54**	

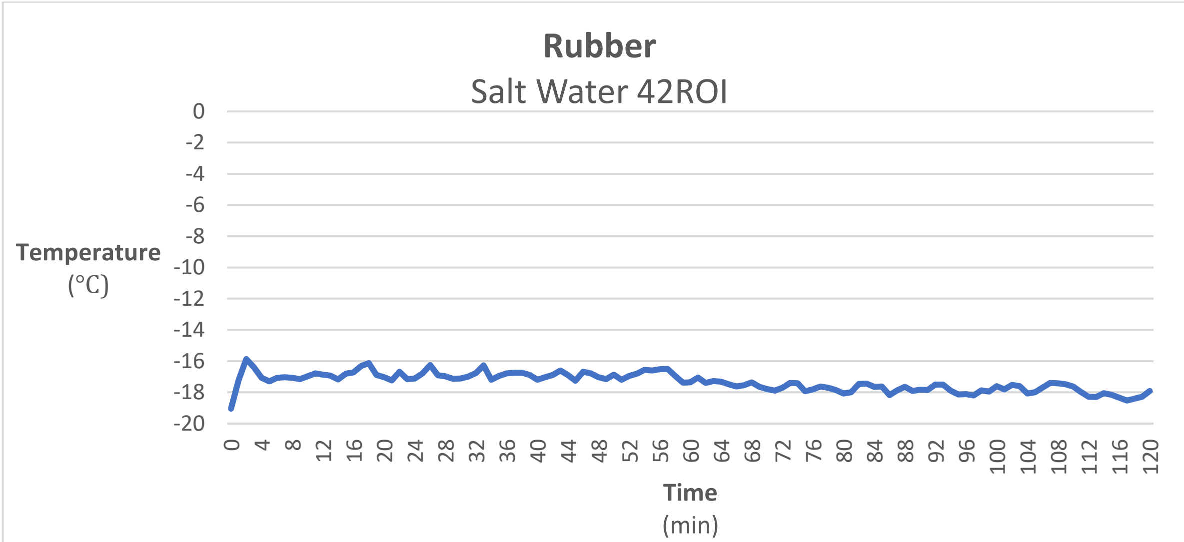

Figure B.21 - Transient Temperature Readings for T-15_ROI42_33PPT_Rub

Figure B.22 - Intermittent Pictures for T-15_ROI42_33PPT_Rub (30,60,90,120 minutes)

Figure B.23 - Step Thickness Pictures for T-15_ROI42_33PPT_Rub (Top, Middle, Bottom)

Appendix C - **Freshwater Impact Test Results**

Table C-1 - Freshwater Aluminum Impact Test

	Impact Test				
Weight	Initial	Final		Ice Removed	
Total	9.081 kg	8.564 kg		Weight	0.517 kg
Ice	0.72 kg	0.203 kg		Percentage	71.81%

Table C-2 - Freshwater Aluminum Impact Test Properties

Aluminum Step	8.361	kg
Mass of Boot	5.534	kg
lbf to Newtons	4.448	
Salinity	0	ppt
Humidity	**79%**	
	.5 hr	75%
	1 hr	79%
	1.5 hr	81%
	2 hr	81%

Figure C.1 – Freshwater Pre and Post Aluminum Impact Pictures

Table C-3 - Freshwater Open Cell Impact Test

	Impact Test				
Weight	Initial	Final		Ice Removed	
Total	9.333 kg	9.183 kg		Weight	0.150 kg
Ice	0.557 kg	0.407 kg		Percentage	26.93%

Table C-4 - Freshwater Open Cell Impact Test Properties

Grated Step	8.776	kg
Mass of Boot	5.534	kg
lbf to Newtons	4.448	
Salinity	0	ppt
Humidity	**78%**	
	.5 hr	73%
	1 hr	76%
	1.5 hr	80%
	2 hr	81%

Figure C.2 – Freshwater Pre and Post Open Cell Impact Pictures

Table C-5 - Freshwater Steel Impact Test

	Impact Test								
Weight	Initial		Final			Ice Removed			
Total	12.418	kg	12.364	kg		Weight	0.054	kg
Ice	0.47	kg	0.416	kg		Percentage	11.49%	

Table C-6 - Freshwater Steel Impact Test Properties

Steel Step	11.948	kg
Mass of Boot	5.534	kg
lbf to Newtons	4.448	
Salinity	0	ppt
Humidity	**82%**	
	.5 hr	78%
	1 hr	81%
	1.5 hr	85%
	2 hr	85%

Table C-7 - Freshwater Rubber Impact Test

	Impact Test						
Weight	Initial		Final			Ice Removed	
Total	9.081	kg	8.564	kg		Weight	0.517 kg
Ice	0.72	kg	0.203	kg		Percentage	71.81%

Table C-8 - Freshwater Rubber Impact Test Properties

Rubber Step	9.92	kg
Mass of Boot	5.534	kg
lbf to Newtons	4.448	
Salinity	0	ppt
Humidity	**81%**	
	.5 hr	78%
	1 hr	81%
	1.5 hr	82%
	2 hr	84%

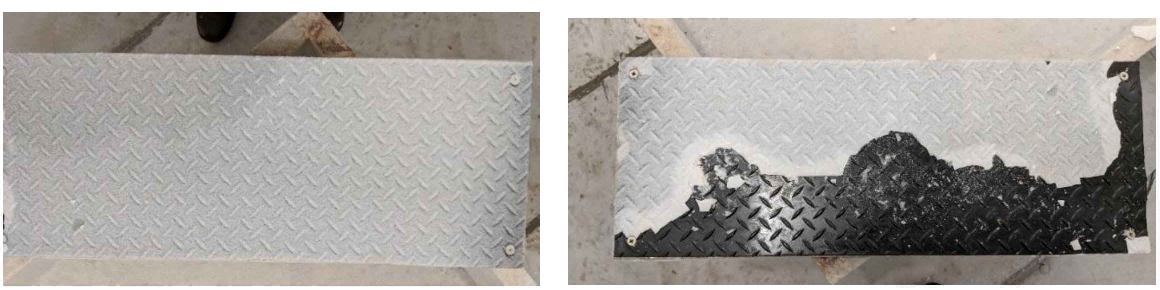

Figure C.3 – Freshwater Pre and Post Rubber Impact Pictures

Appendix D - **Saltwater Impact Test Results**

Table D-1 - Saltwater Aluminum Impact Test

	Impact Test			
Weight	Initial	Final	Ice Removed	
Total	8.928 kg	8.866 kg	Weight	0.062 kg
Ice	0.567 kg	0.505 kg	Percentage	10.93%

Table D-2 - Saltwater Aluminum Impact Test Properties

Aluminum Step	8.361	kg
Mass of Boot	5.534	kg
lbf to Newtons	4.448	
Salinity	34.1	ppt
Humidity	**79%**	
	.5 hr	75%
	1 hr	79%
	1.5 hr	81%
	2 hr	81%

Figure D.1 - Saltwater Pre and Post Aluminum Impact Pictures

Table D-3 - Saltwater Open Cell Impact Test

	Impact Test							
Weight	Initial		Final			Ice Removed		
Total	9.197	kg	9.134	kg		Weight	0.063	kg
Ice	0.421	kg	0.358	kg		Percentage	14.96%	

Table D-4 - Saltwater Open Cell Impact Test Properties

Grated Step	8.776	kg
Mass of Boot	5.534	kg
lbf to Newtons	4.448	
Salinity	35.7	ppt
Humidity	**78%**	
	.5 hr	75%
	1 hr	78%
	1.5 hr	79%
	2 hr	79%

Table D-5 - Saltwater Steel Impact Test

	Impact Test			
Weight	Initial	Final	Ice Removed	
Total	12.65 kg	12.598 kg	Weight	0.052 kg
Ice	0.702 kg	0.65 kg	Percentage	7.41%

Table D-6 - Saltwater Steel Impact Test Properties

Steel Step	11.948	kg
Mass of Boot	5.534	kg
lbf to Newtons	4.448	
Salinity	35.7	ppt
Humidity	**80%**	
	.5 hr	72%
	1 hr	81%
	1.5 hr	83%
	2 hr	84%

Figure D.2 -Saltwater Pre and Post Steel Impact Pictures

Table D-7 - Saltwater Rubber Impact Test

	Impact Test							
Weight	Initial		Final			Ice Removed		
Total	10.445	kg	10.334	kg		Weight	0.111	kg
Ice	0.525	kg	0.414	kg		Percentage	21.14%	

Table D-8 - Saltwater Rubber Impact Test Properties

Rubber Step	9.92	kg
Mass of Boot	5.534	kg
lbf to Newtons	4.448	
Salinity	35.4	ppt
Humidity	**77%**	
	.5 hr	76%
	1 hr	77%
	1.5 hr	77%
	2 hr	78%

Figure D.3 – Saltwater Pre and Post Rubber Impact Pictures

Appendix E: Stair Design Files

ITEM NO.	PART NUMBER	Material	QTY.
1	Side Panel	Steel	2
2	Angled Frame	Steel	3
3	Long Leg	Steel	2
4	Short Leg	Steel	2

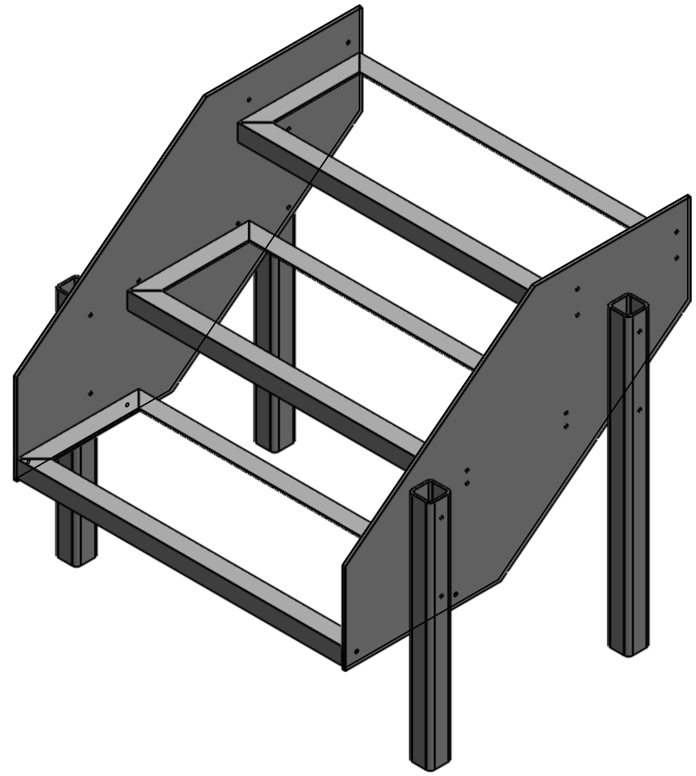

Sheet Notes

Not Pictured

3 x 1/2in Aluminum Treads
3 x 1/2in Steel Treads
3 x 1/4 in Rubber Treads

NEXT ASSY	USED ON
APPLICATION	

UNLESS OTHERWISE SPECIFIED:
DIMENSIONS ARE IN INCHES
TOLERANCES:
FRACTIONAL 1/64
ANGULAR: MACH ±0.1° BEND ±1°
ONE PLACE DECIMAL ±0.1
TWO PLACE DECIMAL ±0.01
THREE PLACE DECIMAL ±0.001

INTERPRET GEOMETRIC TOLERANCING PER:

MATERIAL

FINISH

DO NOT SCALE DRAWING

	NAME	DATE
DRAWN	JRB	AUG 18
CHECKED		
ENG APPR.		
MFG APPR.		
Q.A.		

COMMENTS:

THIRD ANGLE PROJECTION

TITLE:

Stair Model

SIZE	DWG. NO.	REV
A	1 of 7	A

SCALE: 1:16 WEIGHT: SHEET 1 OF 1

5 4 3 2 1

Sheet Notes

Sheet thicknes of
1/4 inch

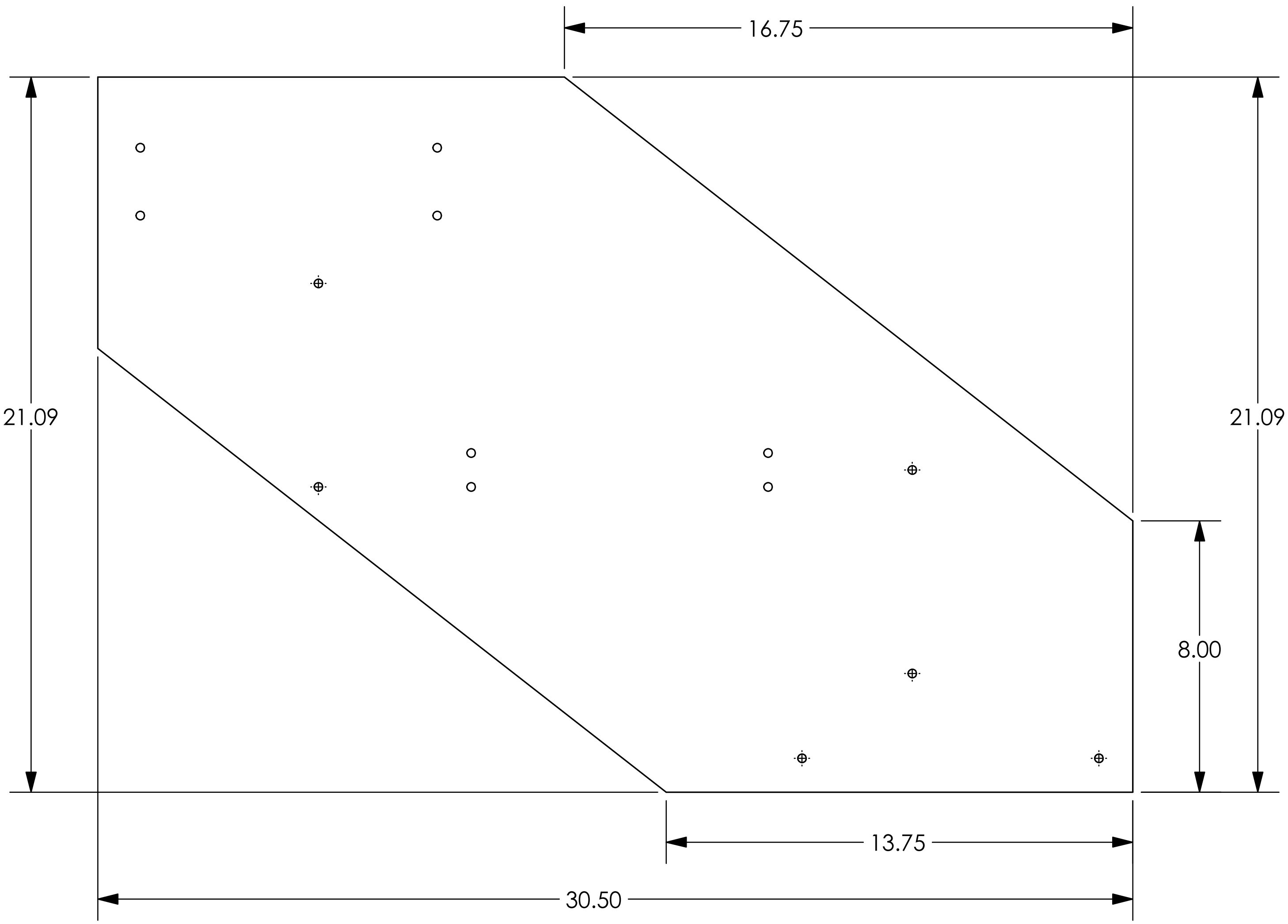

PROPRIETARY AND CONFIDENTIAL

THE INFORMATION CONTAINED IN THIS DRAWING IS THE SOLE PROPERTY OF MEMORIAL UNIVERSITY OF NEWFOUNDLAND. ANY REPRODUCTION IN PART OR AS A WHOLE WITHOUT THE WRITTEN PERMISSION OF MEMORIAL UNIVERSITY OF NEWFOUNDLAND IS PROHIBITED.

NEXT ASSY	USED ON
APPLICATION	

UNLESS OTHERWISE SPECIFIED:
DIMENSIONS ARE IN INCHES
TOLERANCES:
FRACTIONAL 1/64
ANGULAR: MACH ±0.1° BEND ±1°
ONE PLACE DECIMAL ±0.1
TWO PLACE DECIMAL ±0.01
THREE PLACE DECIMAL ±0.001

INTERPRET GEOMETRIC TOLERANCING PER:

MATERIAL

FINISH

DO NOT SCALE DRAWING

	NAME	DATE
DRAWN	JRB	AUG 18
CHECKED		
ENG APPR.		
MFG APPR.		
Q.A.		

COMMENTS:

THIRD ANGLE PROJECTION

TITLE:

Side Panel

SIZE	DWG. NO.	REV
A	2 of 7	A

SCALE: 1:5 | WEIGHT: | SHEET 1 OF 1

5 4 3 2 1

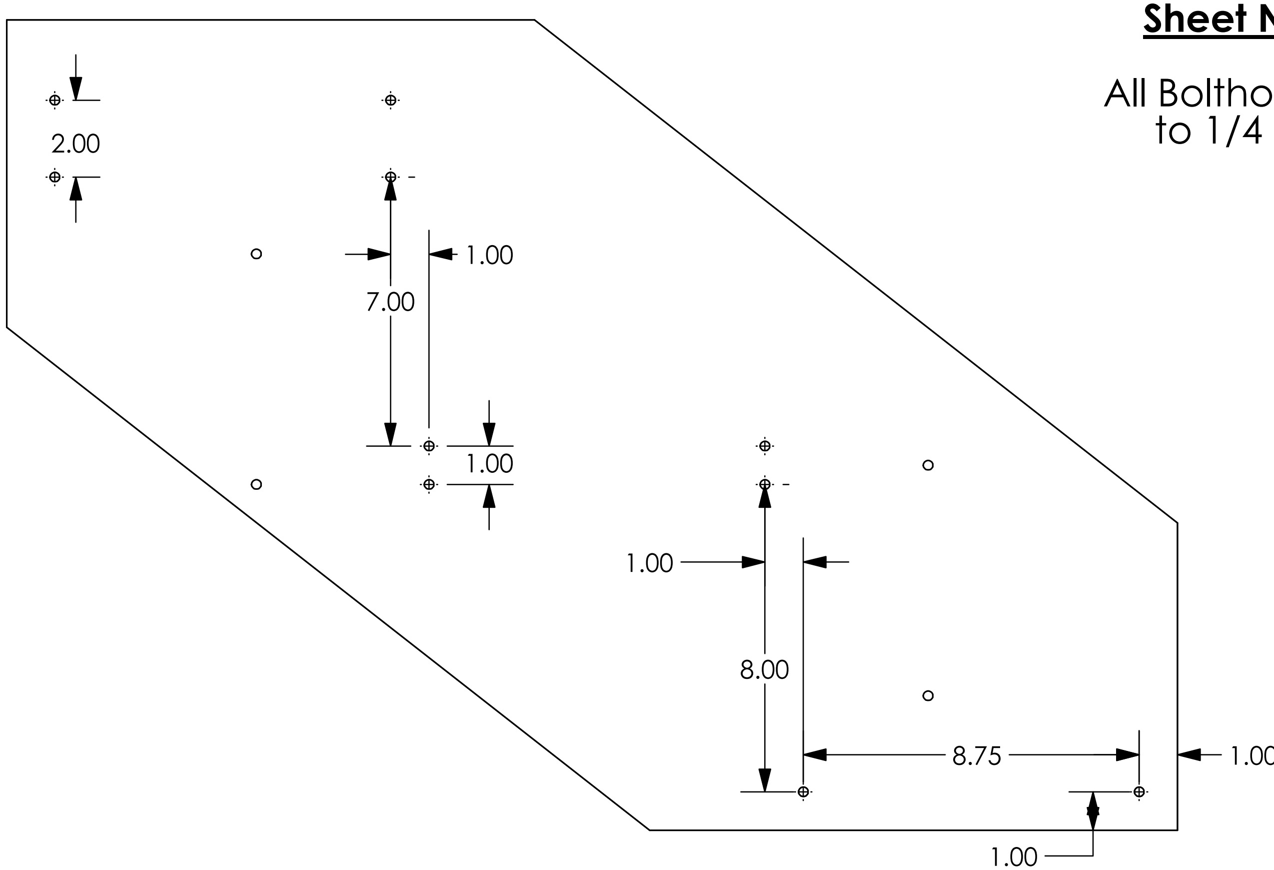

Sheet Notes

All Boltholes cut to 1/4 inch

UNLESS OTHERWISE SPECIFIED:
DIMENSIONS ARE IN INCHES
TOLERANCES:
FRACTIONAL 1/64
ANGULAR: MACH ±0.1° BEND ±1°
ONE PLACE DECIMAL ±0.1
TWO PLACE DECIMAL ±0.01
THREE PLACE DECIMAL ±0.001

INTERPRET GEOMETRIC TOLERANCING PER:

MATERIAL

FINISH

DO NOT SCALE DRAWING

NEXT ASSY | USED ON

APPLICATION

	NAME	DATE
DRAWN	JRB	AUG 18
CHECKED		
ENG APPR.		
MFG APPR.		
Q.A.		

COMMENTS:

THIRD ANGLE PROJECTION

TITLE:

Side Panel Bolt Holes

SIZE A | DWG. NO. 3 of 7 | REV A

SCALE: 1:5 | WEIGHT: | SHEET 1 OF 1

5 4 3 2 1

Sheet Notes

All Bolt holes cut to 1/4 inch

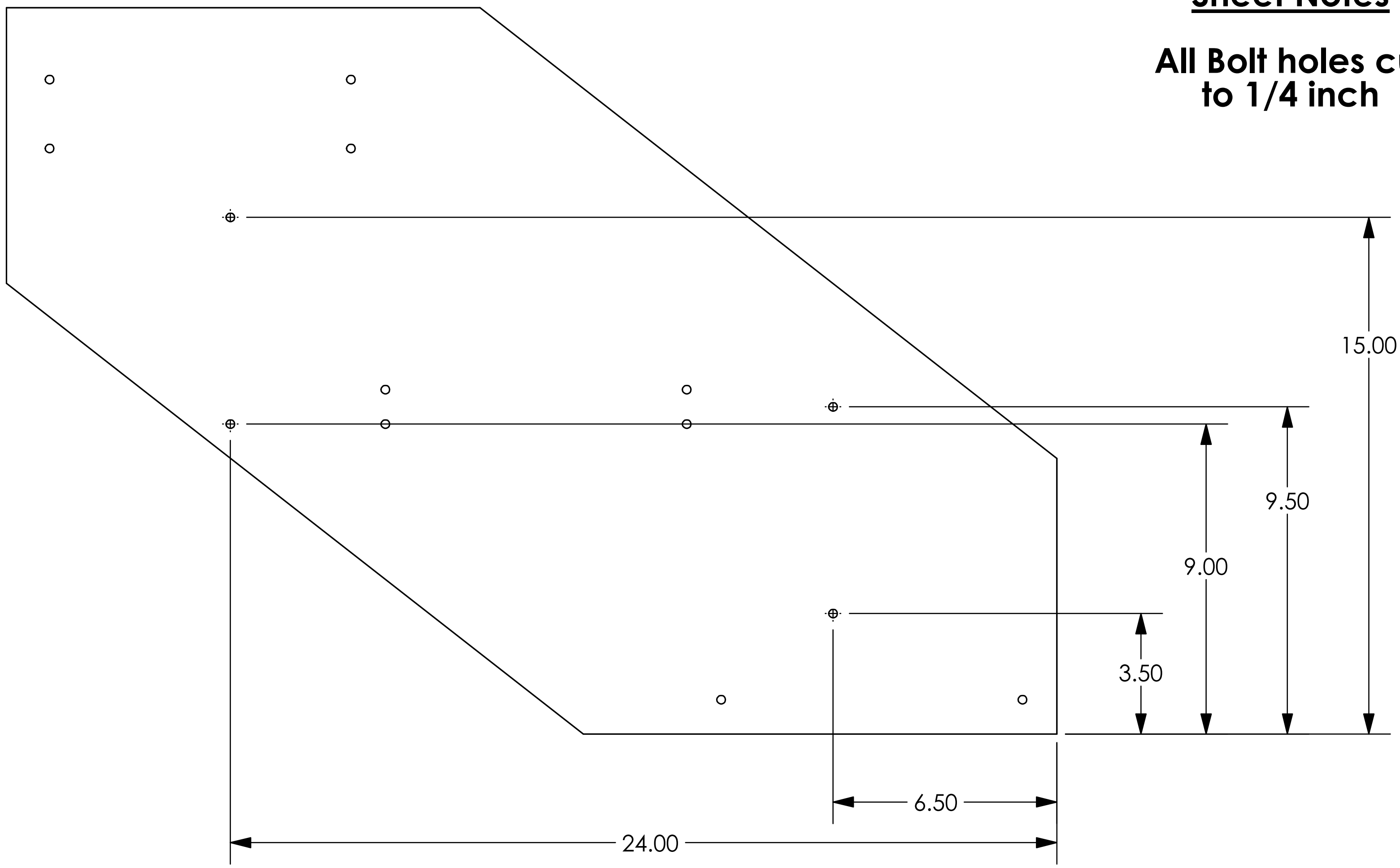

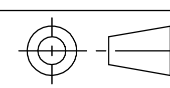

PROPRIETARY AND CONFIDENTIAL

THE INFORMATION CONTAINED IN THIS DRAWING IS THE SOLE PROPERTY OF MEMORIAL UNIVERSITY OF NEWFOUNDLAND. ANY REPRODUCTION IN PART OR AS A WHOLE WITHOUT THE WRITTEN PERMISSION OF MEMORIAL UNIVERSITY OF NEWFOUNDLAND IS PROHIBITED.

NEXT ASSY	USED ON	
APPLICATION		

UNLESS OTHERWISE SPECIFIED:
DIMENSIONS ARE IN INCHES
TOLERANCES:
FRACTIONAL 1/64
ANGULAR: MACH ±0.1° BEND ±1°
ONE PLACE DECIMAL ±0.1
TWO PLACE DECIMAL ±0.01
THREE PLACE DECIMAL ±0.001

INTERPRET GEOMETRIC TOLERANCING PER:

MATERIAL

FINISH

DO NOT SCALE DRAWING

	NAME	DATE
DRAWN	JRB	AUG 18
CHECKED		
ENG APPR.		
MFG APPR.		
Q.A.		

COMMENTS:

THIRD ANGLE PROJECTION

TITLE:

Side Panel Leg Holes

SIZE	DWG. NO.	REV
A	4 of 7	A
SCALE: 1:5	WEIGHT:	SHEET 1 OF 1

5 4 3 2 1

Sheet Notes

Angled Frame with
a thickness of 1/8 inch

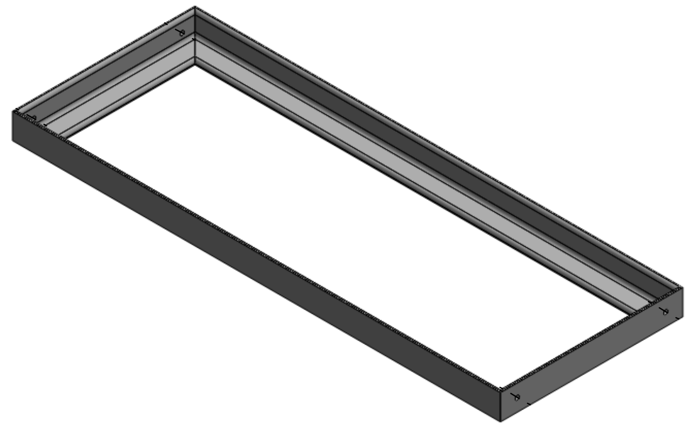

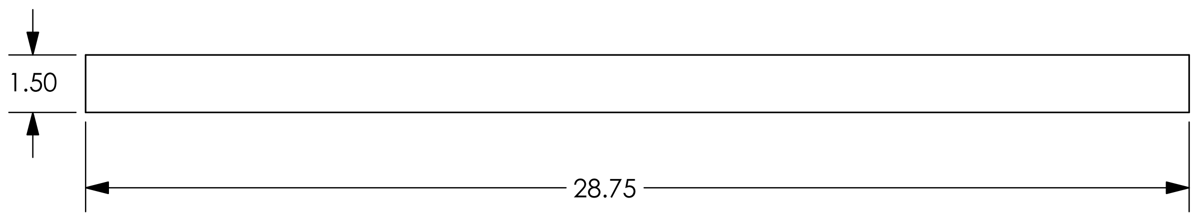

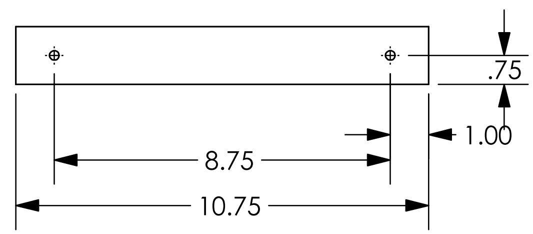

PROPRIETARY AND CONFIDENTIAL

NEXT ASSY	USED ON
APPLICATION	

UNLESS OTHERWISE SPECIFIED:
DIMENSIONS ARE IN INCHES
TOLERANCES:
FRACTIONAL 1/64
ANGULAR: MACH ±0.1° BEND ±1°
ONE PLACE DECIMAL ±0.1
TWO PLACE DECIMAL ±0.01
THREE PLACE DECIMAL ±0.001

INTERPRET GEOMETRIC TOLERANCING PER:

MATERIAL

FINISH

DO NOT SCALE DRAWING

	NAME	DATE
DRAWN	JRB	AUG 18
CHECKED		
ENG APPR.		
MFG APPR.		
Q.A.		

COMMENTS:

THIRD ANGLE PROJECTION

TITLE:

Angled Frame

SIZE	DWG. NO.	REV
A	5 of 7	A

SCALE: 1:5 | WEIGHT: | SHEET 1 OF 1

5 4 3 2 1

Sheet Notes

All bolt holes cut
to 1/4in diameter

Wall thickness of 1/8in

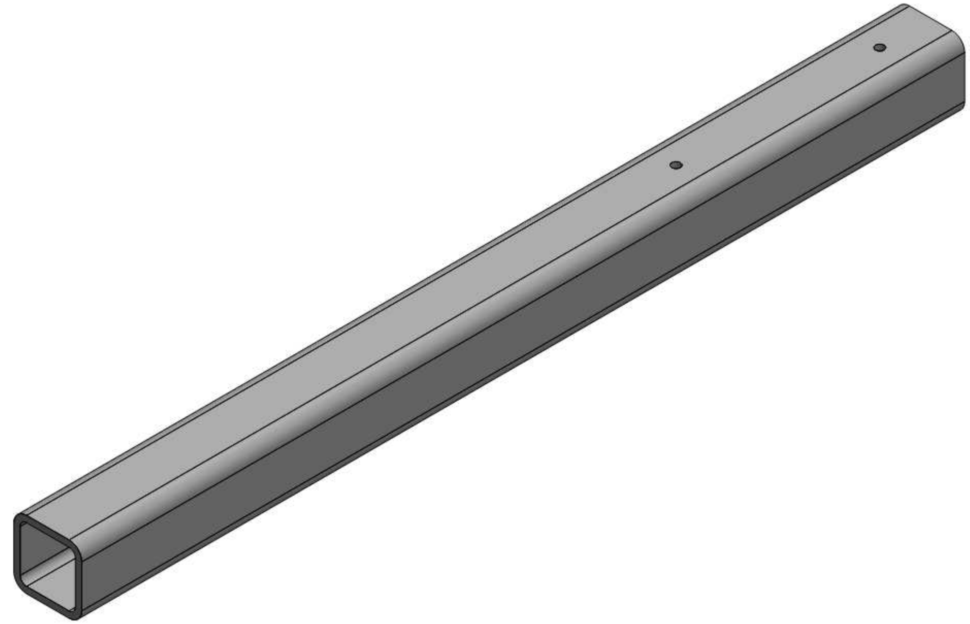

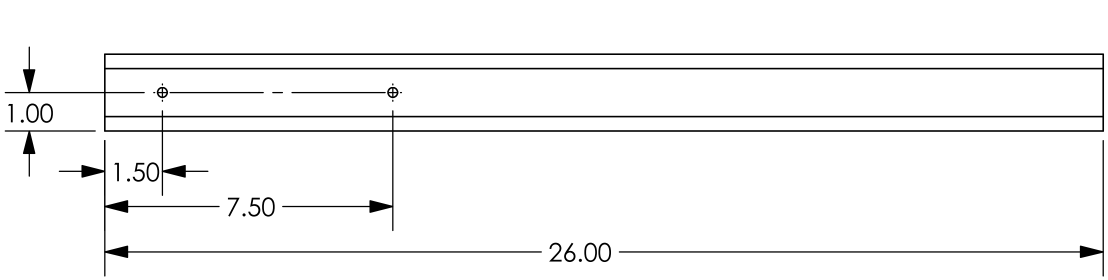

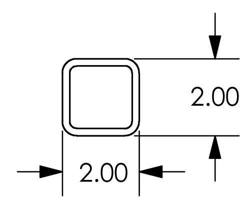

PROPRIETARY AND CONFIDENTIAL

NEXT ASSY	USED ON
APPLICATION	

UNLESS OTHERWISE SPECIFIED:
DIMENSIONS ARE IN INCHES
TOLERANCES:
FRACTIONAL 1/64
ANGULAR: MACH ±0.1° BEND ±1°
ONE PLACE DECIMAL ±0.1
TWO PLACE DECIMAL ±0.01
THREE PLACE DECIMAL ±0.001

INTERPRET GEOMETRIC TOLERANCING PER:

MATERIAL

FINISH

DO NOT SCALE DRAWING

	NAME	DATE
DRAWN	JRB	AUG 18
CHECKED		
ENG APPR.		
MFG APPR.		
Q.A.		

COMMENTS:

THIRD ANGLE PROJECTION

TITLE:

Long Leg

SIZE	DWG. NO.	REV
A	6 of 7	A

SCALE: 1:5	WEIGHT:	SHEET 1 OF 1

5 4 3 2 1

Sheet Notes

Bolt holes cut through
all at 1/4 inch diameter

Wall thickness of 1/8 inch

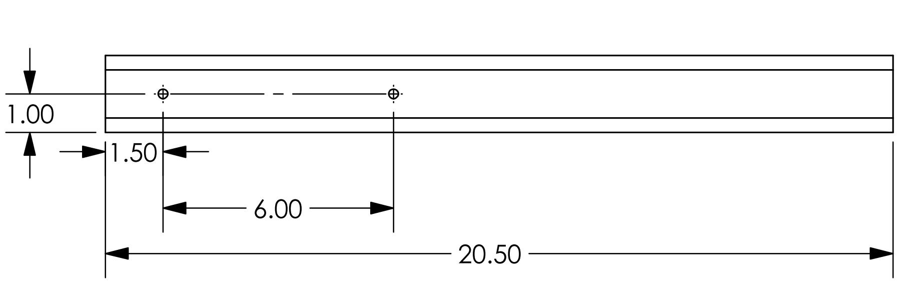

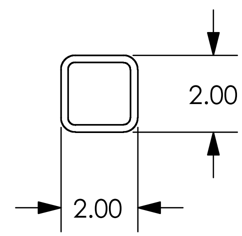

NEXT ASSY	USED ON
APPLICATION	

UNLESS OTHERWISE SPECIFIED:
DIMENSIONS ARE IN INCHES
TOLERANCES:
FRACTIONAL 1/64
ANGULAR: MACH ±0.1° BEND ±1°
ONE PLACE DECIMAL ±0.1
TWO PLACE DECIMAL ±0.01
THREE PLACE DECIMAL ±0.001

INTERPRET GEOMETRIC TOLERANCING PER:

MATERIAL

FINISH

DO NOT SCALE DRAWING

	NAME	DATE
DRAWN	JRB	AUG 18
CHECKED		
ENG APPR.		
MFG APPR.		
Q.A.		

COMMENTS:

THIRD ANGLE PROJECTION

TITLE:

Short Leg

SIZE	DWG. NO.	REV
A	7 of 7	A

SCALE: 1:5 WEIGHT: SHEET 1 OF 1

5 4 3 2 1

Appendix F: Droplet Temperature Calculations

The following analysis is done using the experimental droplet diameter of 792μm and the properties listed below.

Table 0-1 - Air and Water Properties taken from www.engineeringtoolbox.com

Air Properties	
dynamic viscosity	1.64E-05
static viscosity	1.18E-05
thermal conductivity	0.02258
Prantl Number	0.709
static viscosity	1.72E-05
room temperature	-18
airflow	7.487
density	1.225

Water Properties	
density	9.98E+02
thermal conductivity	0.598
specific heat capacity	4180
droplet diameter	7.92E-04
droplet surface area	4.93E-07
droplet volume	6.57E-07

Reynolds Number

$$Re = \frac{Ud}{\mu} = \frac{(7.487)(.000792)}{(.0000118)} = \mathbf{504.3}$$

Nusselt Number

$$Nu = 2.0 + 0.6Pr^{\frac{1}{3}}Re^{\frac{1}{2}} = 2.0 + 0.6(0.709)^{\frac{1}{3}}(504.3)^{\frac{1}{2}} = \mathbf{14.01}$$

Convection Coefficient

$$h = \frac{Nuk}{d_r} = \frac{(14.01)(0.02258)}{(0.000396)} = \mathbf{799.07}$$

Biot Number

$$Bi_r = \frac{hd_r}{k_w} = \frac{(799.07)(.000396)}{(0.598)} = \mathbf{0.53}$$

Alpha

$$\alpha_r = \frac{k_w t}{\rho c_p} = \frac{(0.598)t}{(998)(4180)} = \mathbf{1.43x10^{-7}}\boldsymbol{t}$$

Fourier

$$Fo_r = \frac{\alpha}{{d_r}^{\frac{1}{2}}} = \mathbf{0.914}\boldsymbol{t}$$

Lumped Sum Capacitance

$$\frac{\phi(t)}{\phi_0} = \exp(-3Bi_r Fo_r) = \frac{T - T_\infty}{T_0 - T_\infty}$$

$$T(t) = T_\infty + (T_0 - T_\infty)e^{-3Bi_r Fo_r}$$

$$T(t) = (-18) + \big(20 - (-18)\big)e^{-3(0.53)(0.914t)}$$

$$\boldsymbol{T(t) = 38e^{-1.45t} - 18}$$